Technische Universität München

Wissenschaftszentrum Weihenstephan für Ernährung, Landnutzung und Umwelt

Lehrstuhl für Molekulare Ernährungsmedizin

Impact of gut microbiota composition, liver metabolism and respiratory capacity of peripheral blood mononuclear cells on resting metabolic rate

Gloria-Maria Keppner

Vollständiger Abdruck der von der Fakultät Wissenschaftszentrum Weihenstephan für Ernährung, Landnutzung und Umwelt der Technischen Universität München zur Erlangung des akademischen Grades eines

Doktors der Naturwissenschaften

genehmigten Dissertation.

Vorsitzender:	Prof. Dr. Michael Schemann
Prüfer der Dissertation:	1. Prof. Dr. Martin Klingenspor
	2. Prof. Dr. Karsten Köhler

Die Dissertation wurde am 03. 12. 2019 bei der Technischen Universität München eingereicht und durch die Fakultät Wissenschaftszentrum Weihenstephan für Ernährung, Landnutzung und Umwelt am 24. 03. 2020 angenommen.

Abstract

Obesity is a worldwide health problem with an increasing incidence over the last decades. Treatments include a reduction of energy intake and an increase in energy expenditure, which require a precise knowledge about the daily energy expenditure and its components. Resting metabolic rate (RMR) is with 60 - 80% the biggest component of daily energy expenditure and therefore of special interest. RMR is characterized by a high inter-individual variation. Variables taken into consideration when predicting RMR are sex, age, race, fat mass and fat free mass (FFM). However, even after adjusting RMR for these influencing variables, a residual variation of approximately 30% remains unexplained. In the present work the impact of liver metabolism, gut microbiota composition and the respiratory capacity of peripheral blood mononuclear cells (PBMCs) on RMR variation is analyzed.

To analyze the residual variation of RMR, a general linear regression model was designed, based on the four *enable* cohorts with 488 subjects ranging from 3 to 85 years. At first a mixed effect model was generated with the variables sex, age, fat mass, FFM and body temperature, resulting in a correlation coefficient of R^2 = 0.80. This equation was cross-validated in an independent cohort with a high precision of R^2 = 0.79. The mixed effect model was applied to analyze the influence of clinical blood parameters and blood pressure on RMR variation. Thereby, free triiodothyronine, leukocytes, creatinine, MCHC, systolic blood pressure and heart rate were identified to be significant predictors of RMR. Based on all these variables, a second and more complex statistical model was generated to elucidate the residual variation regarding the influence of liver metabolism, gut microbiota composition and respiratory capacity of PBMCs.

A pilot study with 30 subjects was conducted to analyze the influence of liver fat, as a parameter of liver activity, on RMR variation. Liver fat content was not associated with RMR and did not explain the residual variation of RMR. Gut microbiota composition was determined by 16S rRNA gene sequencing and analyzed in 442 subjects. The analysis of gut microbiota composition on RMR variation was performed by correlation analysis, linear regression analysis, principle component analysis and artificial neural networks. Gut bacterial composition and diversity did not correlate with RMR variation until the level of *Operational Taxonomic Units*. However, an indirect correlation of bacteria on the family level and RMR was found. This correlation was based on an association with FFM, which is the main predictor of RMR. Mitochondrial activity of PBMCs was determined in 179 subjects by high resolution respirometry. Though, the respiratory capacity of PBMCs was not associated with RMR and therefore did not contribute to the residual variation of RMR.

In summary, the results of the present thesis provide new insights into the involvement of liver metabolism, gut microbiota composition and respiratory capacity of PBMCs on RMR variation. Additionally, an equation with high precision to predict RMR is presented.

Zusammenfassung

Übergewicht und Adipositas sind ein weltweites Gesundheitsproblem, das in den letzten Jahrzehnten immer bedeutender wurde. Die Adipositastherapie basiert auf einer Reduzierung der Energiezufuhr und einer Erhöhung des Energieverbrauchs, welche Kenntnisse über den täglichen Energieverbrauch und seine Komponenten erfordert. Der Ruheumsatz ist mit 60 - 80% der größte Anteil des täglichen Energieverbrauchs und ist gekennzeichnet durch eine hohe inter-individuelle Variabilität. Bei der Berechnung des Ruheumsatzes werden Faktoren wie Alter, Geschlecht, Ethnie, Fettmasse und fettfreie Masse berücksichtigt. Jedoch bleibt nach Adjustierung auf die genannten Einflussfaktoren eine Restvariabilität von 30% bestehen. Im Rahmen der vorliegenden Arbeit wurde der Einfluss der Darmmikrobiota-Zusammensetzung, des Lebermetabolismus und der respiratorischen Kapazität von peripheren mononuklearen Zellen des Blutes (PBMCs) auf die Variabilität des Ruheumsatzes analysiert.

Zur Bestimmung der verbleibenden Variation im Ruheumsatz wurde ein allgemeines Regressionsmodell erstellt, das auf den vier *enable* Kohorten mit 488 Probanden zwischen 3 - 85 Jahren basiert. Zunächst wurde ein gemischtes Modell mit den Variablen Geschlecht, Alter, Fettmasse, fettfreie Masse und Körpertemperatur mit einem Korrelationskoeffizienten von R^2 = 0.8 erstellt. Diese Gleichung wurde an einer unabhängigen Studienkohorte mit einem Korrelationskoeffizienten von R^2 = 0.79 validiert. Das gemischte Model wurde verwendet, um den Einfluss klinischer Blutparameter und des Blutdrucks auf die Variation im Ruheumsatz zu analysieren. Dabei wurden das Schilddrüsenhormon (fT_3), Leukozyten, Kreatinin, MCHC, systolischer Blutdruck und Herzfrequenz als signifikante Einflussfaktoren des Ruheumsatzes identifiziert. Basierend auf diesen Variablen wurde ein zweites komplexeres Regressionsmodell erstellt, um den Einfluss der Leber, der Darmmikrobiota-Zusammensetzung und der respiratorischen Kapazität von PBMCs auf den Ruheumsatz zu analysieren.

Im Rahmen einer Pilotstudie mit 30 Probanden wurde der Einfluss des Leberfettgehalts, der als Parameter für die Leberaktivität diente, analysiert. Der Leberfettgehalt korrelierte dabei nicht mit dem Ruheumsatz und erklärt somit nicht die Restvariabilität im Ruheumsatz. Die Darmmikrobiota-Zusammensetzung wurde anhand einer 16S rRNA Gensequenzierung bei 442 Probanden bestimmt. Der Einfluss der Darmmikrobiota auf den Ruheumsatz wurde mittels Korrelationsanalysen, linearer Regressionsanalysen, Hauptkomponentenanalysen und artifizieller neuronaler Netzwerkanalyse analysiert. Die Diversität und Zusammensetzung der Darmbakterien war bis zur Ebene der *Operational Taxonomic Units* nicht mit der Variation im Ruheumsatz assoziiert. Jedoch wurde eine indirekte Korrelation

einiger Bakterienfamilien mit dem Ruheumsatz festgestellt. Diese Korrelation beruhte auf einer Assoziation mit der fettfreien Masse, die ein Haupteinflussfaktor des Ruheumsatzes ist. Die mitochondriale Aktivität von PBMCs wurde anhand von Respirationsmessungen an 179 Probanden bestimmt. Dabei korrelierte die respiratorische Kapazität von PBMCs nicht mit dem Ruheumsatz und trug somit nicht zur Restvariabilität bei.

Zusammenfassend lässt sich sagen, dass die Ergebnisse dieser Dissertation neue Einblicke über den Einfluss der Darmmikrobiota-Zusammensetzung, des Leber-metabolismus und der respiratorischen Kapazität von PBMCs auf den Ruheumsatz des Menschen geben. Außerdem wird eine neue Gleichung mit hoher Präzision zur Berechnung des Ruheumsatzes vorgestellt.

Table of contents

List of Figures

List of Tables

Abbreviations

16S rRNA	16S **r**ibosomal **r**ibonucleic **a**cid
ADP	**a**denosine **d**iphosphate
AIC	**A**kaike **i**nformation **c**riterion
ATP	**a**denosine **t**riphosphate
BIA	**b**ioelectrical **i**mpedance **a**nalysis
BMI	**b**ody **m**ass **i**ndex
BMR	**b**asal **m**etabolic **r**ate
ETS	**e**lectron **t**ransport **s**ystem
FCCP	**c**arbonyl **c**yanide 4-(trifluoromethoxy) **p**henylhydrazone
FFA	**f**ree **f**atty **a**cids
FFG	**f**orearm to **f**ingertip skin temperature **g**radient
fT_3	**f**ree **t**riiodthyronin
GGT	**g**amma-**g**lutamyl**t**ransferase
GPT	**g**lutamate-**p**yruvate-**t**ransaminase
HMRO	**h**igh **m**etabolic **r**ate **o**rgan
LMRO	**l**ow **m**etabolic **r**ate **o**rgan
MCHC	**m**ean **c**orpuscular **h**emoglobin **c**oncentration
MRI	**m**agnetic **r**esonance **i**maging
MRS	**m**agnetic **r**esonance **s**equence
MRT	**m**agnetic **r**esonance **i**maging
NAFLD	**n**on-**a**lcoholic **f**atty **l**iver **d**isease
NASH	**n**on-**a**lcoholic **s**teatohepatitis
OTU	**o**perational **t**axonomic **u**nit
OXPHOS	**ox**idative **phos**phorylation
PBMC	**p**eripheral **b**lood **m**ononuclear **c**ell
PCA	**p**rincipal **c**omponent **a**nalysis
PDFF	**p**roton **d**ensity **f**at **f**raction
RCR	**r**espiratory **c**ontrol **r**atio
RCRu	**r**espiratory **c**ontrol **r**atio **u**ncoupled
RMR	**r**esting **m**etabolic **r**ate
ROS	**r**eactive **o**xygen **s**pecies
SAT	**s**ubcutaneous **a**dipose **t**issue
SUIT	**s**ubstrate **u**ncoupler **i**nhibitor **t**itration
TDEE	**t**otal **d**aily **e**nergy **e**xpenditure
TNZ	**t**hermal **n**eutral **z**one
VAT	**v**isceral **a**dipose **t**issue
WHR	**w**aist to **h**ip **r**atio

1 Introduction

1.1 Resting metabolic rate as the main variable of daily energy expenditure

The occurrence and development of obesity has dramatically increased in the last decades, almost triplicated over 40 years (WHO 2018). A cause for obesity is an imbalance of energy intake and energy expenditure, favored by a chronic positive energy intake. A precise knowledge about the total daily energy expenditure (TDEE) and its components is fundamental to understand the underlying pathology of obesity and implement appropriate therapeutic interventions (Lam and Ravussin 2017).

The major component of TDEE is resting metabolic rate (RMR), accounting for 60 - 80%, followed by physical activity with 10 - 30% and adaptive thermogenesis with 10% (Landsberg 2012). Adaptive thermogenesis stands for metabolic responses like cold (van Marken Lichtenbelt et al. 2009) or diet induced thermogenesis. As RMR is the major component of TDEE, there is a particular interest in the basic principles and how RMR is composed. RMR reflects the metabolic rate necessary to maintain all vital function without any physical activity or additional energy expenses. Therefore, RMR is defined to be determined at rest, in a lying position, in a thermoneutral environment, awake and in a post-absorptive state (10 - 12h after the last meal).

Energy expenditure is determined by measuring heat production, respectively heat loss, either by direct or indirect calorimetry. Early on Atwater described that heat production can be predicted by assessing the consumed oxygen (O_2) and the produced carbon dioxide (CO_2) (Atwater 1905). Today, the measurement of RMR is performed by indirect calorimetry, a real time measurement of O_2 consumption and CO_2 production. Heat production is then calculated by Weir's equation by calculating the 'heat output' (kcal) = $3.9 \times O_2$ (L) + $1.11 \times CO_2$ (L) (Weir 1949). Indirect calorimetry has become the most common and widely used method to measure and calculate energy expenditure. It is an important tool to understand the components of energy expenditure and to accurately predict RMR for obesity intervention (Lam and Ravussin 2017).

RMR can also be predicted by mathematical equations. Several equations haven been generated, since measuring RMR is a complex and time-consuming method, which requires strictly standardized conditions. However, there is a high inter-individual variation in RMR, and the precision of the recommended equations varies. Well-established and commonly used equations are those from Harris-Benedict (Harris and Benedict 1918) and World Health Organization (WHO) (WHO 1985). The Harris-Benedict equation uses the factors weight, height and age, whereas the WHO equation solely uses weight to predict RMR.

However, in current research variables like sex, age, weight, height, fat mass and fat free mass (FFM) are taken into consideration when predicting RMR.

Inter-individual variation of RMR is caused by several factors. The major component contributing to RMR is FFM (Gallagher et al. 1998, Muller et al. 2004, Johnstone et al. 2005, Ravussin et al. 1986, Cunningham 1991). Other factors are age, fat mass and sex (Muller et al. 2004, Javed et al. 2010). Even after adjusting RMR for sex, age, fat mass and FFM a residual variation of approximately 30% remains unexplained (Muller et al. 2004, Javed et al. 2010). Great efforts have been undertaken to elucidate factors contributing to the residual variation in RMR. In terms of obesity research, factors like insulin levels and blood pressure were found to contribute to the inter-individual variation of RMR (Bosy-Westphal et al. 2008). The role of thyroid hormones on energy expenditure was studied in depth, and it is well known that hypo- and hyperthyroidism have an effect on RMR. However, there is no consent about the impact of thyroid hormones on RMR in euthyroid subjects (Bosy-Westphal et al. 2008, Svendsen, Hassager and Christiansen 1993, Spadafranca et al. 2015). Factors like blood pressure, insulin levels and thyroid hormones have been analyzed regarding their influence on RMR, but mostly in the context of obesity or specific diseases and not in healthy individuals.

Understanding the physiological processes determining energy expenditure is important to accurately determine the individual energy requirement and execute weight related interventions. In this context, RMR plays an important role as it is the major component of daily energy expenditure (Landsberg 2012). So far 75% of the inter-individual variation in RMR can be explained (Javed et al. 2010, Muller et al. 2004), leaving the remaining variation unexplained.

1.2 Mitochondria – the energy source of our cells

Mitochondria are the ‘powerhouse’ of our cells and found in almost every eukaryotic cell. In response to acute or chronic energy demands, energy is provided in form of adenosine triphosphate (ATP). Mitochondria generate ATP under the process of oxidative phosphorylation (Figure 1), oxidizing substrates and phosphorylating adenosine diphosphate (ADP). Under the process of substrate oxidation, electrons are accepted by complex I and II and transported along the electron transport chain, consisting of four complexes (complex I - IV). The transport of electrons enables to pump protons from the matrix into the intermembrane space, generating a proton gradient across the inner mitochondrial membrane. This proton gradient is used by the fifth complex, the

ATP-synthase, to produce ATP by ADP phosphorylation. By the process of substrate oxidation, electron transport and proton translocation, oxygen is reduced to water at complex IV. As thereby oxygen is required to produce ATP, this process is called mitochondrial respiration. Oxidative phosphorylation requires approximately 90% of the daily consumed oxygen.
Mitochondrial respiration can be assessed by respiration measurements, assessing the oxygen consumption of cells or isolated mitochondria. A possibility to determine the capacity and efficiency of ATP production in response to energy demands is by measuring the respiratory control ration (RCR) (Brand and Nicholls 2011). RCR describes the increase in respiration in response to ADP and consequently ATP production by ADP phosphorylation. In addition, substrates and inhibitors targeting the individual complexes of the respiratory chain can further elucidate mitochondrial function and dysfunction.

Mitochondria have an essential role in energy supply and therefore are thought to play an important role in metabolic diseases. A reduced capacity of oxidative phosphorylation is observed in metabolic diseases such as fatty liver disease and diabetes (Rontoyanni et al. 2017, Suomalainen and Battersby 2018). Mitochondrial function was mostly analyzed in tissue samples like skeletal muscle or adipose tissue (Jheng et al. 2015, Liesa and Shirihai 2013). Obtaining muscle cells or adipocytes requires the invasive procedure of a biopsy, whereas peripheral blood mononuclear cells (PBMCs) are accessible by a minimal invasive procedure of a venipuncture (Ost et al. 2018). PBMCs are peripheral cells of the blood, characterized by a single round nucleus and mitochondria. PBMCs are a mixed population of immune cells resembled by lymphocytes, monocytes, natural killer cells and dendritic cells (Kleiveland 2015), having important functions during inflammatory processes, thrombosis and immune reactions (Kramer et al. 2014). Diabetes and sepsis lead to inflammatory processes like the activation of lymphocytes and monocytes (Srinivasan et al. 2003), and are associated with changes in the respiratory capacity of PBMCs (Hartman et al. 2014, Belikova et al. 2007). As PBMCs are immune cells, the systemic inflammation of diabetes and sepsis are reflected in the respiratory capacity of PBMCs. PBMCs are circulating cells of the blood and are directly affected by metabolic stress, responding to systemic changes and signals, like the inflammatory processes. Consequently, mitochondria of blood cells have a potential as biomarker for clinical diagnostics and biomedical research to detect early on systemic changes. However, mitochondrial activity of PBMCs in healthy subjects has not deeply been analyzed.

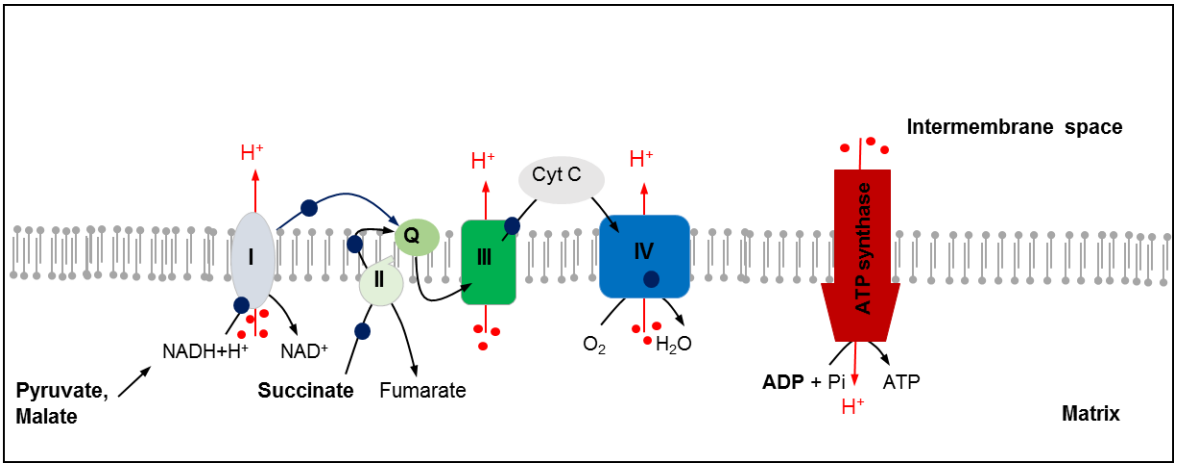

Figure 1: Mitochondrial respiratory chain. Depicted are the four complexes (I - IV) of the electron transport chain and ATP-synthase. Electrons from $NADH+H^+$ and succinate are accepted by complex I, respectively complex II. The flow of electrons along the electron transport chain are presented in dark blue. Protons are pumped into the intermembrane space by complex I, II and IV, generating a proton gradient, which is used by the ATP-synthase to phosphorylate ADP. Protons and their respective flow are depicted in red.

1.3 Gut microbiota in the context of energy metabolism

The human gut is colonized by almost 38 billion bacteria, just as many cells as the human body possesses (Sender, Fuchs and Milo 2016). This is a complex ecosystem with various tasks and functions like protection against pathogens, synthesis of vitamins, stimulation of the immune system and supporting the digestion of hard-to-digestible food components such as fibers. The four largest bacterial strains are *Firmicutes*, *Bacteroidetes*, *Proteobacteria* and *Actinobacteria*, presenting 99% of gut bacteria (Eckburg and Relman 2007).

Gut microbiota composition is highly variable between individuals. The development of the gut microbiome starts already with the mode of delivery and is further influenced by nutrition, antibiotic treatments, drugs, stress and sleeping rhythm (Rodriguez et al. 2015, Tilg and Kaser 2011, Milani et al. 2017). A highly diverse gut microbiome indicates a healthy colonization of the gut, which describes the variety of microorganisms. A diverse microbiome is important to react and adapt to changing environmental conditions. Recently, gut microbiota diversity was found to be reduced in patients with chronic diseases (Gong et al. 2016, Li et al. 2019, Bajaj et al. 2019) and obese people (Mosca, Leclerc and Hugot 2016, Lozupone et al. 2012), suggesting a gut microbiome of diseased subjects cannot as easily adapt to environmental changes as a healthy microbiome.

Besides a reduced diversity, gut microbiota composition is associated with obesity. Transplantation of germ-free mice with an obese microbiome resulted in weight gain

whereas transplantation of a lean microbiome did not result in weight gain (Turnbaugh et al. 2008, Turnbaugh et al. 2006), suggesting the transplanted gut bacteria to be responsible for weight gain in the host. Moreover, obesity is associated with a different gut microbiota composition with an increased ratio of *Firmicutes* to *Bacteroidetes*, compared to lean subjects (Ley et al. 2005, Abdallah Ismail et al. 2011, Castaner et al. 2018). *Firmicutes* are involved in the digestion of plant-based carbohydrates and fermentable fibers, are able to convert them into short chain fatty acids (Shen, Gaskins and McIntosh 2014, Robert and Bernalier-Donadille 2003) and produce enzymes to split even indigestible carbohydrates such as cellulose (Robert and Bernalier-Donadille 2003), thereby additional energy from the diet is extracted.

Gut microbiota is described to be an important factor affecting energy absorption from the diet and also affecting energy storage (Backhed et al. 2004), having an impact on energy metabolism (Karlsson et al. 2013, Tremaroli and Backhed 2012) and body mass development (Backhed et al. 2004, Turnbaugh et al. 2006). Different proportions of different bacterial strains can alter the efficiency of digestion and absorption of food, like an increased abundance of *Firmicutes*. However, the distinct role of gut microbiota in the context of energy homeostasis, respectively RMR, has not been elucidated so far.

1.4 High and low metabolic rate organs as predictors of resting metabolic rate

Inter-individual variation of RMR is caused by sex, age, race, FFM and fat mass. It is well accepted that RMR decreases by 1 - 2% per decade with advancing age (Keys, Taylor and Grande 1973), which is thought to be due to loss of FFM, respectively muscle mass (Tzankoff and Norris 1977). FFM is the major variable contributing to RMR, due to its large size and high metabolic rate between 54 - 1841 kJ/kg, compared to adipose tissue with a metabolic rate of 11.3 - 14.3 kJ/day (Hallgren et al. 1989). Despite its low metabolic rate, adipose tissue is still an independent predictor of RMR (Johnstone et al. 2005), due to its large size, varying more than any other tissue. The contribution of fat mass to RMR increases with increasing fat mass (Bosy-Westphal et al. 2009b), explaining the increased RMR of obese subjects. However, at great adiposity with more than 40% of fat mass the contribution of fat mass to RMR is reduced, supposable due to a reduced specific metabolic rate of fat mass (Bosy-Westphal et al. 2009b).

FFM accounts for 30 - 60% of RMR variation and was therefore analyzed in several studies regarding its influence on RMR (Gallagher et al. 2006, Javed et al. 2010, Bosy-Westphal et al. 2004). FFM is positively associated with RMR stating an increasing FFM being associated with an increasing RMR. Nonetheless, the correlation of FFM and RMR is not constant, as RMR decreases with increasing body weight, in case of a disproportional

increase in muscle mass (Weinsier, Schutz and Bracco 1992). However, FFM is not a homogenous tissue and is resembled by high and low metabolic rate organs (Muller et al. 2002). High metabolic rate organs (HMRO) are heart, liver, kidneys, spleen and brain, characterized by a high metabolic rate like heart and kidneys having a metabolic rate of 1841 kJ/kg (Elia 1992, Muller et al. 2002, Weinsier et al. 1992). HMRO account for approximately 6% of FFM but contribute about 60 -70% to RMR (Figure 2) (Gallagher et al. 1998). In contrast, skeletal muscle as a low metabolic rate organ (LMRO), has a metabolic rate of 54 kJ/kg (Weinsier et al. 1992), represents more than 50% of FFM, but contributes only 22% to RMR (Gallagher et al. 1998). The decline in RMR associated with age is not just due to the decline in muscle mass, but also due to the decline of heart mass, respectively metabolic rate of the heart (Bosy-Westphal et al. 2003). Determining the size and calculating the respective metabolic rate of HMRO can explain additionally 5% of the inter-individual variation of RMR (Javed et al. 2010). However, measuring only organ size ignores the fact that the organ metabolic rate decreases with increasing organ mass (Wang et al. 2001). In addition, fat infiltration in non-adipose tissue might affect the specific organ metabolic rate (Perseghin et al. 2002, Bosy-Westphal et al. 2004), but the distinct consequences are not fully understood.

Commonly, high and low metabolic rate organs are combined in FFM and are not further differentiated. Measuring and adjusting RMR for organ sizes and specific metabolic rates of high and low metabolic rate organs can further elucidate the intra-individual variation of RMR.

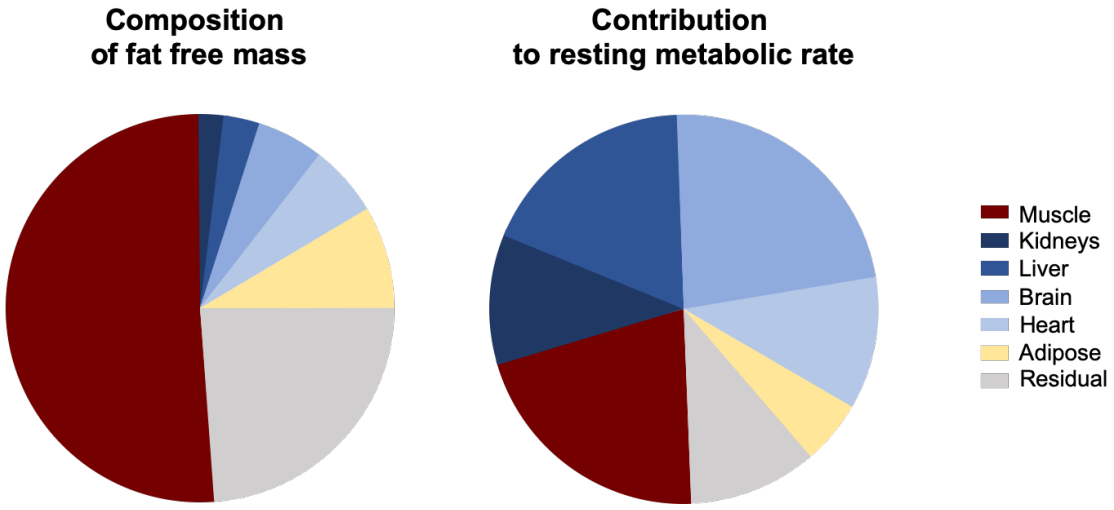

Figure 2: Contribution of organs and tissues to fat free mass and resting metabolic rate. The major component of fat free mass is skeletal muscle with 50.4 ± 4.1%, followed by adipose tissue with 5.2 ± 2.0%. Kidneys, liver, brain and heart constitute 6.7 ± 1.1% of fat free mass. The high metabolic rate organs kidneys, liver, brain and heart account together for 58.0 ± 4.8% of resting metabolic rate (kidneys ~ 10%, liver ~ 20%, brain ~ 22%, heart ~ 5%). Skeletal muscle contributes with 22.5 ± 3.4% and adipose tissue with 3.9 ± 1.3% to resting metabolic rate. Graph and values are adapted from Gallagher et al. (1998).

1.5 Objective of the present work

Obesity and its associated diseases are a global health problem with an increasing incidence. Obesity is usually the consequence of a chronic positive energy balance and treatment strategies include a reduction in energy intake and energy expenditure. Resting metabolic rate (RMR) is the major component of daily energy expenditure and therefore of special interest. However, RMR is characterized by a high inter-individual variation which cannot completely be explained by the variables sex, age, race, fat mass and fat free mass, leaving a residual variation unexplained.

The aim of this PhD thesis is to analyze the residual variation of RMR, regarding the influence of gut microbiota composition, liver metabolism and respiratory capacity of peripheral blood mononuclear cells (PBMCs).

A basis of this work was to generate a statistical model to obtain the residual variation of RMR. Anthropometric data and all raised clinical parameters from the cross-sectional *enable* study, consisting of 488 subjects, are used for model generation. Linear regression analysis is performed by stepwise including the variables to identify predictors and generate a model to predict RMR. This general model to predict RMR allows the examination of further parameters contributing to RMR, by adjusting RMR for the influencing variables and calculating the residual variation. First, the respiratory capacity of PBMCs is analyzed regarding their influence on the residual variation of RMR. Respiratory capacity of PBMCs is assessed by high-resolution respirometry of freshly isolated PBMCs from 179 subjects, a subsample of the *enable* cohort. Substrates, inhibitors and uncoupler can assess different respiratory states and determine mitochondrial activity of PBMCs. Second, the influence of gut microbiota composition on RMR variation is analyzed. Gut microbiota composition is determined in fecal samples by 16S rRNA gene sequencing of the whole *enable* cohort (488 subjects). For the analysis of gut microbiota composition on RMR variation, different statistical approaches will be applied like correlation analysis, linear regression analysis, principal component analysis and artificial neural networks. Third, liver activity will be analyzed regarding its influence on RMR variation. A pilot study with 30 subjects was conducted to determine liver activity by measuring liver fat content. Liver fat is measured by a combination of magnetic resonance imaging and magnetic resonance spectroscopy and analyzed regarding the influence on RMR variation by linear regression analysis.

2 Material and Methods

2.1 The *Enable* Cohort

Data was obtained from the cross-sectional *enable* study, consisting of healthy Caucasian subjects recruited at two study centers in Germany, Freising and Nuremberg between April 2016 and March 2018. Subjects were recruited in four age cohorts, aiming 100 children between 3 and 5 years, 100 adolescents and young adults between 18 and 25, 200 middle-aged adults between 40 and 65 years out of whom 100 subjects should be free of any chronic diseases, whereas the other half should be at risk for metabolic syndrome, defined by a waist circumference of > 102 cm in males and > 88 cm in females. For the fourth cohort the aim was to recruit 160 elderlies between 75 and 85 years, 100 subjects from Nuremberg and 60 from Freising. In all age cohorts the aim was to recruit an equal proportion of male and female. Exclusion criteria were: Body mass index (BMI) less than 18.5 kg/m^2 or greater than 35 kg/m^2, smoking, pregnancy and severe diseases. Elderly participants were included when they were free from severe chronic diseases, cognitive impairment and mobile.
Anthropometric parameters, body composition, resting metabolic rate and clinical parameters like blood pressure and blood parameters were measured according to standardized procedures. Gut microbiota composition was determined in fecal samples by 16S rRNA gene sequencing. Sequencing of 16S ribosomal RNA allows to determine and quantify the abundance of bacterial species in a given sample (Claesson, Clooney and O'Toole 2017). Processing and analysis of gut microbiota was performed at the Microbiome Core Facility, ZIEL - Institute for Food and Health, Technical University Munich. Further details about the study procedures and guidelines can be obtained from the local Clinical Trial Register (DRKS-ID: DRKS00009797).
The *enable* study was conducted according to the guidelines laid down by the Declaration of Helsinki. The ethics committees from the Technical University of Munich (number: 452/15) and the Friedrich-Alexander-University Erlangen-Nürnberg (number: 291_15 B) approved all the procedures.

2.2 Peripheral blood mononuclear cells

2.2.1 Isolation of peripheral blood mononuclear cells

The isolation of peripheral blood mononuclear cells (PBMCs) was conducted by density gradient centrifugation by using biocoll (Biochrom, L6115) for separation. The biocoll medium is a gradient medium denser than lymphocytes, monocytes and platelets but less dense than red blood cells and granulocytes. Accordingly, red blood cells will resemble on

the bottom of the tube, PBMCs in the interface between biocoll and diluted plasma and platelets in the top layer of diluted plasma.

Blood samples were taken in 9 ml lithium-heparine monovettes (Nümbrecht, Sarstedt) from an antecubital vein, in a fasted state of the subject. Isolation procedure was conducted directly after taking the blood sample. Blood was diluted with 8 ml PBS (1:1 ratio) and carefully transferred on top of 16 ml biocoll. To reduce the surface tension, first 2 drops of diluted blood were carefully run down the wall of the falcon tube than the residual diluted blood was gently transferred. The tubes were centrifuged for 25 min (400×*g*, accel 1, break 0). The thin PBMC layer between diluted plasma and biocoll was transferred by a sterile Pasteur-pipette (3 ml) to another tube, diluted in 50 ml PBS and centrifuged for 10 min (300×*g*, accel 5, break 9). This washing step was repeated with 30 ml PBS. Counting and assessing the viability of PBMCs was performed by trypan blue staining using an automated cell counter (Countess™, Invitrogen).

2.2.2 Chamber based respirometry to determine mitochondrial activity of PBMCs

Mitochondrial respiration of PBMCs was determined by high resolution respirometry at the Oxygraph-2k (Oroboros Instruments, Innsbruck, Austria). In preparation, respiration chambers were washed five times with demineralized water and calibrated with MiR05 buffer (Table 1) until oxygen concentration and oxygen consumption was stable for at least 30 min.

Table 1: Compounds and preparation of MiR05 buffer

Compound	Final concentration	Molecular weight g/mol	Volume for 1L	Source
EGTA	0.5 mM	340.4	0.190 g	Sigma E 4378
$MgCl_2 \cdot 6H_2O$	3 mM	203.3	0.610 g	Scharlau MA 0036
Lactobionic acid	60 mM	358.3	120 ml of 0.5 M	Aldrich 153516
Taurine	20 mM	125.1	2.502 g	Sigma T 0625
KH_2PO_4	10 mM	136.1	1.361 g	Merck 104873
HEPES	20 mM	238.3	4.77 g	Sigma H 7523
D-Sucrose	110 mM	342.3	37.65 g	Roth 4621.1
BSA	1 g/l		1 g	Sigma A 6003 fraction V

All listed compounds (except for lactobionic acid) were dissolved in 800 ml H_2O with a magnetic stirrer at 30°C. After adding 120 ml of K-lactobionic stock solution, pH was adjusted with 5 M KOH (Sigma, P 1767) to 7.1, at 30°C. At the end, the final volume was adjusted with H_2O to 1 L.

K-lactobionate stock solution was prepared by dissolving 35.83 g lactobionic acid in 100 ml H_2O, adjusting pH to 7.0 with KOH and adjusting to the final volume of 1 L with H_2O.

After Mir05 buffer was calibrated to oxygen concentration of air, 6 million cells in 100 µl MiR05 were transferred into each of the chambers. At first a stable basal respiration was obtained, approximately 5 - 10 min after applying the cells. Cells were permeabilized by digitonin, followed by a stepwise application of substrates, inhibitors and uncouplers (Table 2). To determine different respiratory states, two different protocols were established with a different order of substrates, inhibitors and uncouplers (Figure 14, Figure 15). At the end, non-mitochondrial respiration was determined by inhibiting complex III with antimycin A. Non-mitochondrial respiration was afterwards subtracted from all other values of the respiration measurement.

Table 2: Substrates, inhibitors and uncoupler of the respiration measurement

Chemical	Final concentration	Source
Digitonin	2 µM	Sigma-Aldrich D5628
Pyruvate	5 mM	Sigma-Aldrich P2256
Malate	5 mM	Sigma-Aldrich M9138
Succinate	5 mM	Sigma-Aldrich 398055
ADP	5 mM	Sigma-Aldrich A2754
Oligomycin	2.5 µg/ml	Sigma-Aldrich O4876
FCCP	0.5 µM	Sigma-Aldrich C2920
Rotenone	1 µM	Sigma-Aldrich R8875
Antimycin A	2.5 µM	Sigma-Aldrich A8674

2.3 Liver spectroscopy - Pilot study

2.3.1 Study design

The influence of liver fat on RMR variation was analyzed in a pilot study with 32 subjects. Proton density fat fraction (PDFF) was measured by using a proton coil to determine liver fat content. Subjects for this pilot study were recruited based on the phenotyping data from the *enable* platform Z, to obtain as far as possible a high amount of liver fat content. The primary selection criterium was visceral fat content, determined by body composition analysis, based on the hypothesis, that liver fat content correlates with the amount of visceral fat.

The examination of the subjects took place at two institutes of the Technical University of Munich. At the study center in Freising, the physical examination of height, weight, body composition, waist and hip circumference, blood sampling, blood pressure and body temperature was conducted. Additionally, RMR was measured by indirect calorimetry. These physical examinations were performed in addition to the phenotyping process of *enable*, since some subjects were phenotyped one year before. Liver fat content was assessed by magnetic resonance imaging (MRI) and magnetic resonance spectroscopy (MRS) at the Klinikum rechts der Isar, Department of Diagnostic and Interventional Radiology.

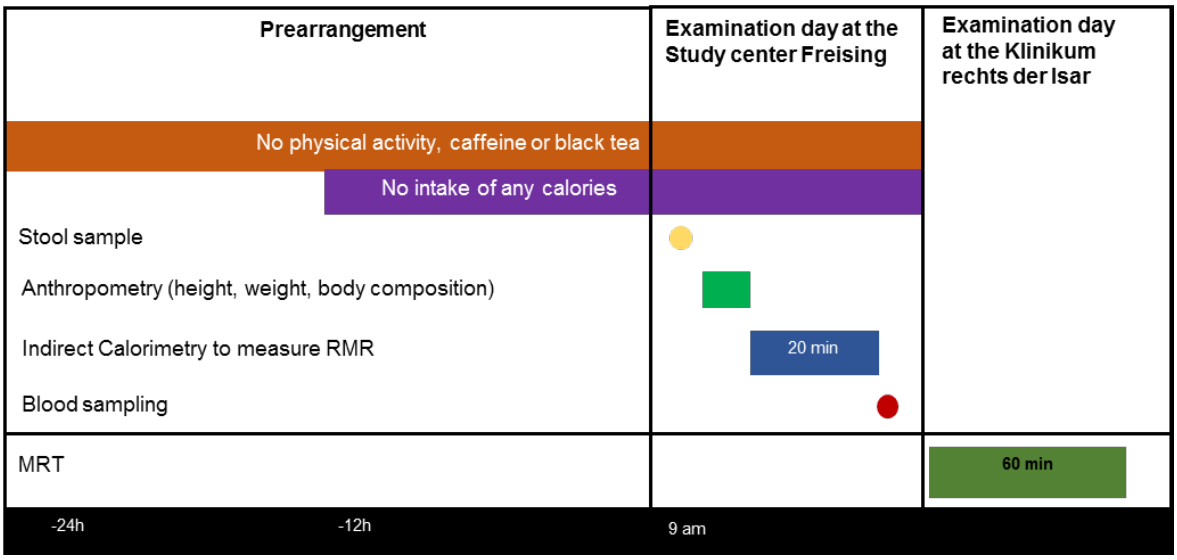

Figure 3: Flow chart of the pilot study to investigate liver fat on RMR variation. Depicted are the different time points for taking the stool sample (yellow), anthropometric measurement (bright green), indirect calorimetry (blue) and blood sampling (red). The MRT scan took place on another day, within two weeks bevor or after the physical examination at the study center in Freising.

2.3.2 Study population

Subjects for the pilot study were recruited from the middle-aged adults (40 - 65 years). For this pilot study 33 subjects were recruited, aiming an equal proportion of male and female. As subjects were recruited from the *enable* cohort, the same inclusion and exclusion criteria were applied, and some additional exclusion criteria due to contraindication of MRT analysis.

Exclusion criteria due to contraindication for the MRT scan:

- Implanted defibrillator
- Artificial heart valve

- Cardio seal
- Non safety MR-compatible aneurysm-clips
- Implanted magnetic metal part (screw, plaque from operations)
- Cochlear implant
- Metal splint or garnet splint
- Acupuncture needle
- Insulin pump
- Tattoos and permanent make-up
- Non removable piercings
- Lung diseases (e.g. asthma)
- Diseases of central nervous system (e.g. cerebrovascular insufficiency, multiple sclerosis, craniocerebral injury)
- Claustrophobia

2.3.3 Ethics

This pilot study was conducted according to the guidelines laid down by the Declaration of Helsinki. All procedures were approved by the ethics committee of the Technical University of Munich (number: 197/17 S). The study was registered at the German Clinical Trial Register (DRKS-ID: DRKS00013549). Subjects were included after written consent was obtained.

2.3.4 Phenotyping and body composition

Physical examination of the subjects was performed at the study center in Freising, after an overnight fast. Body weight and body composition, including fat mass and fat free mass (FFM), were measured by Bioelectrical Impedance Analysis (BIA), using a Seca medical Body Composition Analyzer 515 (Seca, Hamburg, Germany). Body composition by BIA is measured by an alternating current of 800 mA and 50 kHz, running through the body for 70 sec. Body composition can be determined by measuring resistance and reactance of the current, as the electrical current can flow through muscle tissue, but fat tissue creates a resistance. Body height (in cm, to the nearest of 0.1 cm) was measured without shoes using a stadiometer (Seca, Hamburg, Germany). Body temperature was measured with an ear thermometer by the nearest of 0.1°C (Braun Thermoscan, IRT 4020).

2.3.5 Indirect calorimetry to measure resting metabolic rate

Resting metabolic rate (RMR) was measured by indirect calorimetry using a face mask (Metalyzer 3B, Cortex Biophysik GmbH). To avoid any interactions with digestions or muscle activity, subjects were asked to avoid any physical activity on the day before the

examination. Subjects were asked to fast overnight (at least 8 - 10 hours) and not to consume any caffeinated products or any other drinks except for water. Subjects were accommodated in a quiet room, in a supine position for 10 min before the indirect calorimetry measurement was conducted for 20 min. During the measurement subjects were instructed not to move or fall asleep. RMR was determined by measuring O_2 (ml/min) consumption and CO_2 (ml/min) production rates every 5 -10 sec and converted to RMR by using the abbreviated Weir equation (Weir 1949):

RMR (kJ/day) = $((3.9 \times (VO_2) + 1.1 \times (VCO_2)) \times 1.44) \times 1.48 \times 4.184$

2.3.6 Blood sampling

Blood sampling was performed after indirect calorimetry measurement to avoid the excitement from blood sampling on RMR. Samples were taken from an antecubital vein by using a butterfly valve and were analyzed by the clinical laboratory service Synlab in Munich.

Table 3: Clinical blood parameters of the pilot study

Parameter	Sample	Center of Analysis
Fasted blood glucose	2.7 ml NaF	Synlab, Munich
Small blood analysis*	2.7 ml EDTA	
HDL, LDL	7.5 ml serum	
Triglycerides		
Cholesterol		
Creatinine		
CRP sensitive		
Samples for possible additional analysis	9 ml EDTA without gel	Science Lab
	7.5 ml serum	
Total blood volume	**29.4 ml**	

* Erythrocytes, hemoglobin, MCV, hematocrit, MCHC, RDW, platelets, leukocytes

2.3.7 Liver fat determined by magnetic resonance spectroscopy

To determine liver fat, visceral (VAT) and subcutaneous (SAT) adipose tissue, the abdominal region of subjects was scanned on a 3.0 T whole-body scanner (Ingenie 3.0 T, Philips Healthcare, Best, Netherlands) with an anterior and posterior coil arrays, at the Klinikum rechts der Isar, Department for Diagnostic and Interventional Radiology.

Measurement was performed by a set of axial two-point Dixon images with the imaging parameters: TR = 4.0 ms, T1/T2 = 1.32/2.6 ms, flip angle = 10°, bandwidth = 1004.0

Hz/pixel, acquisition voxel size = 1.5 × 2 × 5 mm^3, 44 slices in 2 stacks. To minimize breathing artifacts, scans were performed in a single breath-hold. Analysis of SAT and VAT was performed by a semi-automated segmentation tool with Matlab (The MathWorks, Inc., Natick, Massachusetts, USA, 2016b), developed at the Department of Interventional Radiology.

Liver fat was determined by PDFF at a single-voxel region of interest with 20 mm diameter, at nine liver segments. Presented is the mean PDFF of all nine liver segments.

2.4 Statistical analysis

Linear regression modeling was performed by stepwise inclusion of the variables based on increasing R^2 and decreasing Akaike-Information Criterion (AIC), to determine best fitting model. AIC determines the quality of a statistical model by calculating the goodness of fit and the simplicity of the model, under- and overfitting are thereby taken into consideration. Analysis of linear regression and mixed effect models was performed by using RStudio (RStudio, Inc., Boston, MA, 2016b). Any other statistical analysis was performed by GraphPad Prism 6 (GraphPad Software, Inc., La Jolla, USA). Data are presented as means ± standard deviation (SD) and *P*-values < 0.05 were considered significant. Heat-maps were generated in RStudio with level plot (lattice). All other graphs were created by GraphPad Prism 6.

The Tanita-balance, scale to measure body composition, has embedded an equation to predict RMR with five constants, which are not specified in the corresponding patent (EP1195138). Since all other variables of the equation were known, the constants were mathematically determined with an independent cohort of 20 male individuals by using Matlab (The MathWorks, Inc., Natick, Massachusetts, USA, 2018b).

Analysis of the gut microbiota profile was performed with RStudio using the Rhea script (Lagkouvardos et al. 2017). Heat-maps and principal component analysis were performed with RStudio. Neural network analysis was calculated with Matlab (The MathWorks, Inc., Natick, Massachusetts, USA, R2018b) by using the Levenberg-Marquardt algorithm with one hidden layer of 10 neurons (Figure 4).

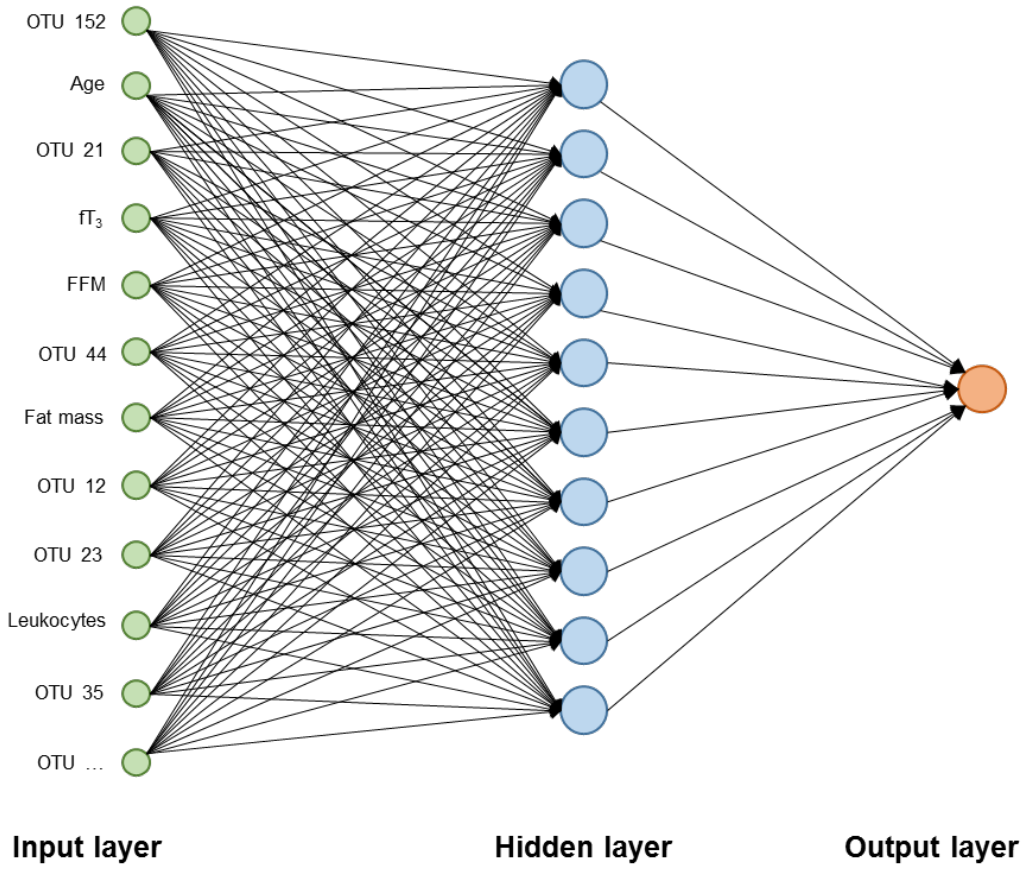

Figure 4: Schematic overview of a neural network structure. The input layer presents alls variables used by the neural network to calculate the output layer. The neural network consisted of one hidden layer with ten neurons, 'comunicating' back and forth with the input layer to calculate the output layer, based on the Levenberg-Marquardt algorithm. Each arrow presents the connection of the output and the input of the other layer. In this example, the output layer is the prediction of RMR by the anthropometric and clinical parameters. The presented variables of the input layer are only examples, as all variables cannot be depicted in this graph. For proof of principle of the neural network the variables accounting for the inter-individual variation of RMR, FFM, fat mass, body temperature, fT_3, Leukocytes, Creatinine, MCHC, systolic blood pressure and heart rate, were mixed among all variables of the gut microbiota to predict RMR.

3 Results

3.1 Linear regression models to predict resting metabolic rate

Resting metabolic rate (RMR) is with 60 - 70% the major component of daily energy expenditure. Being the biggest component, RMR plays an important role in determining the energy requirement in obesity treatment and clinical studies. Measuring RMR is a complex and time-consuming method, which requires strictly standardized conditions. Therefore, several equations have been generated to predict RMR, like the equation from Harris-Benedict (Harris and Benedict 1918) and World Health Organization (WHO) (WHO 1985). However, there is a high inter-individual variation in RMR, and the precision of these equations varies.

Well-known factors contributing to the variation of RMR are sex, age, height, weight, fat mass, and fat free mass (FFM). Adjusting RMR for these influencing variables is a prerequisite to compare individuals independent from their physical characteristics and body composition. These predictors can be used to calculate RMR, if a measured RMR is not available. The aim of this thesis was to generate a new prediction equation, for general use in clinical studies. Aside from that, the prediction equation should serve as a basis for the analysis of liver metabolism, gut microbiota composition and respiratory capacity of peripheral blood mononuclear cells (PBMCs) on RMR variation. For the general linear regression model, the *enable* cohort was used, consisting of four different age groups between 3 and 85 years.

3.1.1 Physical characteristics of the *enable* study cohort

Overall 488 subjects (247 male, 241 female) of four age cohorts were recruited at two study centers, Freising and Nuremberg (Table 4). At the study center in Freising, 34 children consisting of 19 boys and 15 girls, 94 adolescents and young adults with 46 male and 48 female subjects, 202 middle aged adults with an equal distribution of male and female subjects were recruited. Subjects of the elderly cohort were recruited in Freising and Nuremberg. Altogether, 157 elderly subjects were phenotyped (100 Nuremberg, 57 Freising), consisting of 80 male and 77 female subjects. Subjects of the *enable* study were healthy, represented in a mean BMI of 25.24 kg/m^2. In the cohort of middle-aged adults, the mean BMI with 27.49 kg/m² was slightly elevated due to the aim to recruit half of the middle-aged adults with the risk for metabolic syndrome. Nevertheless, these subjects did still meet the inclusion and exclusion criteria and were therefore free of any severe or chronic diseases.

Table 4: Physical characteristics of the *enable* cohort

	All			**Children**			**Adolescents**			**Adults**			**Elderly**		
	(N=247 M, 241 F)			**3-5 years (N=19 M, 15 F)**			**18-25 years (N=46 M, 48 F)**			**40-65 years (N=101 M, 101 F)**			**75-85 years (N=80 M, 77 F)**		
	Mean	±	SD	Mean	±	SD	Mean	±	SD	Mean	±	SD	Mean	±	SD
Age (years)	51.5	±	24.0	4.3	±	0.9	22.2	±	2.0	52.4	±	6.9	78.2	±	2.7
Weight (kg)	72.4	±	21.2	18.1	±	3.9	68.2	±	11.7	82.2	±	16.5	74.0	±	13.5
Height (cm)	166.9	±	18.5	109.4	±	9.4	175.5	±	9.7	172.6	±	9.2	166.9	±	9.0
Fat mass (kg)	23.4	±	11.7	3.4	±	1.8	14.3	±	6.2	28.1	±	11.0	27.2	±	8.2
FFM (kg)	49.2	±	14.5	14.7	±	3.2	53.9	±	11.9	54.1	±	11.0	47.4	±	10.1
Body temperature (°C)	36.4	±	0.4	36.8	±	0.4	36.6	±	0.3	36.3	±	0.3	36.4	±	0.4
BMI (kg/m^2)	25.2	±	5.2	14.9	±	1.6	22.1	±	2.5	27.5	±	4.5	26.5	±	4.0
RMR (kJ/day)	6577.0	±	1353.6	4273.2	±	727.4	7022.0	±	1174.1	6969.5	±	1222.6	6315.7	±	1140.6

3.1.1.1 Comparison of body composition determined by different devices

Fat free mass and fat mass are two variables contributing most to the variability of RMR. Determining body composition is therefore of great importance to analyze the variability in RMR. Body composition was determined with bioelectrical impedance analysis by two different devices. At the study center in Freising, the Seca balance and the BodPod device were used to measure body composition of the adolescents, middle aged adults and elderly, whereas for the children only the BodPod device was used. At the study center in Nuremberg subjects were only measured by the Seca balance. To analyze if there is a difference in measuring body composition, the cohorts of adolescents, middle aged adults and elderly (Freising) were compared in body weight and body composition determined by the two devices. Comparing the Seca and BodPod device, no significant differences were detected for the body weight (data not shown), fat mass and FFM ($P < 0.001$) (Figure 5).
In conclusion, the two devices determine in equal manner fat mass and FFM since there were no significant differences in body weight and composition. In the following analysis, data about body composition was therefore not corrected for the different devices.

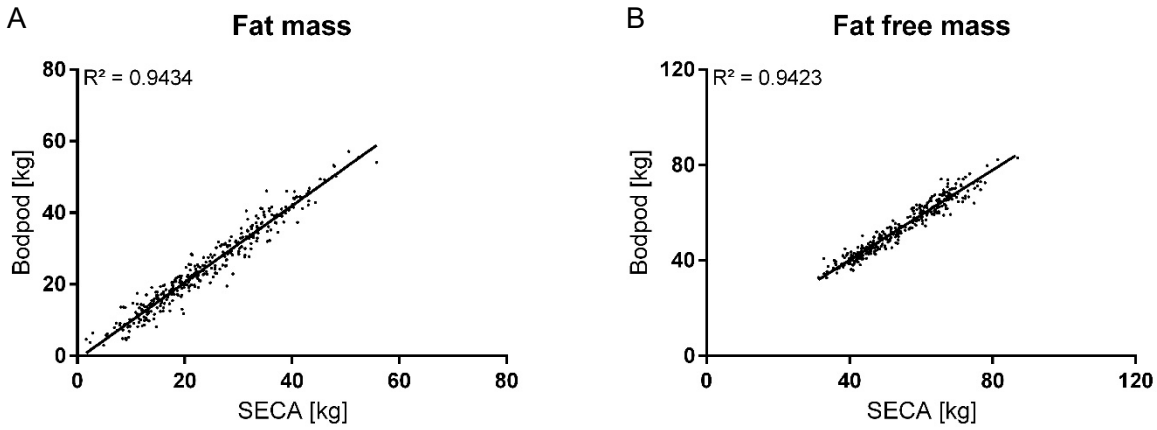

Figure 5: Body composition determined by BodPod and Seca. Comparison of (**A**) fat mass and (**B**) FFM determined by Seca and BodPod, N = 353. No significant differences ($P < 0.001$) in fat mass and FFM measured by Seca and BodPod.

3.1.2 Mixed effect model to predict resting metabolic rate

Resting metabolic rate can be calculated by mathematical models, based on the variables determining RMR. The Harris-Benedict (Harris and Benedict 1918) and WHO (WHO 1985) equation were developed decades ago and primarily focus on weight, height and age. Nowadays variables like sex, age, fat mass and FFM are taken into consideration when predicting RMR (Gallagher et al. 2006, Muller et al. 2004). The aim of this study was to generate a new equation to predict RMR. This equation should be applicable for the general use in clinical studies and a wide range of subjects.

All *enable* cohorts, ranging in age from 3 - 85 years, were used to generate a prediction equation by linear regression analysis. By stepwise including parameters into the regression analysis, factors contributing to the variation in RMR were identified. Potential predictors contributing to RMR were body mass, height, sex, age, fat mass, FFM and body temperature. Regression analysis started with the strongest predictor of RMR the FFM, which accounted for 74% of the variation. By adding body temperature, R^2 improved to 0.7556. In the next steps first sex than fat mass and age were added to the regression analysis, resulting in a R^2 of 0.7942 (Table 5). Selection criteria for the improved model was an increasing R^2 and decreasing Akaike information criterion (AIC). The AIC determines the quality of a statistical model by calculating the goodness of fit and the simplicity of the model, under- and overfitting are thereby taken into consideration.

Table 5: Modeling of regression analysis to predict RMR

Step	Variable	Multiple R^2	Adjusted R^2	AIC
1	FFM (kg)	0.7443	0.7438	7730.675
2	Body temperature (°C)	0.7566	0.7556	7708.790
3	Sex	0.7613	0.7598	7701.284
4	Fat mass (kg)	0.7763	0.7745	7671.671
5	Age (years)	0.7963	0.7942	7628.091
6	Random factor = Child	0.7994		7590.890

Adjusted R^2 is adjusted for the number of predictors in the model.

Having a differentiated look at the measured and predicted RMR of the four age cohorts, a difference in the slopes can be observed (Figure 6). The three adult cohorts, adolescents, middle-aged and elderly have almost the same slope, whereas children have a different slope (Figure 6). Including children as a random factor, improved the slope and brought it in the direction of the adult cohorts (Figure 6), resulting in a mixed effect model. The random

factor “child” was only referred to FFM. The mixed effect model explained 79.9% of variation in RMR by five variables (Table 6) with the following equation:

RMR (kJ/day) = - 7540.6 - 263.3 × **sex** - 7.8 × **age**(years) + 25.8 × **fat mass**(kg) + (79.2 + (**child**) × 34.4)) × **FFM**(kg) + 277.9 × **body temperature**(°C)

Sex: male = 0, female = 1. Random factor child: Child (3-5 years) = 1, Adult (18-85) = 0, referred to FFM

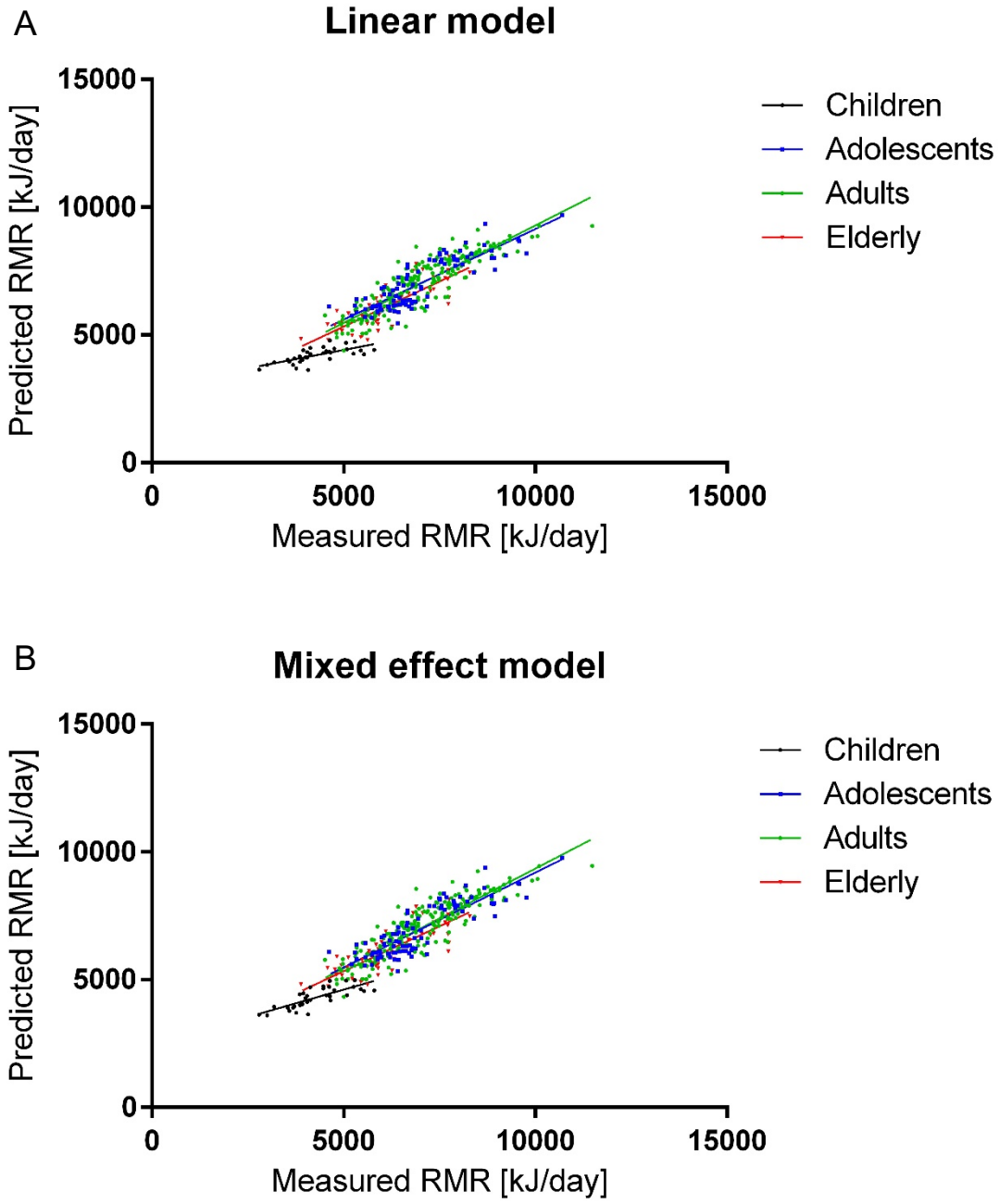

Figure 6: Measured and predicted RMR of the four *enable* cohorts. (A) Predicted RMR is calculated by linear regression analysis with the variables sex, age, fat mass, FFM and body temperature (N = 488). Each cohort is presented in a different color **(B)** Predicted RMR is calculated by a mixed effect model with the fixed factors sex (male = 0, female = 1), age, fat mass, FFM, body temperature and the random factor "child", which is referred to FFM (N = 488). Cohorts are differentiated by colors.

A detailed look at the coefficients of the individual variables cooperated in the mixed effect model illustrates their positive or negative contribution to RMR (Table 6). Sex and age have a negative coefficient, meaning female have a lower RMR than male, respectively describing the decline of RMR with increasing age. Fat mass, FFM and body temperature have all positive coefficients, presenting an increase in fat mass, FFM and body temperature being associated with an increase in RMR. Different coefficients of FFM were determined for children and adults, since the random factor "child" was related to FFM. This means that in children FFM has a higher impact on RMR than in adults (Table 6).

Table 6: Mixed effect model to predict RMR

Model and variable	Coefficient	Std. Error	*P-value*	R^2
Model 1: RMR = sex[1] + age + fat mass + FFM + body temperature				**0.7994**
Intercept	-7540.6	2968.0	0.011	
Sex	-263.3	94.2	0.005	
Age (years)	-7.8	1.7	0.000	
Fat mass (kg)	25.8	3.1	0.000	
FFM (kg)				
Child[2]	113.6	21.2	0.000	
Adult	79.2			
Body temperature (°C)	277.9	80.5	0.000	

N = 488, [1]Male = 0, Female = 1, [2]Child (3 - 5 years)

Comparing predicted and measured RMR can visualize the precision of an equation. Predicting RMR with the new established equation (Table 6) and correlating it to the measured RMR resulted in a R^2 of 0.7994, as calculated by the regression analysis with the mixed effect model (Figure 7). Presented is a simple statistical model for the general use to predict RMR of a wide range of age, based on five anthropometric and clinical parameters. Adjusting RMR for sex, age, fat mass, FFM and body temperature reduced the variation in RMR, remaining a variation about 20% unexplained (Figure 7). The residual variation of RMR was further elucidated in a more complex statistical model.

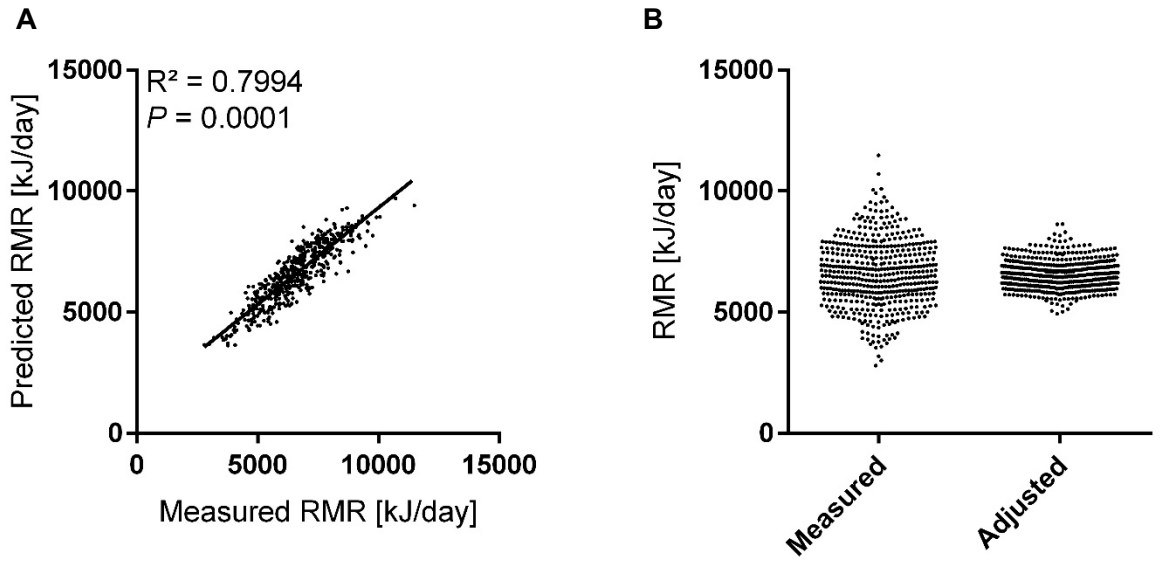

Figure 7: Measured, predicted and adjusted RMR with the new generated equation. (A) RMR is predicted by the mixed effect model with the variables sex, age, fat mass, FFM, body temperature and the random factor 'child'. Predicted RMR is correlated with measured RMR (N = 486). **(B)** Measured and adjusted RMR presenting the remaining variation in RMR after adjusting for the variables sex, age, fat mass, FFM and body temperature with the coefficients calculated by the mixed effect model, N = 486.

3.1.3 Linear regression analysis to elucidate the influence of blood parameters on the inter-individual variation of resting metabolic rate

Inter-individual variation of RMR is mainly determined by sex, age, fat mass, and body temperature. Even after adjusting RMR for these variables a variation of 20% remains unexplained.

To further analyze the variation in RMR, beyond the previous explained factors (sex, age, fat mass, body temperature) a subpopulation of the *enable* cohort was used. RMR was analyzed regarding the influence of clinical blood parameters and blood pressure. Since no blood samples were taken from the children, a subpopulation was used for this analysis consisting of the three adult cohorts' adolescents, middle-aged and elderly. In total 452 subjects (225 male, 227 female) were analyzed. Physical characteristics of this subpopulation are described in Table 7.

Table 7: Physical characteristics of the *enable* subpopulation

	All (N=452)	Female (N=227)	Male (N=225)
	Mean ± SD	Mean ± SD	Mean ± SD
Age (years)	55.1 ± 20.8	54.3 ± 21.1	56.0 ± 20.6
Height (cm)	171.1 ± 9.7	164.5 ± 6.9	177.7 ± 7.4
Weight (kg)	76.4 ± 15.6	68.4 ± 13.1	84.5 ± 13.6
Body temperature (°C)	36.4 ± 0.4	36.4 ± 0.3	36.4 ± 0.4
Fat mass (kg)	24.5 ± 9.9	25.8 ± 10.2	23.1 ± 9.3
FFM (kg)	52.2 ± 11.6	42.8 ± 6.0	61.7 ± 7.5
RMR (kJ/day)	6748.9 ± 1229.6	5951.6 ± 803.7	7553.3 ± 1048.0
Leukocytes (N/nl)	5.8 ± 1.5	6.0 ± 1.6	5.6 ± 1.3
fT_3 (pg/ml)	3.2 ± 0.4	3.1 ± 0.4	3.4 ± 0.4
Creatinine (mg/dl)	0.8 ± 0.2	0.7 ± 0.1	0.9 ± 0.2
MCHC (g/dl)	34.1 ± 0.6	33.8 ± 0.8	34.4 ± 0.9
Systolic blood pressure (mmHg)	130.3 ± 19.2	126.4 ± 20.4	134.3 ± 17.2
Diastolic blood pressure (mmHg)	83.0 ± 9.7	81.8 ± 9.8	84.1 ± 9.5
Heart rate (bpm)	62.2 ± 9.9	63.8 ± 10.1	60.5 ± 9.4

To analyze the effect of blood parameters and blood pressure on RMR the previous developed mixed effect model was used as a baseline to predict RMR (Table 6). The variables, from the mixed effect model, sex, age, fat mass, FFM and body temperature were used in a linear regression analysis to predict RMR of the subpopulation (Table 8). Thereby, non-significant predictors like sex (P = 0.057) were excluded, resulting in model 2. In this subpopulation the effect size of fat mass, FFM and body temperature was stronger than in the mixed effect model and therefore rendered sex to be a non-significant predictor of RMR. Non-significant variables in a linear regression model hold the risk of overfitting and are therefore excluded. The initial model (model 2), includes the variables, age, fat mass, FFM and body temperature, which explain 74.3% of the variability in RMR.

The effect of blood parameters and blood pressure on RMR was analyzed with the residual variation after eliminating the effect of age, fat mass, and FFM and body temperature. The residual variation of RMR presents the remaining variation between the measured and predicted RMR, which cannot be explained by the variables age, fat mass, FFM and body temperature. Identifying possible candidates influencing RMR variation, a correlation analysis was performed with the residual variation and all available blood parameters, which were raised in the *enable* phenotyping process (Table 9). After correcting for multiple testing according to Benjamini-Hochberg the residuals correlated significantly with fT_3 (P = 0.0002),

leukocytes (P = 0.011), creatinine (P = 0.01), MCHC (P = 0.002), systolic blood pressure (P = 0.0005), heart rate (P = 0.01) and diastolic blood pressure (P = 0.0018) (Table 9). Blood parameters and blood pressure significantly correlating with the residuals of RMR were additionally analyzed in an individual linear regression analysis to obtain a more detailed overview (Figure 8). To further analyze if blood parameters could improve the linear regression model and explain part of the residual variation in RMR, blood parameters were included in the linear regression model (Table 8). In this step, only blood parameters significantly correlating with the residuals of RMR were added to the regression analysis. The clinical blood parameters fT_3 (P < 0.0001), leukocytes (P < 0.0001), creatinine (P = 0.009), MCHC (P = 0.017), systolic blood pressure (P < 0.001) and heart rate (P = 0.001) appeared to be significant predictors of RMR and accounted for additional 3.5 percentage points of the variation in RMR. Whereas diastolic blood pressure was not a significant predictor of RMR (P = 0.42, data not shown) and was therefore excluded in the further analysis. By including the blood parameters and blood pressure in the linear regression model the coefficient of determination was improved from 0.7433 to 0.7777 and the AIC decreased from 6934.5 to 6876.7 (Table 10).

Table 8: Linear regression models and blood parameters.

Model and variable	Coefficient	Std. Error	*P-value*	R^2
Model 1: RMR = sex+ age + fat mass + FFM + body temperature				**0.745**
Intercept	-7652.3	3218.5	0.018	
Sex	-263.5	138.0	0.057	
Age (years)	-7.4	2.1	0.000	
Fat mass (kg)	21.3	4.2	0.000	
FFM (kg)	77.2	6.1	0.000	
Body temperature (°C)	285.5	86.7	0.001	
Model 2: RMR = age + fat mass + FFM + body temperature				**0.743**
Intercept	-8593.3	3176.1	0.007	
Age (years)	-4.6	1.7	0.005	
Fat mass (kg)	16.4	3.4	0.000	
FFM (kg)	87.5	2.7	0.000	
Body temperature (°C)	292.1	86.4	0.000	
Model 3: RMR = fat mass + FFM + body temperature + blood pressure + blood parameter + heart rate				**0.777**
Intercept	-11276.5	3349.8	0.000	
Age (years)	-6.8	2.0	0.000	
Fat mass (kg)	13.1	3.3	0.000	
FFM (kg)	85.5	3.2	0.000	
Body temperature (°C)	217.6	84.0	0.009	
fT_3 (pg/ml)	243.2	79.6	0.002	
Leukocytes (N/nl)	51.7	20.4	0.011	
Creatinine (mg/dl)	-626.6	212.1	0.003	
MCHC (g/dl)	102.7	36.5	0.005	
Systolic blood pressure (mmHg)	7.9	1.8	0.000	
Heart rate (bpm)	9.6	3.0	0.001	

Table 9: Correlation analysis of blood parameters and residuals of RMR

Blood parameter	R^2	*P-value*
Free Triiodothyronine (fT_3)	0.0302	0.0002*
Mean Corpuscular Hemoglobin Concentration (MCHC)	0.0207	0.0022*
Creatinine	0.0144	0.0108*
Leukocytes	0.0143	0.0113*
Red Cell Distribution Width (RDW)	0.0114	0.0234
Hemoglobin	0.0098	0.0362
Free Thyroxine (fT_4)	0.0002	0.7250
Thyroid-Stimulating Hormone (TSH)	0.0000	0.8929
Insulin	0.0005	0.6356
C-Reactive Protein	0.0006	0.5998
Ferritin	0.0008	0.5465
Iron	0.0068	0.0806
Uric acid	0.0009	0.5132
Urea	0.0035	0.2057
Low-Density Lipoprotein (LDL)	0.0008	0.5369
High-Density Lipoprotein (HDL)	0.0001	0.8289
Triglycerides	0.0000	0.9795
Cholesterol	0.0022	0.3140
Fasted blood glucose	0.0010	0.4972
Lactic Acid Dehydrogenase (LDH)	0.0026	0.2735
Gamma-Glutamyl Transferase (GGT)	0.0018	0.3635
Glutamate-Pyruvate Transaminase (GPT)	0.0000	0.9992
Glutamate-Oxaloacetate Transaminase (GOT)	0.0035	0.2063
Packed cell volume	0.0041	0.1746
Mean corpuscular volume (MCV)	0.0000	0.8801
Mean Hemoglobin concentration/ erythrocyte (HBE)	0.0012	0.4608
Systolic blood pressure	0.0272	0.0005*
Diastolic blood pressure	0.0216	0.0018*
Heart rate	0.0276	0.0004*

*significant according to Benjamini-Hochberg correction for multiple testing

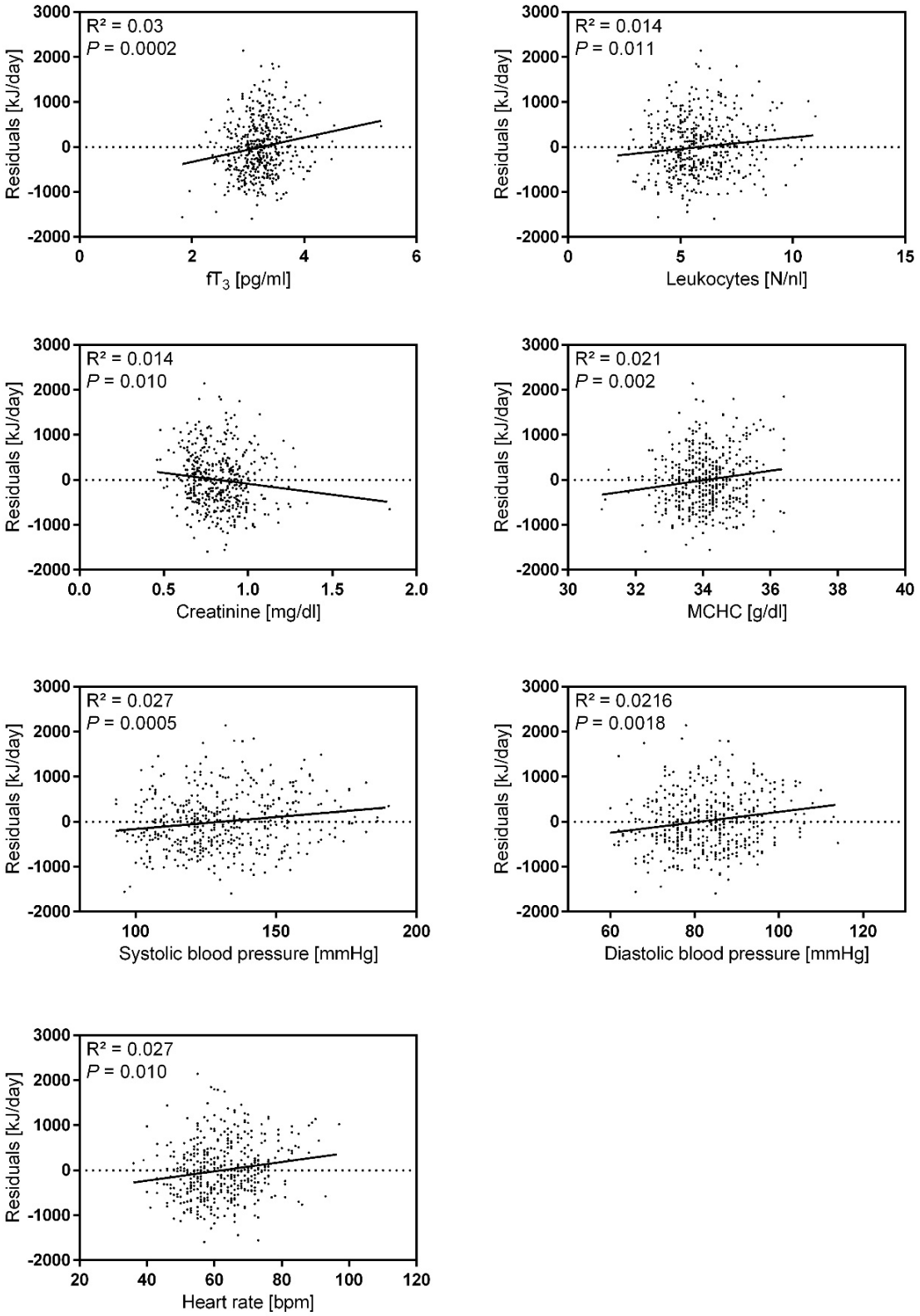

Figure 8: Blood parameters and pressure correlating with the residuals of RMR. Presented are only blood parameters and blood pressure significantly correlating with the residuals of RMR, after correcting for multiple testing according to Benjamini-Hochberg. Residuals were calculated with the variables age, fat mass, FFM and body temperature and the coefficients of the linear model 2 (**Table 8**), N = 446-449.

Table 10: Linear regression modeling

Model	Variable	Multiple R^2	Adjusted R^2	AIC
2	RMR = age + fat mass + FFM + body temperature	0.7456	0.7433	6934.5
3	RMR = age + fat mass + FFM + body temperature + fT_3 + leukocytes + creatinine + MCHC + systolic blood pressure + heart rate	0.7828	0.7777	6876.7

The correlation analysis of clinical blood parameters, blood pressure and the residuals of RMR revealed new variables directly correlating with RMR. The impact of these variables on RMR was not only due to the interaction with other factors contributing to RMR, because their influence on RMR was analyzed after removing the effect of known influencing variables.

RMR is highly variable between individual subjects and is influenced by several factors. In the regression analysis the contribution of the individual factors was determined by the coefficient, for example if a variable is contributing positively or negatively to RMR. Thus, the coefficient makes it difficult to visualize the relative contribution of the individual variable. Therefore, the relative contribution of the variables contributing to RMR was calculated.

Part of the residual variation was set to be due to technical and biological variation. Intra-individual variation was determined in a separate small cohort of 20 male subjects in the age between 18 and 40 years (Schicker 2017). Within three weeks, three repeated measurements were conducted to determine intra-individual variation. Across the three weeks the mean RMR of these 20 male subjects was 8994.07 kJ/day with a SD of 1061.97 kJ/day, resulting in a mean CV_{intra} of 4.6 $\pm$ 2.3%. The variation within one subject was used to calculate the overall mean variation within a subject. The mean within subject variation was used to calculate the contribution to the overall inter-individual variation by dividing the square of within subject variation by the SD of the inter-individual variation $(219.15^2)/(1061.97^2) = 0.043$. Meaning that 4.3% of the inter-individual variation was due to technical and biological intra-individual day-to-day variation.

First, the contribution of the variables incorporated in the mixed effect model was calculated. In the mixed effect model FFM is the strongest predictor and the biggest contributor to RMR with 55.88%. The second strongest predictor is fat mass, contributing with 11.63% to RMR. Body temperature and age contribute almost equally to RMR with 5.27% and 5.07% (Figure

9). Including the intra-individual variation to the factors contributing to the variation of RMR, 15.79% of RMR variation remained unexplained.

In a second step the relative contribution of the variables from the linear regression model with blood parameters and blood pressure was calculated (model 3, Table 8). FFM was still the strongest predictor of RMR, followed by fat mass. However, the effect of both variables was reduced by including blood parameters and blood pressure to the regression analysis. Among the clinical parameters fT_3 and creatinine are the strongest variables contributing to RMR, followed by systolic blood pressure. Creatinine, fT3 and systolic blood pressure are even stronger predictors as fat mass, age and body temperature. Considering 4.3% of the variation be due to technical and intra-individual variation, 18% of variation in RMR remained unexplained, presenting an improvement of the model by 3.4% (Figure 9), compared to the linear regression model without blood parameters and blood pressure Figure 10, B).

The major part of RMR is determined by FFM and fat mass. Effect of both variables was reduced by including additional parameters to the regression model. This implies an interaction of FFM and fat mass with the included blood parameters and blood pressure and implies an indirect contribution of FFM and fat mass to RMR variation.

FFM and fat mass are both heterogeneous tissues. The reduced effect size by including the clinical parameters demonstrates that the contribution of FFM and fat mass to RMR variation is not only due to the mass of these tissues, but rather due to the different components of these tissues. To analyze the interaction of the variables cooperated in the linear regression mode to predict RMR a correlation analysis was performed (Figure 10). This presented an interaction of FFM with MCHC, creatinine and fT_3. Fat mass showed a positive correlation with systolic blood pressure, heart rate and leukocyte number. The correlation analysis demonstrated the interaction of the individual variables and explained the reduced effect size of FFM and fat mass by including additional variables to the linear regression model.

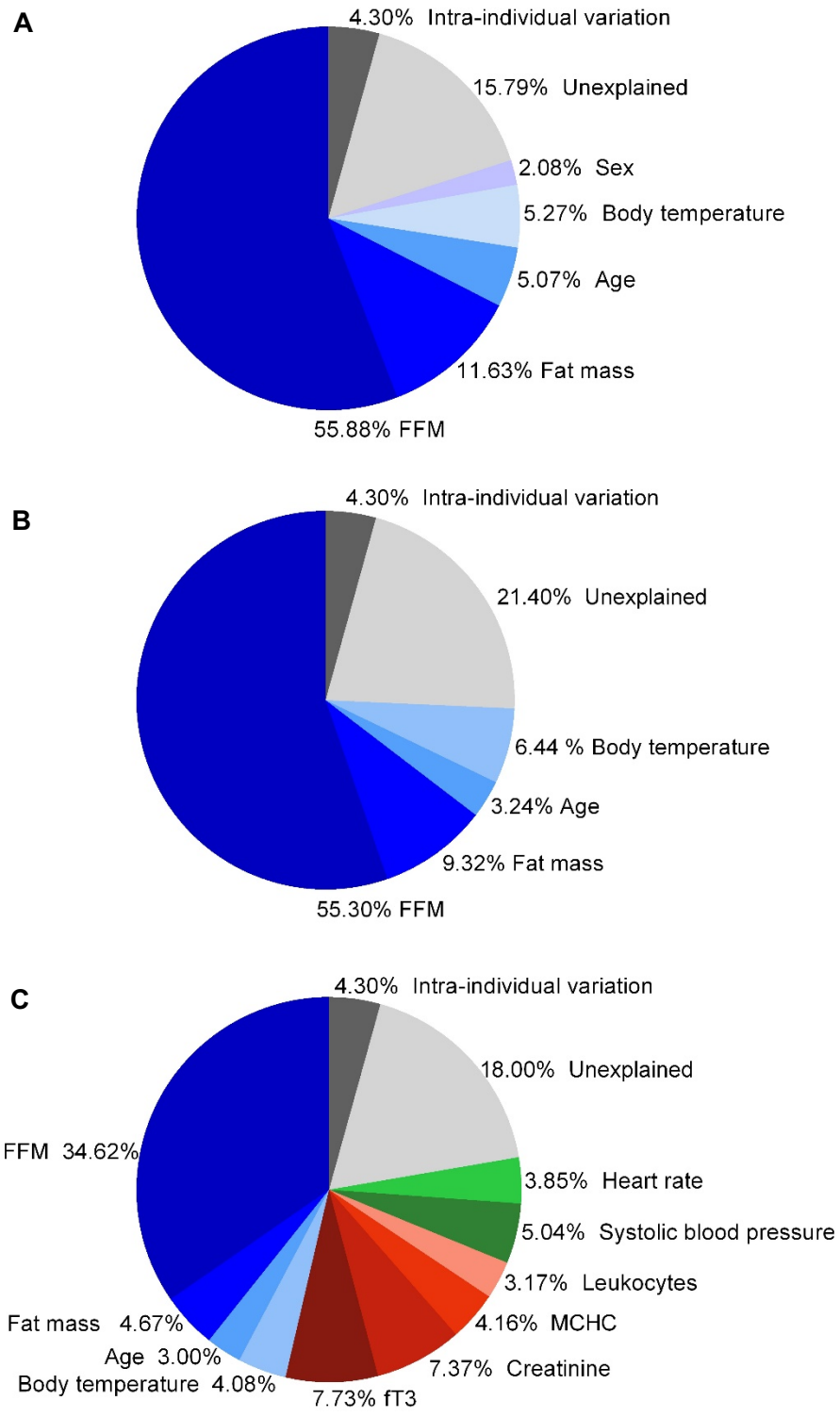

Figure 9: Relative contribution of the different variables influencing RMR variation.(**A**) Variables cooperated in the mixed effect model (model 1, **Table 6**). Contribution of the variables to RMR was calculated with the coefficient from the mixed effect model, N = 488. (**B**) Variables of the linear regression model 2 of the three adult cohorts N = 452. (**C**) Variables of the linear regression model 3 (**Table 8**). Particular contribution was calculated by the coefficient of the linear regression analysis, N = 452. (**A-C**) Intra-individual variation presents biological and technical variation, measured and calculated in a separate small study cohort of 20 male subjects.

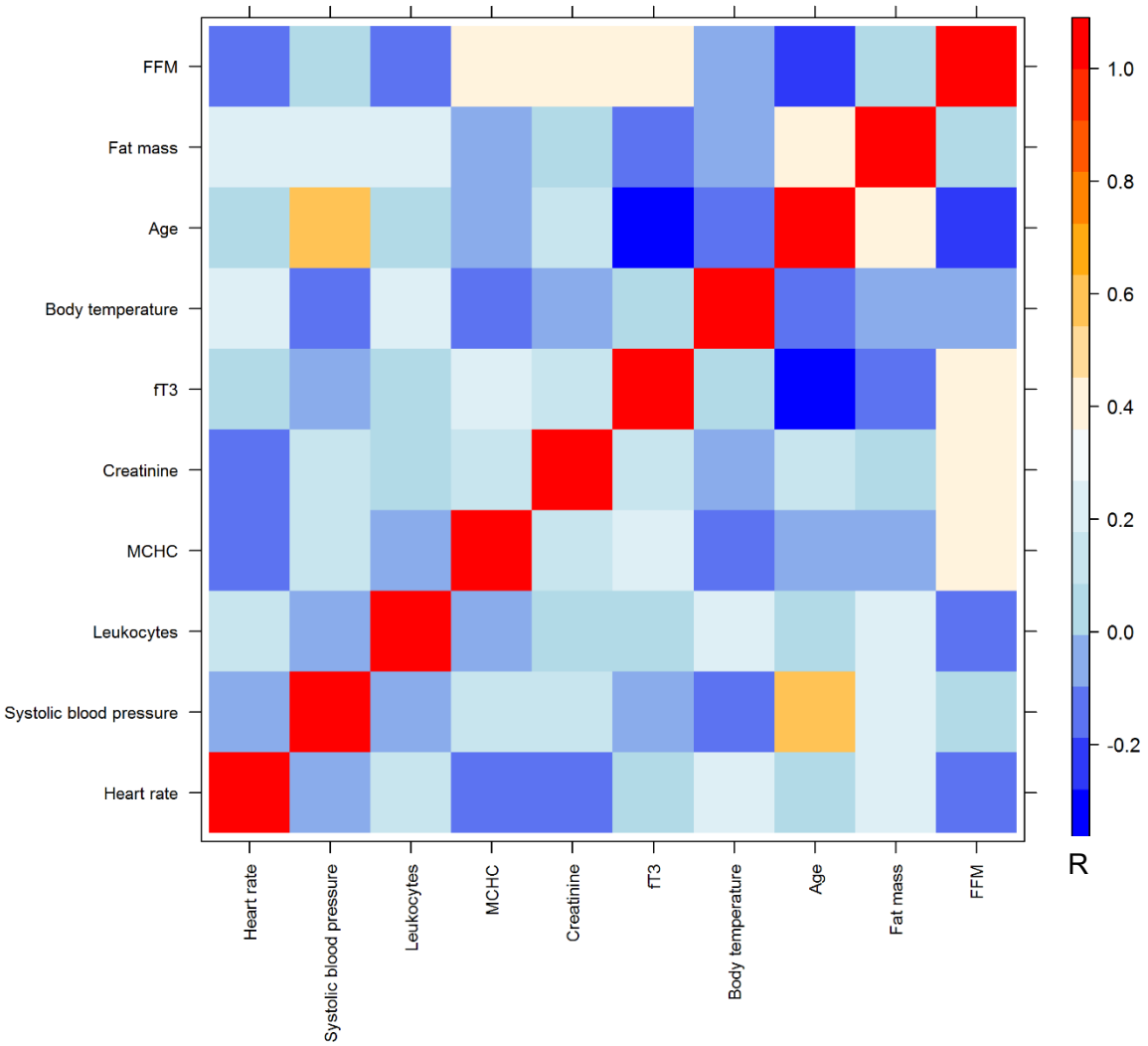

Figure 10: Correlation analysis of the variables from the linear regression model. Pearson's coefficient of correlation of the variables cooperated in the linear regression model 3 (**Table 8**).

3.1.4 Cross validation of the new prediction equation by an independent cohort

Determining the quality of the newly developed equation required an application on an independent study cohort. Based on the new formula RMR was predicted of an independent cohort and compared with the measured RMR to verify the quality of the equation.

To cross-validate the new developed equation a study cohort from Munich was used, consisting of 417 subjects. This validation cohort was defined by 268 female and 149 male subjects in the range of 19 to 73 years, a sub cohort of a previously described cohort (Drabsch et al. 2018). Subjects of the validation cohort were selected based on the inclusion and exclusion criteria set in the *enable* cohort, to have a comparable cohort without diseased subjects. RMR and all physical parameters, which are included in the equation to predict RMR, were differed significantly ($P < 0.0001$) from the *enable* cohort (Table 11). RMR was calculated with the variables sex, age, fat mass, FFM and body temperature from the mixed effect model (Table 6). To validate the precision of the equation, the predicted RMR was analyzed in a linear regression analysis with the measured RMR, which resulted in a high coefficient of determination of 0.7902 (Figure 11). The coefficient of determination of the validation cohort was as high as in the *enable* cohort with an R^2 of 0.7994 and not significantly different from the *enable* cohort. This demonstrates that the newly established equation of the mixed effect model has a high precision to calculate and thereby predict RMR in a widespread age cohort of 19 to 73 years.

The equation was applied in an independent study cohort to compare measured and predicted RMR. Prediction of RMR was reproduced with the same precision as in the original cohort, presenting a high quality of the newly developed equation.

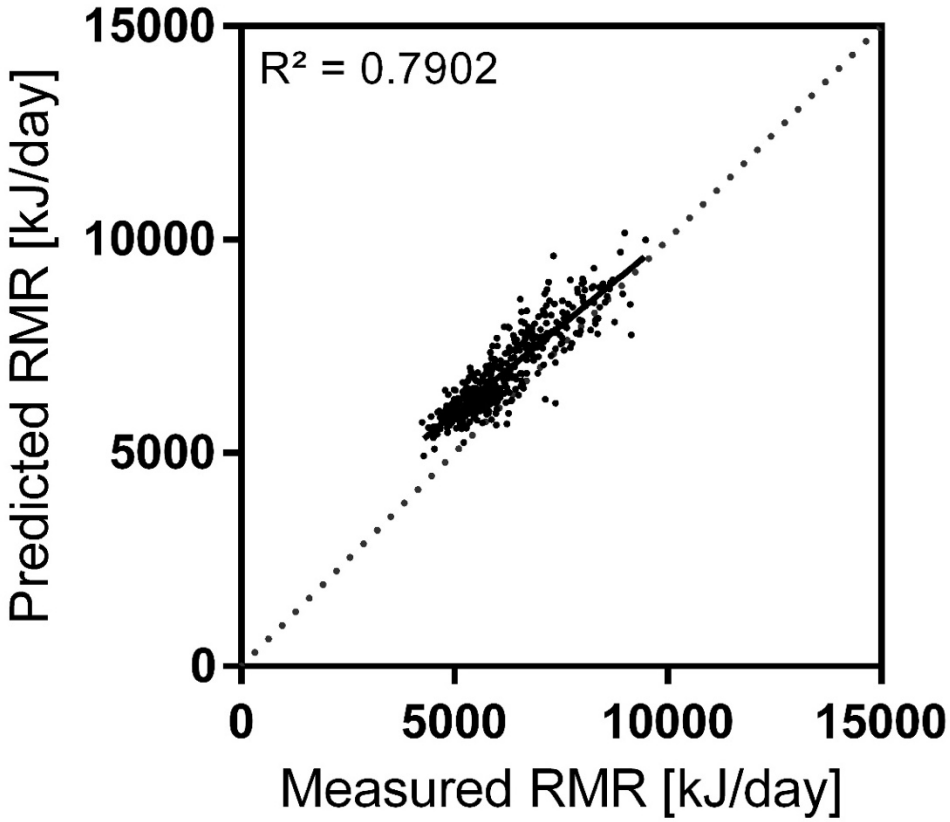

Figure 11: Cross validation of the newly developed equation by an independent cohort. Predicted RMR was calculated with the variables sex, age, fat mass, FFM and body temperature from the mixed effect model (**Table 6**). Measured RMR was determined by indirect calorimetry. Presented is the linear regression analysis of measured and predicted RMR calculated in the validation cohort, N = 417. Predicted RMR significantly correlated with measured RMR ($P < 0.0001$).

Table 11: Physical characteristics of the *enable* and validation cohort

	***Enable* – all** (N=247 M, 241 F)	***Enable* – Children** 3-5 years (N=19 M, 15 F)	***Enable* – Adolescents** 18-25 years (N=46 M, 48 F)	***Enable* – Adults** 40-65 years (N=101 M, 101 F)	***Enable* – Elderly** 75-85 years (N=80 M, 77 F)	**Cross-validation Cohort** 19-73 years (N=149 M, 268 F)
Age (years)	51.5 ± 24.0	4.3 ± 0.7	22.2 ± 2.0	52.4 ± 6.8	78.2 ± 2.7	31.1* ± 11.8
Weight (kg)	72.4 ± 21.2	18.1 ± 3.9	68.2 ± 11.0	82.2 ± 16.5	74.0 ± 13.5	70.6 ± 13.0
Height (cm)	166.7 ± 18.5	109.4 ± 9.4	175.5 ± 9.7	172.6 ± 9.1	166.9 ± 9.0	172.6* ± 9.9
Fat mass (kg)	23.4 ± 11.7	3.4 ± 1.8	14.3 ± 6.2	28.1 ± 11.0	27.2 ± 8.2	16.6* ± 8.3
FFM[2] (kg)	49.2 ± 14.5	14.6 ± 3.2	53.9 ± 11.9	54.1 ± 11.0	47.4 ± 10.1	54.1* ± 11.7
Body temperature (°C)	36.4 ± 0.4	36.8 ± 0.4	36.6 ± 0.3	36.3 ± 0.3	36.4 ± 0.4	36.5* ± 0.5
RMR[3] (kJ/day)	6577.0 ± 1353.6	4273.2 ± 727.4	7022.0 ± 1174.1	6969.5 ± 1222.6	6315.7 ± 1140.6	6193.2* ± 1066.8

[1]All values are presented as means ± SDs

[2]FFM = fat free mass

[3]RMR = resting metabolic rate

*significantly different from the '*enable* – all' (unpaired t test) $P < 0.0001$

3.1.5 Comparison of the new equation with common prediction equations

Calculating RMR by a prediction equation is a common practice in clinical studies and research to estimate the energy requirement of the individual subject. For this purpose, several equations have been published like the equation from Harris-Benedict (Harris and Benedict 1918) and the Schofield equation, which is recommended by WHO (WHO 1985). However, these equations have been established decades ago with various subjects and ethnicities. These equations are also embedded in several bioelectrical impedance analysis (BIA) scales and indirect calorimetry devices to provide a reference value for the measured RMR.

The newly established equation to predict RMR was compared with the commonly used equation from Harris-Benedict and WHO. Additionally, the well-known equation from Kleiber (Kleiber 1947) and the equation embedded in the Tanita scale (EP1195138) were analyzed regarding their accuracy to predict RMR (Table 12). The Tanita scale is a BIA scale to measure body composition. By using the enable data set measured and predicted RMR, calculated by the WHO equation, revealed a coefficient of determination of 0.75 (Figure 12). Among the well-established equations, the WHO equation predicted RMR with the highest accuracy, followed by the Tanita scale. Predicting RMR by Kleiber's law resulted in a strong underestimation of RMR for children. However, Kleiber's Law describes the correlation between body mass and metabolic rate of animals and was not designed to predict RMR of humans. In this setting Kleiber's law was used out of curiosity, how well it can predict RMR of humans. Even though the prediction was not as precise as the other equations presented in this work, Kleiber's law was able to predict RMR of humans.

All reference equations were able to predict RMR with a high coefficient of determination between 0.6 and 0.75, whereas the newly developed equation presents a coefficient of determination of 0.80. However, the reference equations were developed on other data sets with various ethnicities, age and BMI groups and might therefore result in a better prediction in other study cohorts, respectively the data set they were established.

Table 12: Common equations to predict RMR

Equation	Sex	Age	RMR (kJ/day)
Present work	Male and female	3-85 years	= - 7540.6 - 263.3 * sex[1] - 7.8 * age[2] + 25.8 * fat mass[3] + (79.2 + (child[4]) * 34.4)) * FFM[5] + 277.9 * body temperature[6]
Harris-Benedict-Equation	Male	21-70 years	= 66.47 + 13.7 * weight[7] + 5 * height[8]– 6.8 * age[2] * 4.184
	Female	21-70 years	= 655.1 + 9.6 * weight + 1.8 * height – 4.7 * age * 4.184
WHO	Male	3-10 years	= (22.7 * weight[7] + 495) * 4.184
		18-30 years	= (15.3 * weight + 679) * 4.184
		30-60 years	= (11.6 * weight + 879) * 4.184
		> 60 years	= (13.5 * weight + 487) * 4.184
	Female	3-10 years	= (22.5 * weight + 499) * 4.184
		18-30 years	= (14.7 * weight + 496) * 4.184
		30-60 years	= (8.7 * weight + 829) * 4.184
		> 60 years	= (10.5 * weight + 596) * 4.184
Kleiber	Male and female	(Quelle)	= 283 *weight$^{0.75}$
Tanita scale	Male and female	>9 years	= (A*FFM*FFM + B*FFM + C*(1/age) + D*weight + E[9])*4.184

[1] male = 0, female = 1; [2]age in years; [3]fat mass in kg; [4]children = 3 - 5 years, adults = 18 - 85 years; [5]FFM = fat free mass in kg; [6]body temperature in °C; [7]weight in kg, [8]height in cm; [9]A = 0.08, B = 15.0, C = 2616.2, D = 3.8, E = 203.3, these constants were mathematically determined.

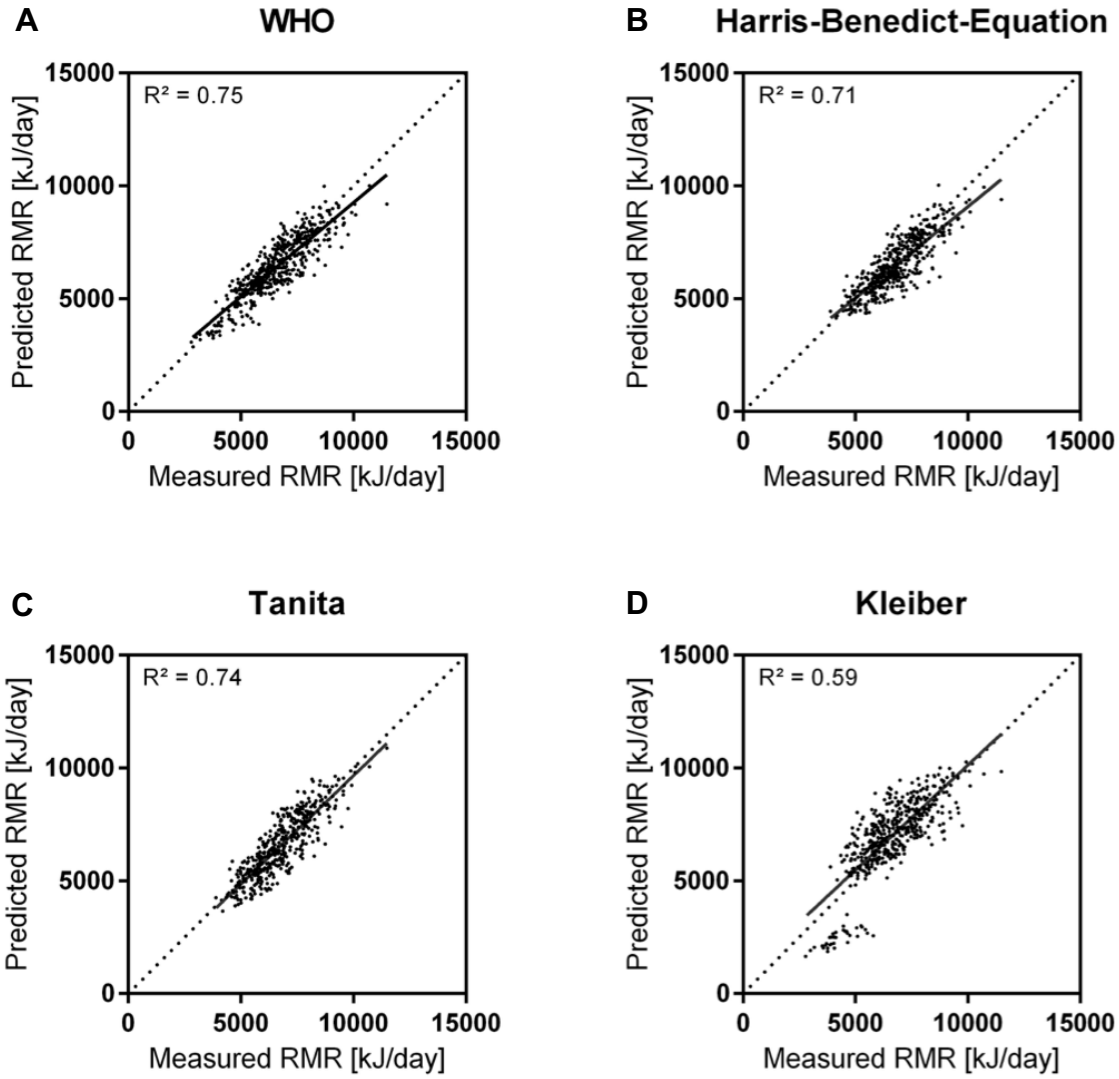

Figure 12: Common equations to predict RMR. Measured and predicted RMR of the *enable* cohort, calculated by different equation (N = 488). Detailed information about the individual equation are presented in **Table 12**. For all equations a significant correlation of measured and predicted RMR was observed ($P < 0.0001$).

3.2 Peripheral blood mononuclear cells and resting metabolic rate

Mitochondria are the 'powerhouse' of our cells, where ATP as an energy source is generated. To study the effect of mitochondrial activity on inter-individual variation of RMR the respiratory capacity of peripheral blood mononuclear cells (PBMCs) was determined. PBMCs are peripheral cells of the blood with a single round nucleus and mitochondria and are easily accessible by a blood sample. As PBMCs are circulating cells of the blood they are directly affected by metabolic stress and respond to changes like inflammatory processes. PBMCs might reflect processes globally affecting RMR variation. Therefore, PBMCs were used as a biomarker to assess mitochondrial activity and its influence on RMR variation.

3.2.1 Methodical approaches to determine respiratory capacity of PBMCs

3.2.1.1 Protocols to measure mitochondrial respiration of PBMCs

In the process of analyzing the mitochondrial activity of PBMCs, two different protocols were established to determine the different respiratory states of PBMCs in a chamber based respirometry.

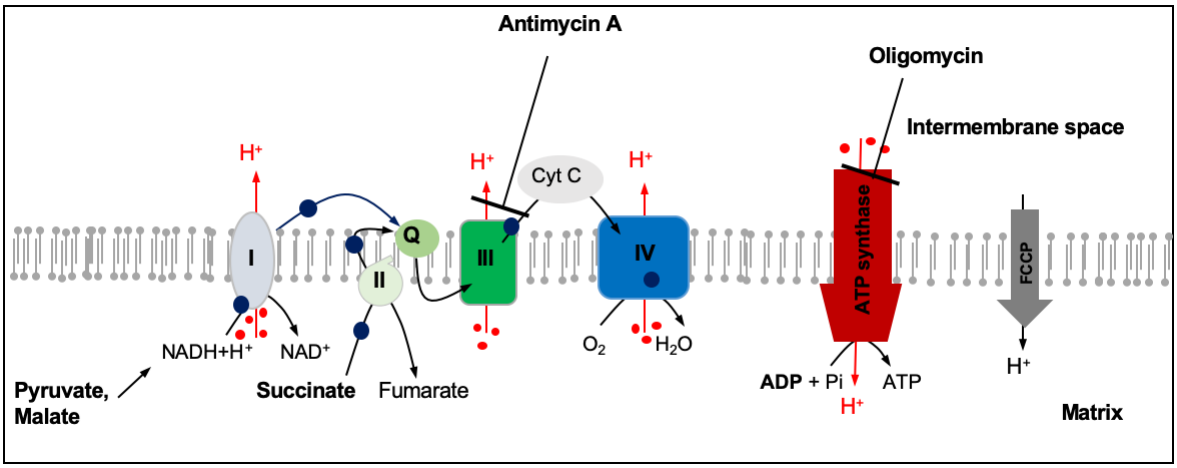

Figure 13: Mitochondrial respiratory chain with substrates inhibitors and uncouplers. Depicted are the four complexes of the electron transport chain (ETS) and ATP-synthase. Protons and their respective flow are depicted in red, the flow of electrons along the electron transport chain are presented in dark blue. Substrates, uncouplers and inhibitors and their access points at the respiratory chain are presented in bold.

The first protocol is the so-called Substrate-Uncoupler-Inhibitor-Titration (SUIT) protocol (Figure 14). As the name implies in this protocol substrates, uncoupler and inhibitors are combined and titrated. The aim of this protocol was to determine as far as possible all respiratory states in one protocol by applying different substrates and inhibitors. Therefore, cells were permeabilized with digitonin to be accessible for substances like pyruvate,

malate, succinate and ADP. In a first step pyruvate and malate were applied to provide the substrate NADH+H$^+$ for complex I, followed by succeeding injection of ADP to induce ADP phosphorylation, determining oxidative phosphorylation (OXPHOS) under complex I substrates. Next, succinate was applied to provide substrates in excess for complex II and thereby determining the OXPHOS capacity under all available substrates for the electron transport chain. Followed by leak respiration under oligomycin to inhibit the ATP-synthase. Leak respiration presents the minimal respiration, compensating for the proton leak across the inner mitochondrial membrane. The maximal uncoupled respiration was measured by titrating FCCP. Last, non-mitochondrial respiration was determined by applying antimycin A to inhibit complex III and thereby the electron flow.

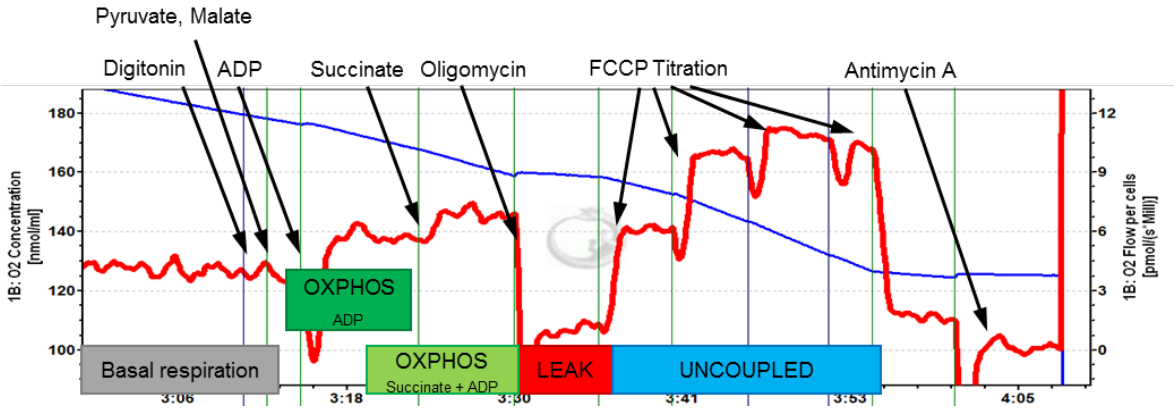

Figure 14: SUIT protocol to measure mitochondrial activity of permeabilized PBMCs. Respiration protocol to determine the different respiratory states under the combination of substrate, uncoupler and inhibitors in a chamber based respirometry. Basal respiration is determined with intact cells at the beginning of the measurement without the addition of any substrates or inhibitors (presented in grey). In dark green the state of the OXPHOS capacity under the substrates pyruvate, malate and ADP is presented, in light green the OXPHOS capacity under the addition of succinate. Leak respiration (depicted in red) was determined after inhibiting the ATP-synthase by oligomycin and the uncoupled respiration was determined by a titration of FCCP (blue). Non-mitochondrial respiration was determined by inhibiting complex III with Antimycin A. The red slope presents the oxygen consumption [pmol/million cells] and the blue slope the oxygen concentration [nmol/ml] in the chamber.

The second protocol was the so-called succinate-rotenone protocol (Figure 15). In this protocol, complex I is inhibited by rotenone and therefore the electrons can only enter the electron transport chain through complex II. After permeabilizing the cells by digitonin and inhibiting complex I by rotenone, succinate was applied as a substrate for complex II and following OXPHOS capacity was measured by supplying ADP for the ADP phosphorylation. Leak respiration was determined in the presence of oligomycin to inhibit the ATP-synthase, followed by an FCCP titration to determine maximal uncoupled respiration. In the last step, non-mitochondrial respiration was assessed by inhibiting complex III with antimycin A.

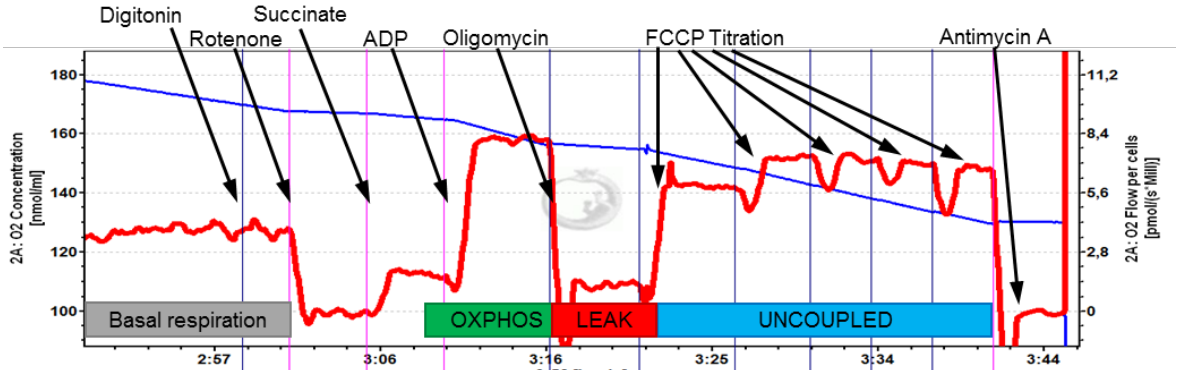

Figure 15: Succinate-rotenone protocol to measure mitochondrial activity of permeabilized PBMCs. The different respiratory states are determined under the substrate succinate and the inhibition of complex I through rotenone. Basal respiration is determined with intact cells at the beginning of the measurement without the addition of any substrates or inhibitors. After permeabilization of the cells by digitonin, rotenone was supplied to inhibit complex I, followed by succinate to provide electrons for complex II. OXPHOS (green) capacity was determined by supplying ADP to stimulate ADP phosphorylation. Leak (red) respiration was determined by inhibiting the ATP-synthase with oligomycin followed by a titration of FCCP to assess maximal uncoupled respiration (blue). Non-mitochondrial respiration was determined by inhibiting complex III with antimycin A. The red slope presents the oxygen consumption [pmol/million cells] and the blue slope the oxygen concentration [nmol/ml] in the chamber.

3.2.1.2 Respiratory states in the substrate uncoupler inhibitor titration protocol

SUIT protocols are a combination of substrates, uncoupler and inhibitors to assess the different respiratory states like the OXPHOS and electron transfer system (ETS) and leak respiration. There are different possibilities how to assess leak, OXPHOS and ETS capacity in the SUIT protocol. In the following the effect and consequences of the different options to determine the respiratory states in the SUIT protocol are evaluated for PBMCs.

Proton leak is defined as the oxygen consumption compensating for proton leak across the inner mitochondrial membrane. Proton leak contributes with 20 - 25% to the metabolic rate of liver cells and even up to 50% of skeletal muscle cells (Brand et al. 1999, Rolfe and Brand 1996). Liver and skeletal muscle contribute as high metabolic rate organs to RMR variation, therefore also this proton leak contributes to RMR. A damaged inner-mitochondrial membrane would lead to an increased proton leak, which might affect RMR variation.
The uncoupled respiration determines the respiratory capacity of the ETS independent from the capacity of the ATP-synthase to phosphorylate ADP. By measuring uncoupled respiration information about the coupling efficiency of substrate oxidation and ADP-phosphorylation can be obtained. An increased uncoupled respiration above the OXPHOS capacity may indicate a limited ATP-synthase activity, resulting in a reduced ATP production. A reduced capacity to produce ATP might therefore affect energy homeostasis, respectively RMR.
Leak respiration can either be determined by inhibiting the ATP-synthase with oligomycin (protocol 1) or by a prolonged waiting time after permeabilizing the cells with digitonin (protocol 2, Figure 16). A prolonged waiting time after permeabilization with digitonin resulted in a decreased OXPHOS capacity (Figure 16, protocol 2). By comparing the two respiratory states of leak respiration, oligomycin was found to induce a more stable leak respiration (Figure 16). However, oligomycin inhibited the effect of FCCP and therefore it was not possible to assess the real uncoupled respiration (Figure 17).

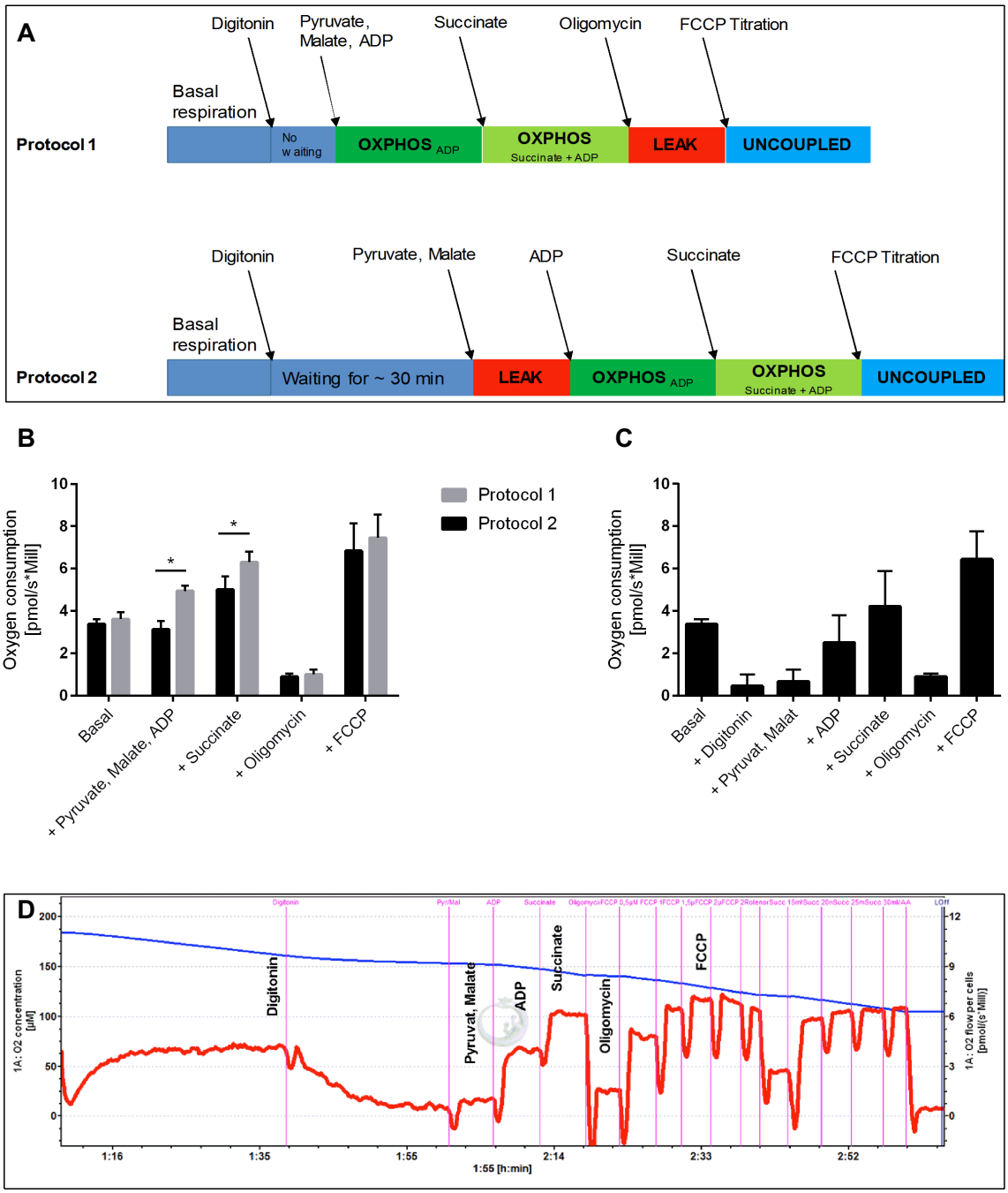

Figure 16: Effect of digitonin on leak and OXPHOS capacity in two different SUIT protocols. Respiratory states of two different SUIT protocols were assessed in fresh isolated PBMCs. (**A**) Two different SUIT protocols with the different steps to assess OXPHOS, leak and uncoupled respiration. Protocol 1 measured OXPHOS capacity directly after permeabilizing the cells with digitonin and therefore oligomycin was used to determine leak respiration. In protocol 2 leak respiration was determined after permeabilizing the cells by digitonin and providing the substrates pyruvate and malate. (**B**) Comparison of the OXPHOS capacity in the two different SUIT protocols, by protocol 1 and 2, N = 4. (**C**) Comparison of the leak respiration, either determined by permeabilizing with digitonin with a prolonged waiting time or by inhibiting the ATP-synthase with oligomycin, N = 4 (**D**) Representative trace of a respiration measurement where the different states of leak respiration were determined.

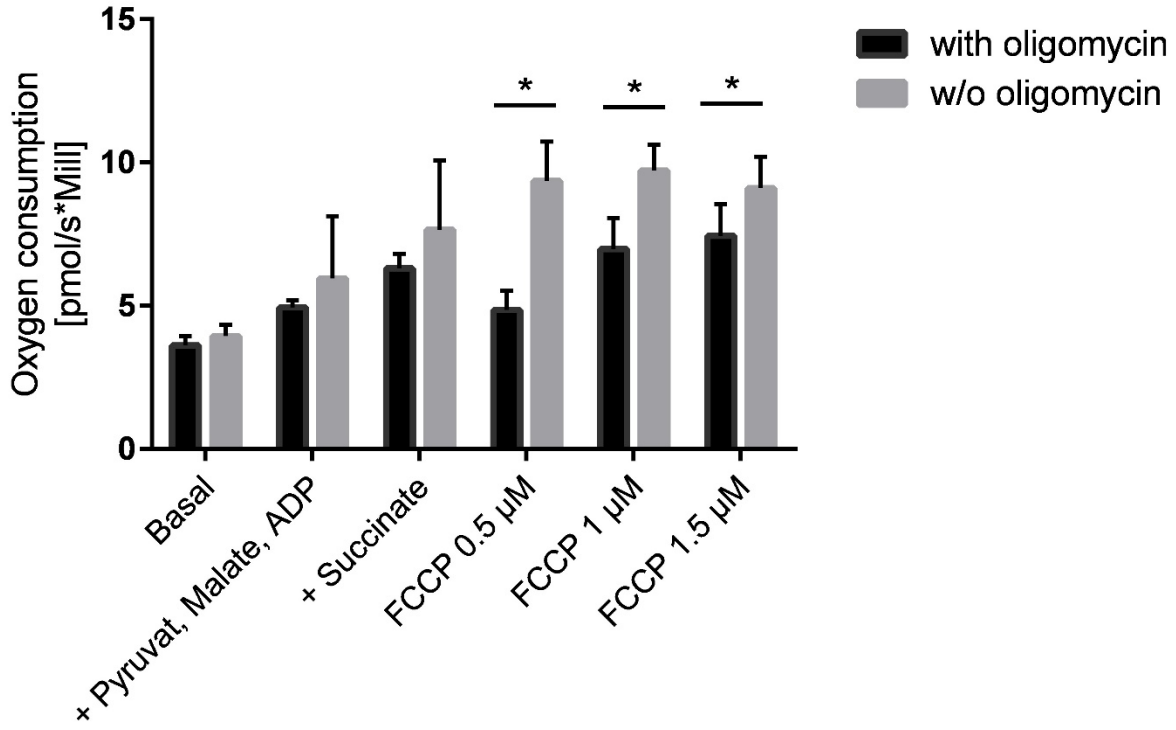

Figure 17: Effect of oligomycin on the uncoupled respiration induced by FCCP. Oxygen consumption rate of permeabilized PBMCs was assessed in a chamber based respirometry. Cells were permeabilized by digitonin. Uncoupled respiration was determined by titrating the uncoupler FCCP until the maximal uncoupled respiration was reached. Compared is the uncoupled respiration either in the presence (black) or in absence (grey) of oligomycin, N = 4.

SUIT protocol determines the uncoupled respiration based on the activity of complex I and II (Figure 14). In the succinate-rotenone protocol complex I is inhibited by rotenone at the beginning of the measurement. Consequentially, the uncoupled respiration is measured without the activity of complex I (Figure 15).

The aim of the following experiment was to include an uncoupled respiratory state in the SUIT protocol based on complex II activity. By inhibiting complex I with rotenone, after the cells were fully uncoupled by FCCP, the oxygen consumption decreased dramatically (Figure 18 A). The respiration was rescued by a high amount of succinate up to 25 mM, but did not reach the same oxygen consumption as before. The uncoupled respiration based on complex II in the SUIT protocol was compared with the uncoupled respiration in the succinate-rotenone protocol, as it should be the same respiratory state. The comparison revealed a significantly ($P < 0.0001$) reduced uncoupled respiration in the SUIT compared to the succinate-rotenone protocol (Figure 18 B). Therefore, it was not possible to include an uncoupled respiratory state based on complex II activity in the SUIT protocol. The results

of this experiment demonstrated that the order and combination of substrates and inhibitors are important to determine the same respiratory states in PBMCs.

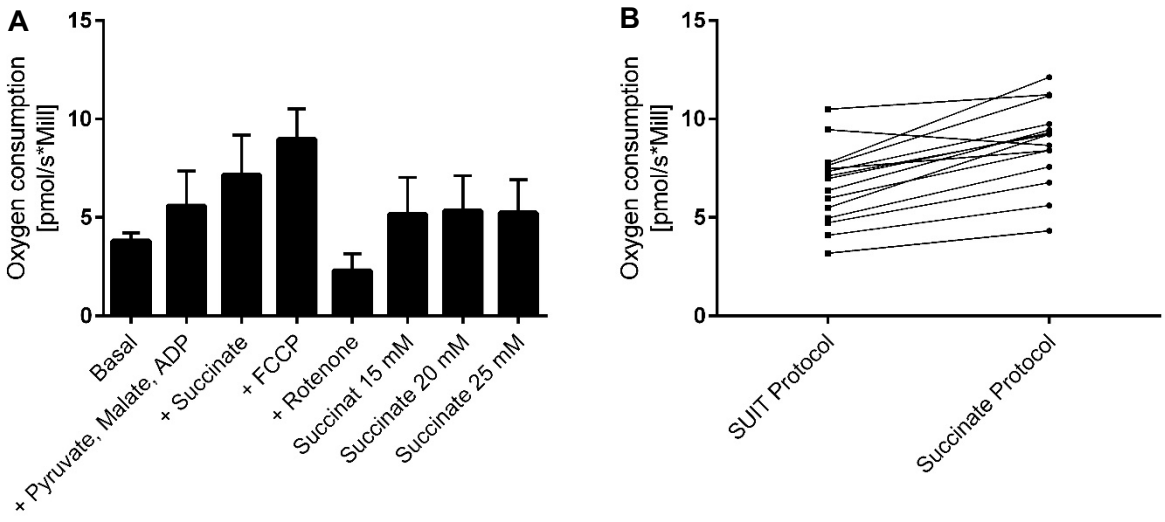

Figure 18: Effect of rotenone on the uncoupled respiration in the SUIT protocol. An additional uncoupled respiratory state, based on complex II activity was assessed in freshly isolated and permeabilized PBMCs. (**A**) Consecutive states of the respiration measurement in the SUIT protocol with the addition of rotenone and succinate at the end, N = 11. (**B**) Uncoupled respiration based on complex II activity was significantly lower in the SUIT protocol compared to the succinate-rotenone protocol ($P < 0.0001$), N = 15.

Assessing mitochondrial activity of PBMCs by high-resolution respirometry is ideally performed on freshly isolated PBMCs. In human trials, blood samples of several subjects are not always taken at the same time and therefore the isolation of PBMCs cannot start immediately. The aim of the following experiment was to assess the effect of a delayed start of isolation from the blood sample on the mitochondrial activity of PBMCs.

Determining the effect of a delayed start of isolation, all blood samples were taken in the morning at 8am. Half of the blood samples were used to directly isolate PBMCs, the other half was stored on a tube roller and isolation started six hours later. Comparison revealed no significant difference in the oxygen consumption rate ($P > 0.05$) between freshly isolated PBMCs and PBMCs isolated six hours later (Figure 19). This result illustrates the possibility to store a blood sample and start the isolation procedure time-delayed after taking the blood sample without having an effect on the mitochondrial activity.

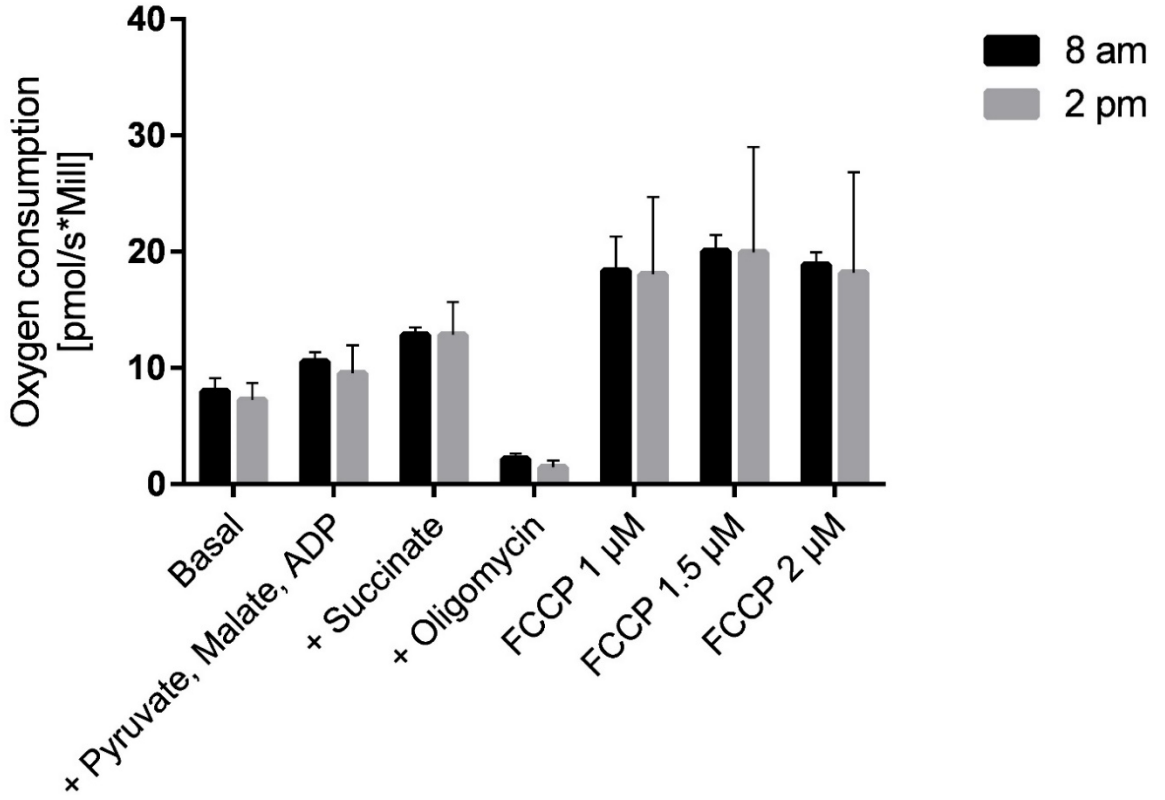

Figure 19: Time effect of a delayed isolation on mitochondrial activity of PBMCs in the SUIT protocol. All blood samples were taken in the morning. Mitochondrial activity of freshly isolated PBMCs was compared with PBMCs isolated six hours after taking the blood sample. In the mean while blood samples were stored on a constant moving tube roller at room temperature to avoid separation of plasma and cellular components. Presented are three biological replicates consisting of four technical replicates, which were used to calculate the daily mean.

3.2.2 Respiratory capacity of PBMCs as a biomarker for mitochondrial activity and their influence on resting metabolic rate variation

Mitochondria are found in most eukaryotic cells and are the central organelle to produce energy in form of ATP. PBMCs are circulating cells of the blood and might reflect global processes affecting RMR variation. To study the influence of mitochondrial activity on the inter-individual variation of RMR, the respiratory capacity of PBMCs was assessed.

Mitochondrial activity of PBMCs was assessed in 179 subjects from three *enable* cohorts adolescents, middle-aged adults and elderly (Table 13). These subjects were selected randomly based on the time schedule if it was possible to measure PBMCs, and if enough blood was available. Physical characteristics of the 179 subjects were not significant different from the physical characteristics of the overall *enable* cohort (Table 13). Looking into the distribution of the subjects from the PBMC cohort the 179 subjects were equally

distributed in the whole *enable* cohort (Figure 20). A correlation analysis confirmed no significant difference between measured and predicted RMR of the PBMC sub cohort and the overall *enable* cohort (Figure 20). As there are no differences in the physical characteristics and the distribution of the subjects from the PBMC sub cohort, this presents a good representative sample for the whole *enable* cohort to study the influence of mitochondrial activity on RMR variation.

Table 13: Physical characteristics of the *enable* sub cohort for the PBMC analysis

	Enable All (N=247 M, 241 F)			**PBMC cohort (N=88 M, 91 F)**		
	Mean	±	SD	Mean	±	SD
Age (years)	51.5	±	24.0	49.1	±	20.5
Weight (kg)	72.4	±	21.2	75.7	±	16.1
Height (cm)	166.9	±	18.5	171.8	±	9.9
Fat mass (kg)	23.4	±	11.7	23.2	±	10.8
FFM (kg)	49.2	±	14.5	52.5	±	11.7
Body temperature (°C)	36.4	±	0.4	36.4	±	0.3
BMI (kg/m^2)	25.2	±	5.2	25.5	±	4.6
RMR (kJ/day)	6577.0	±	1353.6	6781.3	±	1266.8

All parameters of the 'PBMC cohort' are not significant different from the '*enable* all cohort', two-tailed t-test ($P > 0.05$)

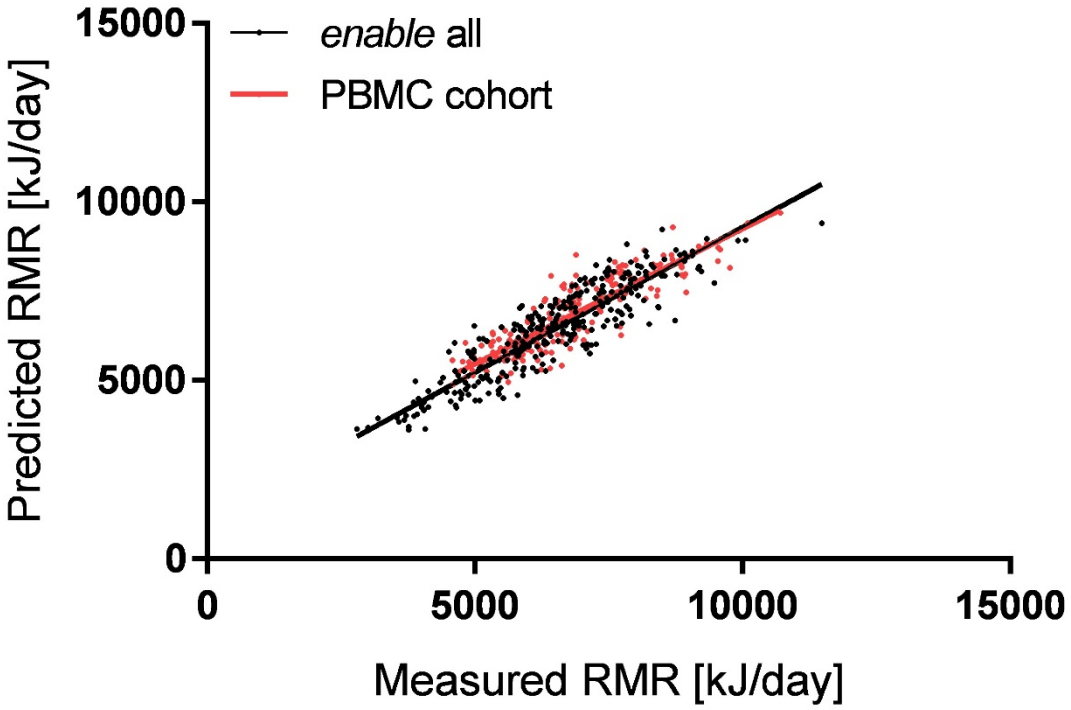

Figure 20: Measured and predicted RMR of the PBMC and *enable* cohort. Predicted RMR was calculated with the variables sex, age, fat mass, FFM and body temperature based on the mixed effect model, with the random variable 'child'. Subjects were divided into the subjects with the additional assessment of the respiratory capacity of PBMCs (depicted in red) and the remaining subjects of the *enable* cohort (presented in black). Slopes and intercept of measured and predicted RMR were not significantly different between the e*nable* and PBMC sub cohort (P = 0.25). *Enable* cohort: N = 309, PBMC cohort: N = 179.

Analyzing the inter-individual variation of RMR, a residual variation remained, which was not explained by sex, age, fat mass, FFM and body temperature. To investigate if the respiratory capacity of PBMCs has an influence on the inter-individual variation of RMR, the analysis was performed with the residual variation after adjusting for the known influencing variables. The residuals of RMR were calculated based on the mixed effect model (Table 6) with the variables sex, age, fat mass, FFM and body temperature and the random factor 'child'. In this case, not the complex linear regression model 3 with all the blood parameter was used, as some of the blood parameters might interfere with the respiratory capacity of PBMCs and therefore the influence of PBMC activity on inter-individual variation of RMR may possibly not been detectable. For example, leukocytes accounted for 3.17% of the inter-individual variation in RMR. Lymphocytes are part of leukocytes and belong to the PBMC fraction. By adjusting RMR for the leukocyte number, part of the influence of the respiratory capacity of PBMCs might already been taken away.

All different respiratory states of the SUIT protocol were analyzed individually whether they explain part of the residual variation of RMR (Figure 21). No respiratory state of the SUIT protocol correlated with the residuals of RMR ($P > 0.05$). The same analysis was performed for all respiratory states of the succinate-rotenone protocol, resulting in a non-significant correlation with the residuals of RMR (data not shown). Differences in the respiratory capacity of the different respiratory states like leak or maximal uncoupled respiration did not account for part of the inter-individual variation in RMR. The respiratory control ratio (RCR) is an indicator for mitochondrial inner membrane integrity and metabolic scope, as determined by monitoring the increase in respiration in response to ADP or a chemical uncoupler. In other words, the RCR describes the ability of the mitochondria to produce ATP depending on the demand of ATP or achieving maximal respiration to defend a proton leak. Differences in coupled and uncoupled respiratory control ratio could not explain part of the residual variation in RMR.

Summing up, individual differences in the respiratory capacity of PBMCs were not associated with the residual variation of RMR.

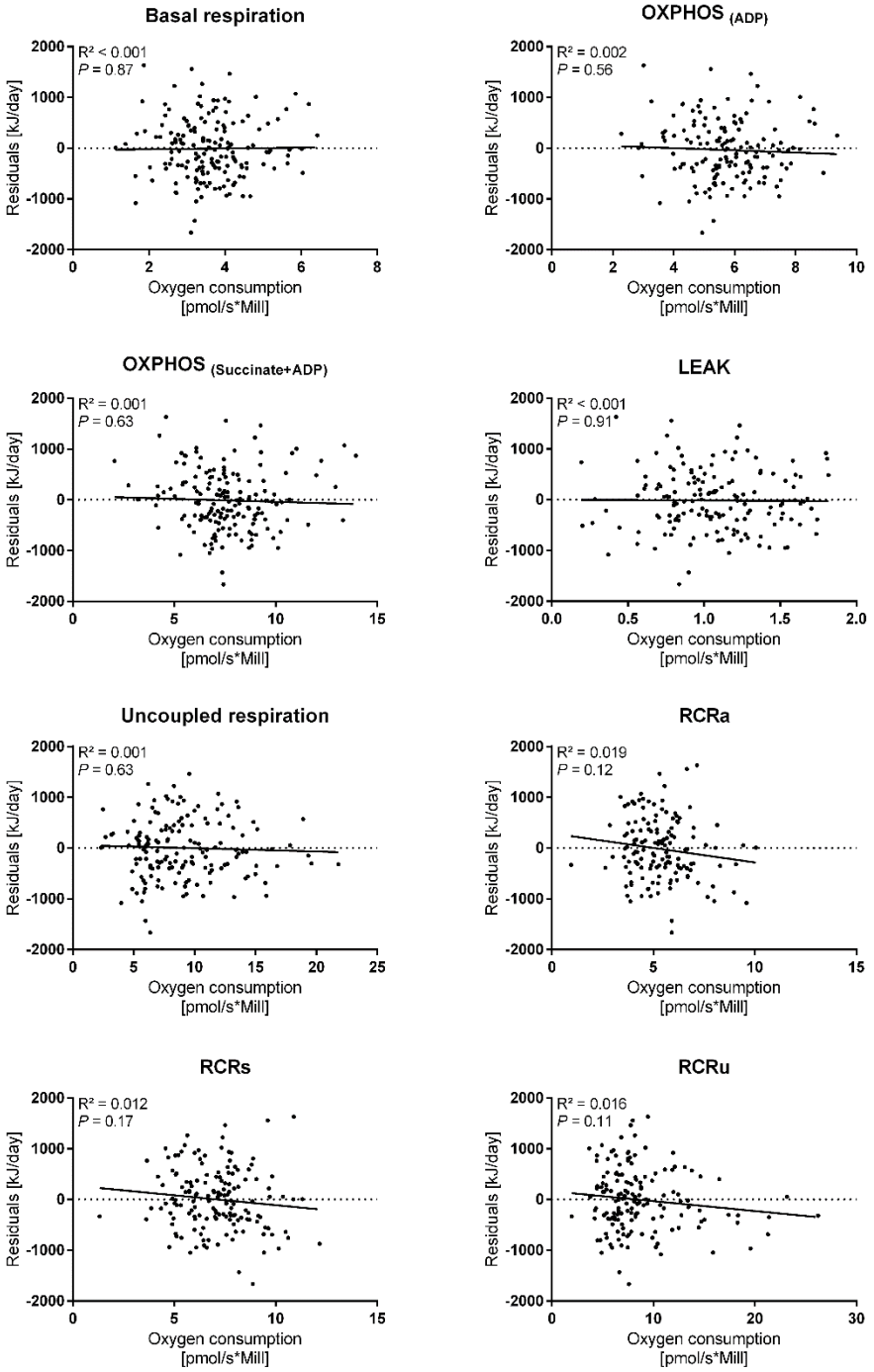

Figure 21: Respiratory states of the SUIT protocol and residuals of RMR. Residuals of RMR were calculated with the variables sex, age, fat mass, FFM, body temperature and the random factor 'child' from the mixed effect model 1 (**Table 6**). Presented are the different respiratory states of the SUIT protocol. Basal respiration was determined at the beginning without the addition of any substrates or inhibitors. $OXPHOS_{(ADP)}$ presents the OXPHOS capacity with the substrates pyruvate, malate and ADP. $OXPHOS_{(succinate + ADP)}$ presents the OXPHOS capacity with the substrates pyruvate, malate, succinate and ADP. Leak respiration was determined with oligomycin and uncoupled respiration by FCCP. The respiratory control ratio (RCR) were calculated with the leak respiration under oligomycin. RCRa stands for the RCR calculated with the $OXPHOS_{(ADP)}$, RCRs with the $OXPHOS_{(succinate + ADP)}$ and RCRu with the uncoupled respiration, N = 166.

3.2.3 Declining mitochondrial activity of PBMCs with increasing age

In the process of aging, a general decline in physiological processes was associated with a decline and altered function in mitochondrial activity (Lopez et al. 2013, Ames, Shigenaga and Hagen 1995, Sebastian, Palacin and Zorzano 2017).

The *enable* cohorts were used to study the behavior of mitochondrial activity of PBMCs over three age cohorts of young adults, middle-aged adults and elderly subjects. Mitochondrial respiration of PBMCs was determined in chamber-based respirometry and the different respiratory states of the succinate-rotenone protocol were compared between the three age cohorts (Figure 22). In the basal respiration, the OXPHOS capacity and the uncoupled respiration a trend towards a reduced oxygen consumption was observed for the cohort of elderly. Whereas in the leak respiration a significantly increased oxygen consumption was observed for the elderly compared to the middle-aged adults. The tendency of a decreased maximal uncoupled respiration and an increased leak respiration led to a significantly reduced uncoupled respiratory control ratio (RCRu) for the elderly compared to the middle-aged adults. RCRu describes the ability of mitochondria to achieve maximal respiration by defending a chemically induced proton leak. A reduced respiratory capacity of PBMCs in elder subjects was observed, mainly possessed by an increased proton leak.

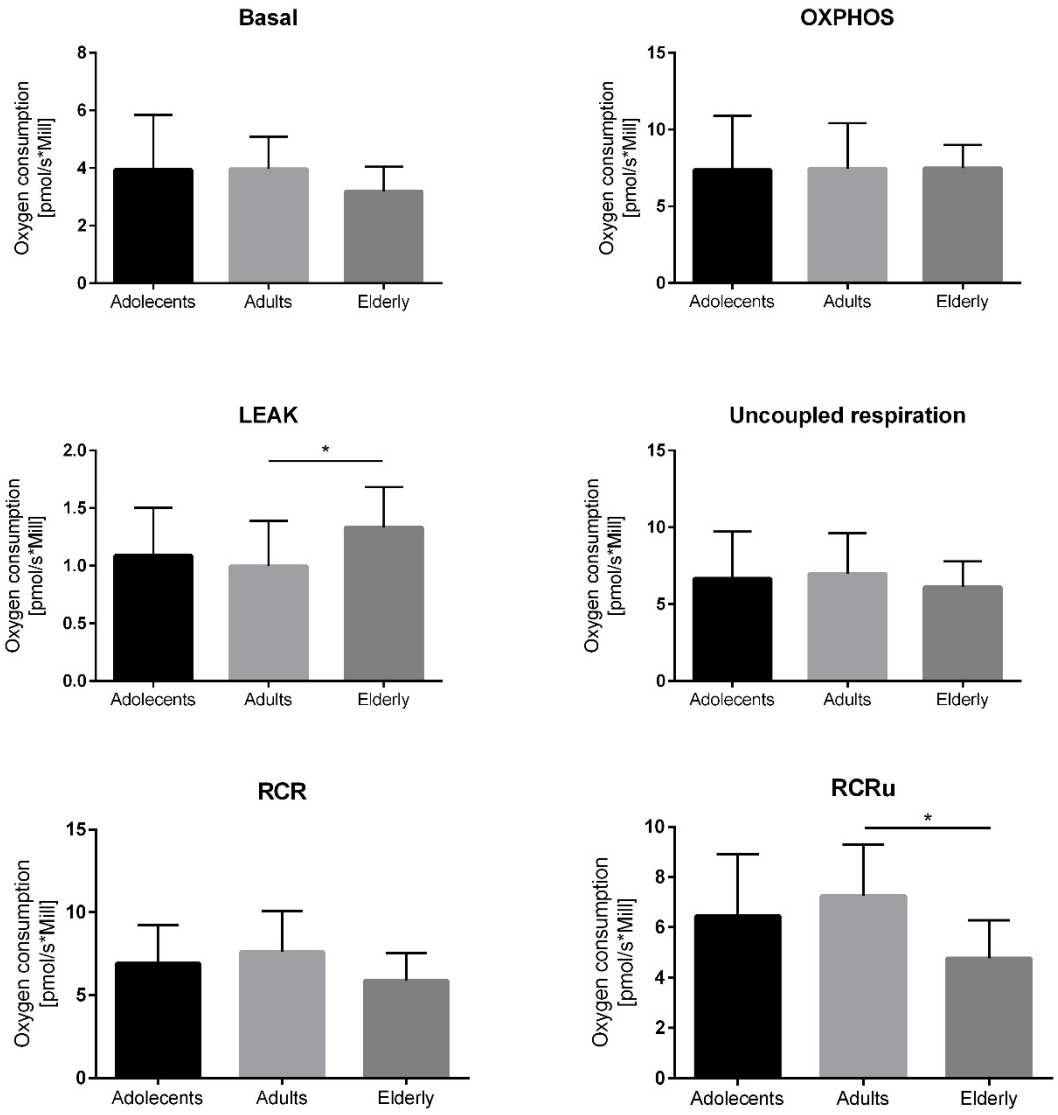

Figure 22: Respiratory states of PBMCs in the succinate-rotenone protocol, differentiated by age cohorts. Oxygen consumption rate of freshly isolated PBMCs from the succinate-rotenone protocol (**Figure 15**). Each respiratory state was differentiated by the age cohort to analyze the effect of aging in the context of mitochondrial function of PBMCs. Basal respiration was determined with intact cells, without any additional substrates. Leak respiration was significantly increased ($P < 0.05$) in the cohort of elderly compare to the middle-aged adults. RCRu was significantly decreased ($P < 0.05$) in the cohort of elderly compared to the middle-aged adults, N = 11 - 54.

3.3 Gut microbiota composition and inter-individual variation of RMR

The human gut is a complex ecosystem consisting of multiple bacteria. These bacteria have several functions like the digestion of hard-to-digestible food components such as fibers, activation of the immune defense and to displace pathogens. If it comes to changes of the gut microbiota composition, it can have different consequences. In the context of obesity research, a different composition of the two dominant gut bacteria *Firmicutes* and *Bacteroidetes* was found. Obese subjects have a higher amount of *Firmicutes* and a reduced amount of *Bacteroidetes* (Abdallah Ismail et al. 2011, Ley et al. 2005). Gut microbiota of obese subjects was found to be more effective in extracting energy from the diet than the microbiota from lean subjects (Turnbaugh et al. 2006). So far, there is no evidence-based knowledge about the impact of the gut microbiota on the energy metabolism in healthy lean subjects. In the process of identifying further parameters contributing to the inter-individual variation of RMR, the gut microbiota composition and diversity was analyzed in the *enable* cohort.

To investigate the effect of gut microbiota composition on RMR variation, the three adult cohorts of *enable* were used, consisting of 442 subjects (220 male, 222 female, Table 7). Some of the subjects had to be excluded due to missing data on the gut microbiota. First the effect of gut microbiota composition, determined by 16S rRNA gene sequencing was analyzed with measured RMR, not adjusted for any influencing variable. The phylotype richness and Shannon index were analyzed in a linear regression analysis with RMR. The phylotype richness presents the number of observed species per sample and is not corrected for the different abundances of the individual species. The Shannon index stands for the diversity within the *enable* cohort and considers the different abundances of the individual species (Jost 2007). A negative correlation of RMR and species richness was observed (R^2 = 0.02, P = 0.003). The Shannon index presented also a negative correlation with RMR (R^2 = 0.013, P = 0.003, Figure 23).
These results present a correlation of gut microbial composition to be associated with RMR. An increased diversity was associated with a decreased RMR.

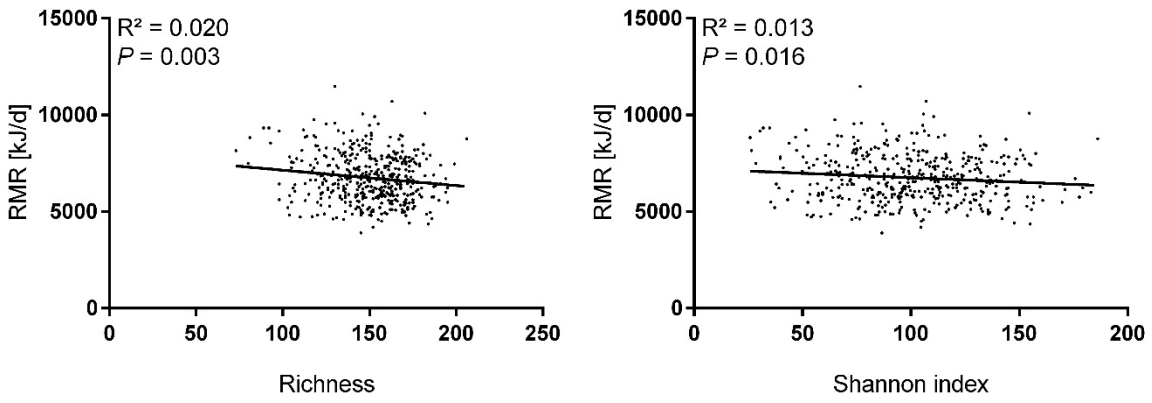

Figure 23: Gut microbiota diversity and RMR in the *enable* cohort. (A) Phylotype richness representing the number of observed species per sample, N = 442. (**B**) Shannon index describing the diversity of bacteria and thereby taking the differential abundances of the individual operational taxonomic units (OTUs) into account, N = 442.

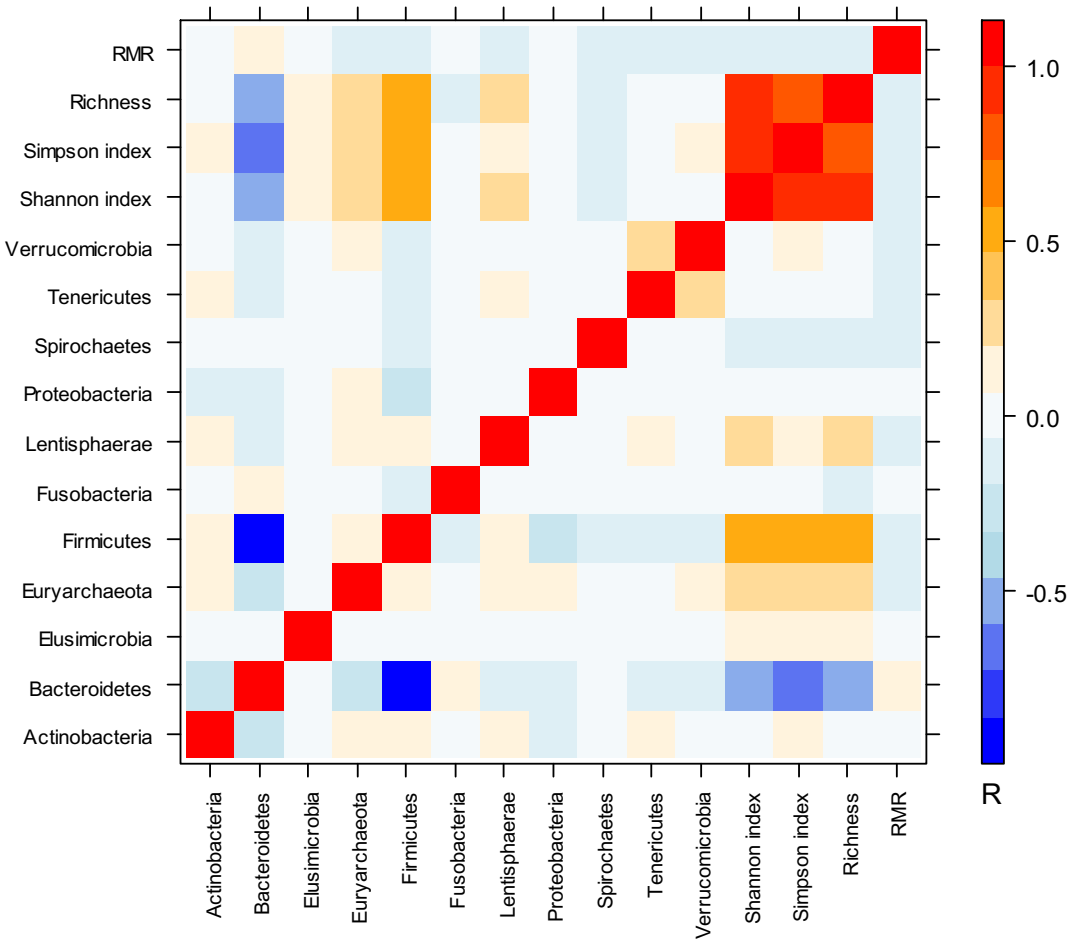

Figure 24: Heat-map of gut microbiota on phylum level and RMR. Pearsons coefficient of correlation of gut microbiota on the phylum level and measured RMR [kJ/day], not adjusted for any influencing variables. Gut bacteria are presented as relative abundances, N = 442.

In the next step, a correlation analysis on the taxonomic levels of phylum, class, order, family, genus and species was performed to identify possible candidates of gut bacteria correlating with RMR. For this analysis the measured RMR was used, not adjusted for any influencing variables. For the bacteria a preselection was carried out, thereby all unknown bacteria were removed prior to the analysis and a threshold of presence in the *enable* cohort was set. Only bacteria being present in at least 60% of the subjects from the *enable* cohort were included in the analysis. To obtain an overview and identify possible candidates of gut bacteria having an influence on RMR heat-maps were generated based on the Pearson's coefficient of correlation. Presented is the correlation analysis from the phylum and family level, which resulted in the highest values of coefficient of correlation compared to the other taxonomic levels.

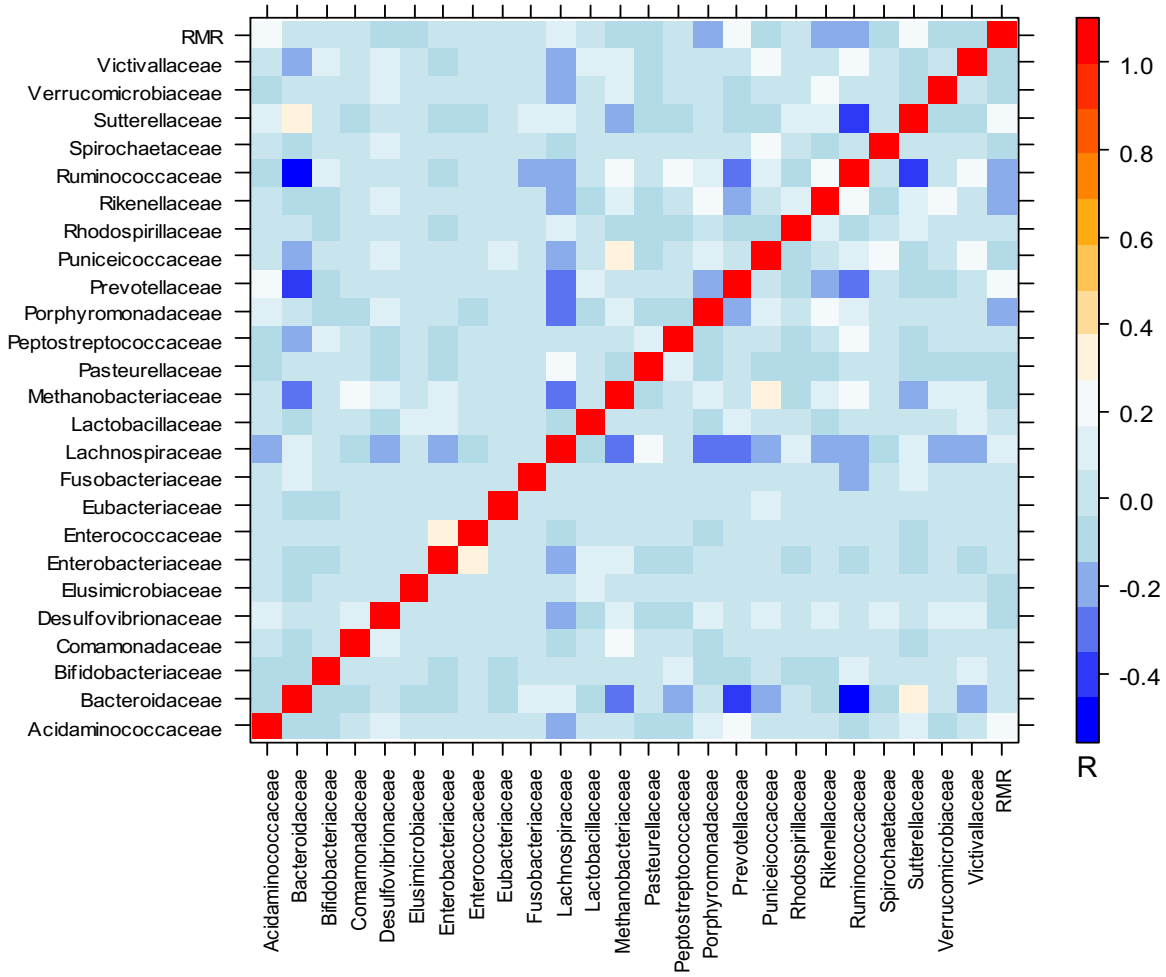

Figure 25: Heat-map of gut microbiota on family level and RMR. Pearson's coefficient of correlation of selected gut microbiota on family level. Bacteria were preselected based on a threshold of being present in at least 60% of the subjects of the *enable* cohort. Unknown bacteria were excluded from the analysis. Correlation analysis was calculated with the relative abundance of the bacteria and the measured RMR [kJ/day], N = 442.

On phylum level, no specific bacteria were identified to correlate with RMR. On the family level, three bacteria *Porphyromondaceae*, *Rikenellaceae* and *Ruminococcaceae* were identified as possible candidates with a coefficient of correlation of 0.2. These three candidates were analyzed more in detail regarding their influence on RMR and if they account for part of the residual variation in RMR, which cannot be explained by variables like sex, age, fat mass or FFM.

Analyzing the relationship of *Porphyromondaceae*, *Rikinellaceae* and *Ruminococcaceae* on RMR variation, these three bacteria were analyzed individually in a linear regression analysis. The sequence abundance of all three bacteria showed a significant ($P < 0.05$) negative correlation with RMR.

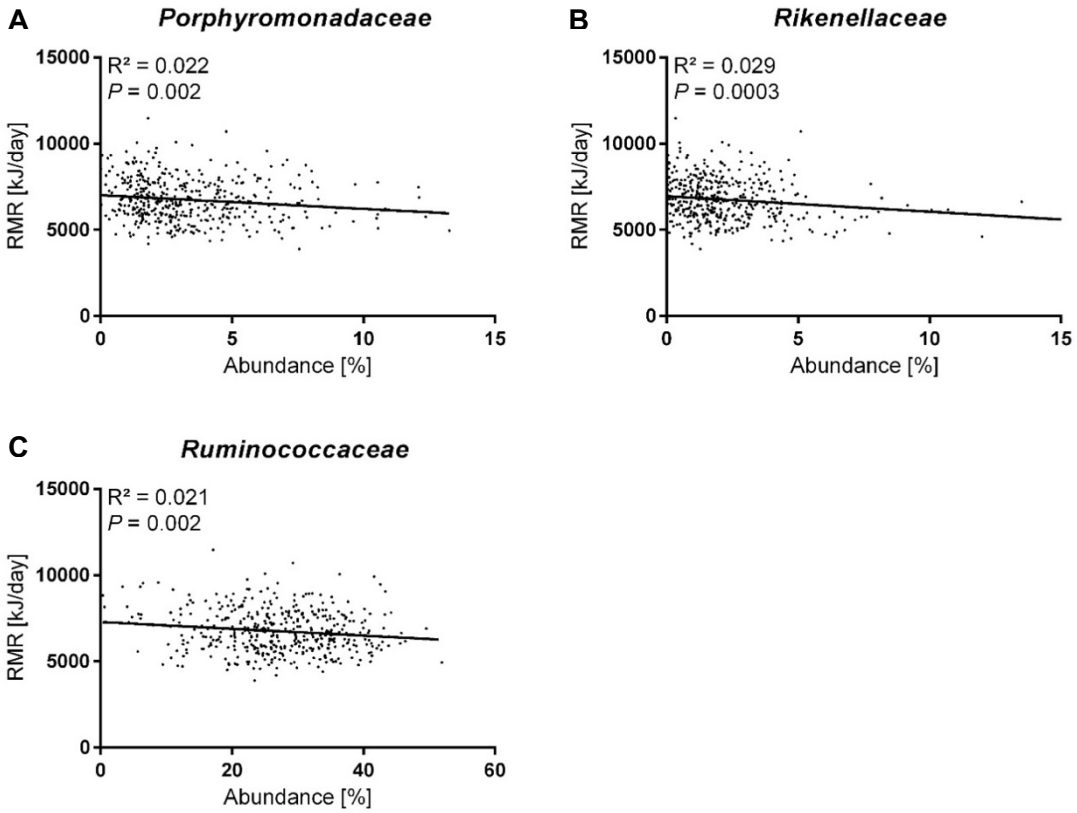

Figure 26: Representative gut microbiota on family level and RMR. Relative sequence abundance [%], in the *enable* cohort of (**A**) *Porphyromondaceae*, (**B**) *Rikinellaceae* and (**C**) *Ruminococcaceae* correlated significantly with measured RMR, based on a linear regression analysis, N = 442.

In conclusion, the diversity of the gut microbiota and the three bacteria *Porphyromondaceae*, *Rikinellaceae* and *Ruminococcaceae* were negatively associated with the measured RMR in the *enable* cohort. A lower RMR was associated with an increased bacterial diversity and an increased abundance of the three bacteria from the family level.

3.3.1 Gut microbiota composition and the residual variation of resting metabolic rate

Analyzing the influence of bacterial diversity and the effect of specific bacterial strains on the variation of RMR, the residual variation of RMR was calculated. Based on the previous established linear regression model the residual variation of RMR was calculated with the variables FFM, fat mass, age, body temperature, fT_3, creatinine, leukocytes, MCHC, systolic blood pressure and heart rate (model 3, Table 8).

The formerly identified parameters richness and Shannon index, describing the *alpha*-diversity of the *enable* cohort, were analyzed regarding their influence on the residual variation of RMR. Additionally, the three identified bacteria from the family level *Porphyromondaceae*, *Rikenellaceae* and *Ruminococcaceae* were investigated in this context.

The observed correlation of RMR and richness (R^2 = 0.02, *P* = 0.003, Figure 23) was not observed by a linear regression analysis with the residuals of RMR and the species richness (*P* = 0.32, Figure 27). Furthermore, the Shannon index was not significantly associated with the residuals of RMR (*P* = 0.63). Both parameters describing the diversity of gut microbiota were not associated with RMR after adjusting RMR for the influencing variables FFM, fat mass, age, body temperature, fT_3, creatinine, leukocytes, MCHC, systolic blood pressure and heart rate. The previously observed correlation of gut microbiota diversity and RMR was obviously due to correlations with other variables accounting for the variation in RMR.

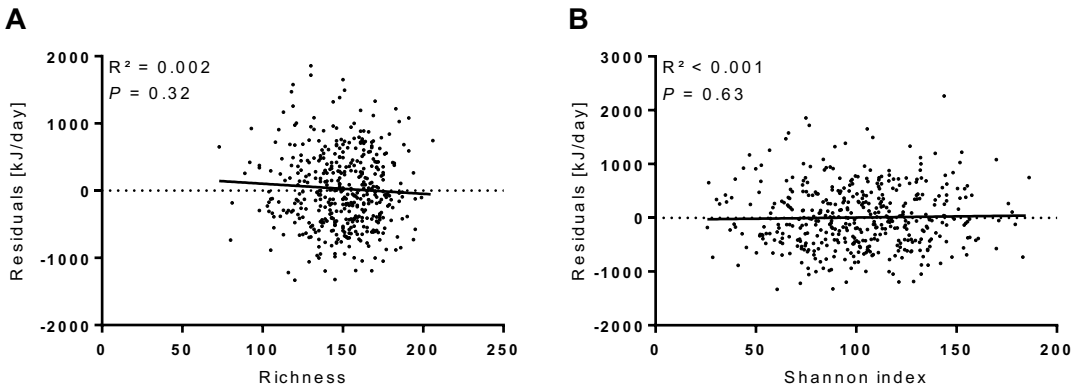

Figure 27: *Alpha*-diversity of the gut microbiota and residuals of RMR (**A**) Phylotype richness, presenting the number of observed species in the *enable* cohort and (**B**) Shannon index effective describing the diversity of gut microbiota in the *enable* cohort by taken the individual abundances into account, N = 442. (**A+B**) Residuals of RMR were calculated with the variables FFM, fat mass, body temperature, fT_3, leukocytes, creatinine, MCHC, systolic blood pressure and heart rate from the linear regression model 3 (**Table 8**).

Investigating the influence of the three bacterial candidates *Porphyromondaceae*, *Rikenellaceae* and *Ruminococcaceae* on RMR the relative abundance of these bacteria was analyzed regarding their influence on the residual variation of RMR in a linear regression analysis. *Porphyromondaceae* (*P* = 0.49), *Rikenellaceae* (*P* = 0.43) and *Ruminococcaceae* (*P* = 0.95) were not significantly associated with the residuals of RMR (Figure 28). The correlation of these three bacteria with RMR disappeared after adjusting RMR for the known influencing variables

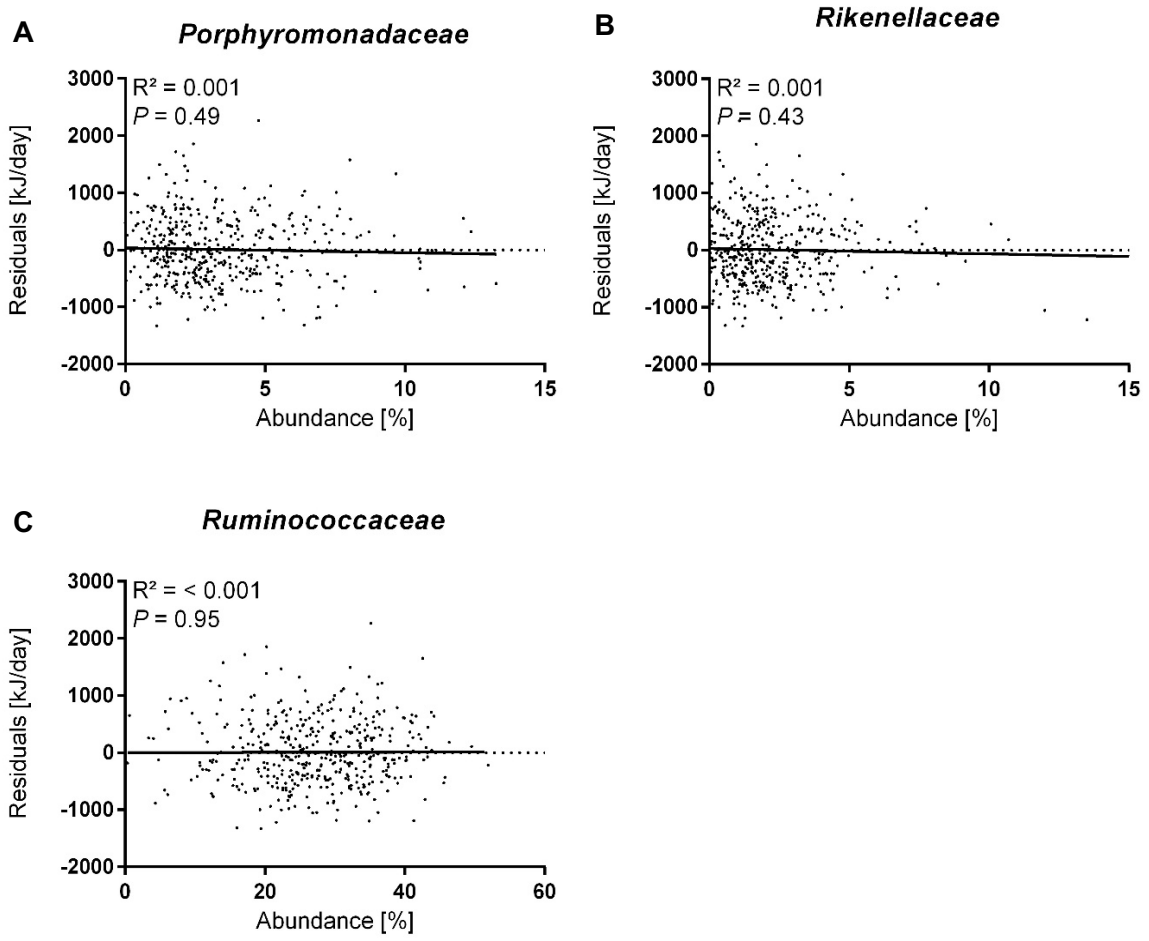

Figure 28: Specific gut microbiota on family level and residuals of RMR. Relative abundance of (**A**) *Porphyromondaceae*, (**B**) *Rikenellaceae* and (**C**) *Ruminococcaceae* in the *enable* cohort, N = 442. (**A-C**) Residuals were calculated based on the linear regression model 3 (**Table 8**), with the variables fat mass, FFM, body temperature, fT_3, leukocytes, creatinine, MCHC, systolic blood pressure and heart rate.

To identify parameters being associated with *Porphyromondaceae*, *Rikenellaceae* and *Ruminococcaceae*, a correlation analysis with these bacteria and all variables known to influence RMR was performed. Analyzing the interaction of *Porphyromondaceae*, *Rikenellaceae* and *Ruminococcaceae* with the variables age, fat mass, FFM, body temperature, MCHC, creatinine, leukocytes, fT_3, systolic blood pressure and heart

rate (Figure 29). This analysis indicated an association of *Ruminococcaceae*, *Rikenellaceae* and *Porphyromondaceae* with FFM (R = 0.2). Furthermore, *Rikinellaceae* and *Porphyromondaceae* seemed to be association with the systolic blood pressure and *Rikenellaceae* with the thyroid hormone fT_3.

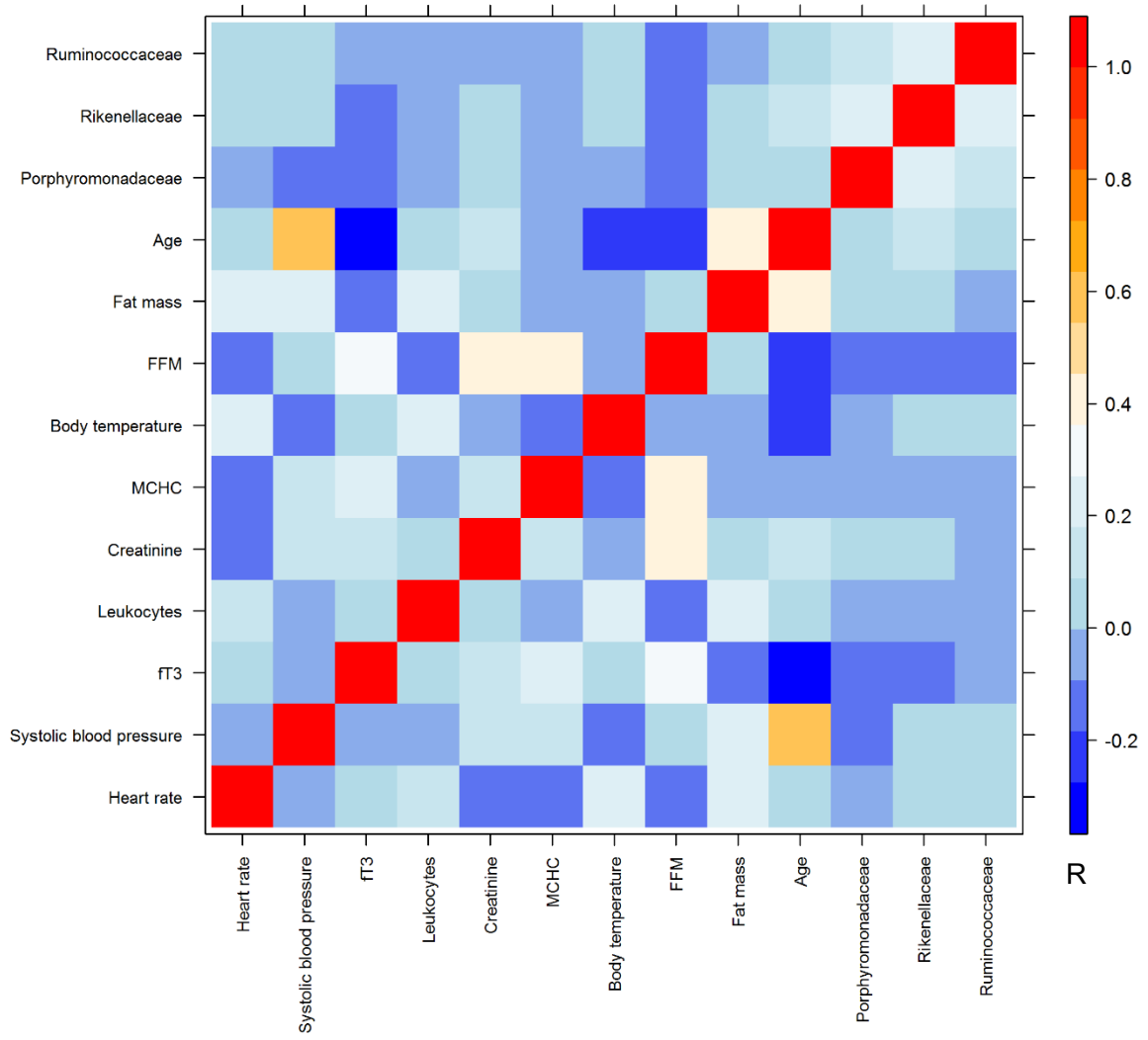

Figure 29: Specific gut microbiota on the family level and physical characteristics of the linear regression model to predict RMR. Pearson's coefficient of correlation of the variables cooperated in the linear regression model (model 3, **Table 8**) to predict RMR, N = 442. The bacteria *Ruminococcaceae*, *Rikenellaceae* and *Porphyromondaceae* are presented as relative abundances. The variables of the linear regression model are presented as follows: age (years), fat mass (kg), FFM (kg), body temperature (°C), MCHC (g/dl), creatinine (mg/dl), leukocytes (N/nl), fT_3 (pg/ml), systolic blood pressure (mmHg) and heart rate (bpm).

Individual linear regression analysis of *Ruminococcaceae*, *Rikenellaceae* and *Porphyromondaceae* with FFM and fat mass revealed a significant correlation of these three bacteria with FFM ($P < 0.05$), whereas *Ruminococcaceae* was not significantly associated with fat mass ($P = 0.336$) (Figure 30). Furthermore, *Porphyromondaceae* and *Rikenellaceae*

showed a significant correlation with fT_3 ($P < 0.001$) and *Porphyromondaceae* was additionally significantly associated with the systolic blood pressure ($P = 0.044$) (Figure 31).

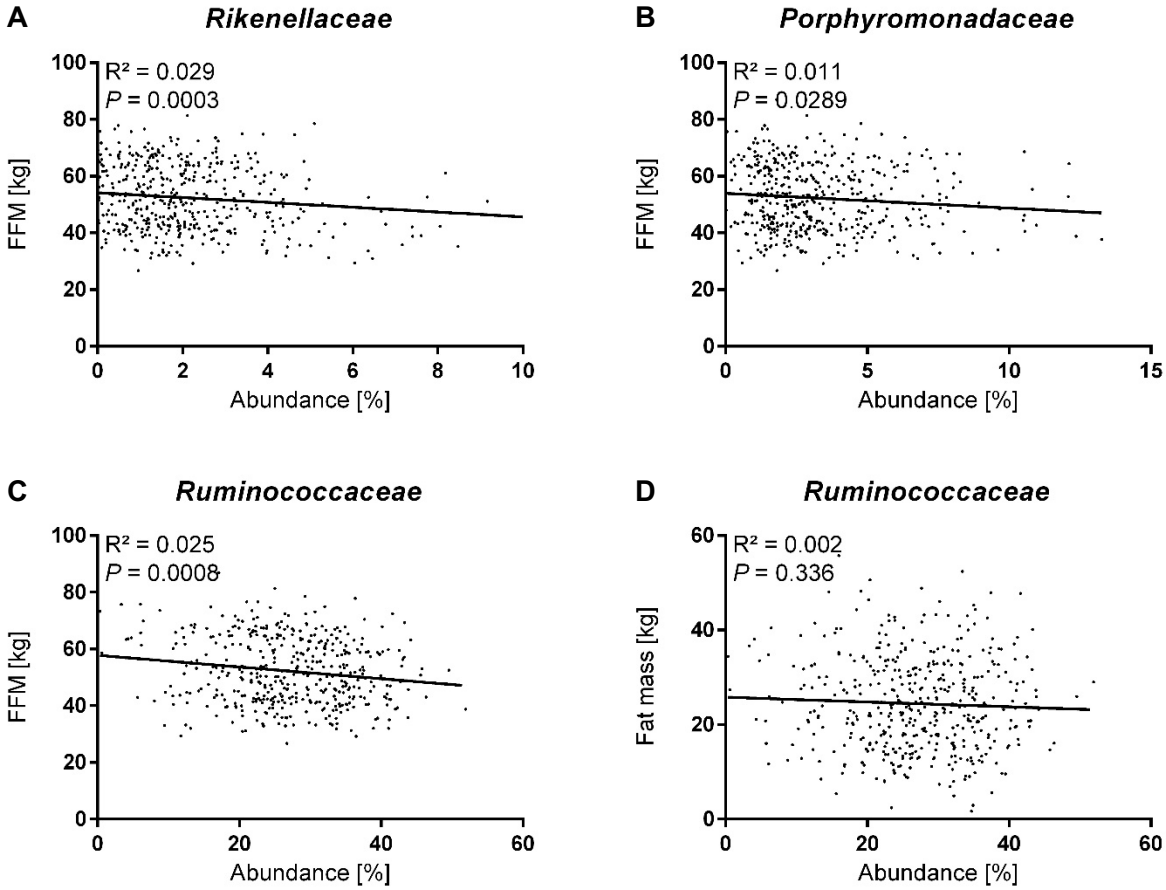

Figure 30: Linear regression analysis of specific gut bacteria with FFM and fat mass. Relative abundance of (**A**) *Rikenellaceae*, (**B**) *Porphyromondaceae* and (**C**) *Ruminococcaceae* significantly correlate with FFM in a linear regression analysis, N = 442. (**D**) The relative abundance of *Ruminococcaceae* does not significantly correlate with fat mass, N = 442.

All three bacterial candidates showed a significant correlation with measured RMR, which disappeared after adjusting RMR for all known influencing variables. Further analysis revealed that the initial correlation of gut microbiota and RMR was due to the variables FFM, thyroid hormone fT_3 and systolic blood pressure, which account for part of the inter-individual variation in RMR. Therefore, we can conclude that these gut bacteria have no direct influence on RMR, but they are associated with variables having an influence on RMR variation.

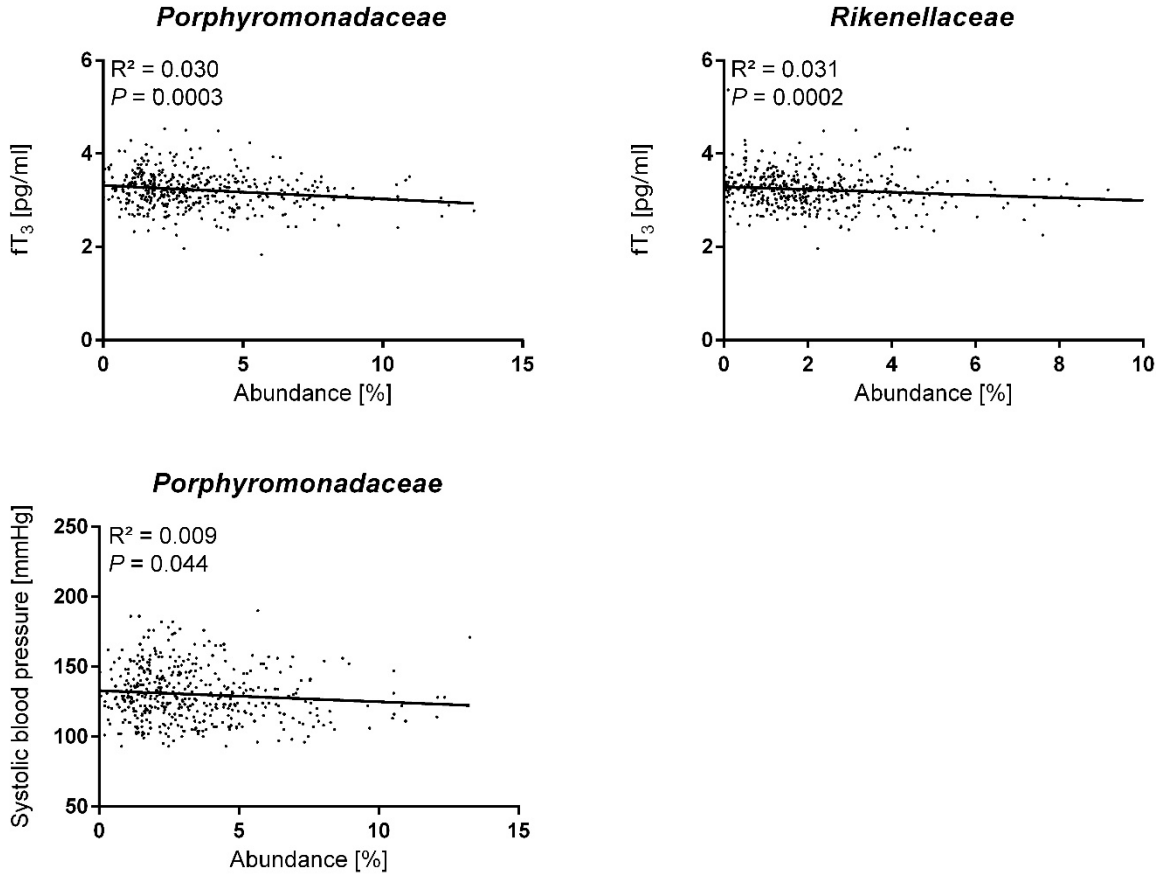

Figure 31: Linear regression analysis of specific gut bacteria with fT_3 and systolic blood pressure. The relative abundance of (**A**) *Porphyromondaceae* and (**B**) *Rikenellaceae* significantly correlated with the amount of thyroid hormone fT_3, N = 442. (**D**) The relative abundance of *Porphyromondaceae* significantly correlated with the systolic blood pressure, N = 442.

3.3.2 Principal component analysis, identifying bacterial cluster influencing resting metabolic rate variation

Analyzing the effect of gut microbiota composition on the residual variation of RMR different statistical procedures were applied. Beside a correlation and linear regression analysis, a principal component analysis (PCA) was performed to simplify a multidimensional data set. A PCA analysis can identify possible cluster of variables, to explain as much variance as possible of the given data set.

The PCA was performed on the taxonomic levels of phylum, class, order, family, genus and species. By analyzing the proportion of variance, the contribution of the individual principal component to the overall variance can be studied. Commonly the first two or three principal components together explain more than 95% of the variance in the data set, depending on the variables going into the analysis. This can also be depicted by the cumulative proportion. In this data set with the gut microbiota of the *enable* cohort, the cumulative proportion of 50% was reached after 18 to 20 principal components. Meaning that these 20 principal components explain 50% of the total variance in the data set and thereby demonstrating a high variance of the data. The principal components explaining most of the variance in the data set were extracted from the PCA and individually analyzed in a linear regression analysis with the residuals of RMR. The residuals of RMR were calculated with the variables FFM, fat mass, body temperature, fT_3, leukocytes, creatinine, MCHC, systolic blood pressure and heart rate, from the previously established linear regression model (model 3,Table 8). By this approach, no principle component was identified to significantly correlate with the residual variation of RMR ($P > 0.05$).

By applying a statistical method to discover possible cluster of variables and explaining as much variance as possible in the present data set, which cannot be detected by humans, no patterns of gut microbiota were identified to correlate with the residual variation of RMR. Concluding that there is on all taxonomic levels no cluster of bacteria detectably contributing to the inter-individual variation in RMR.

3.3.3 Artificial neural network analysis to identify cluster of gut microbiota influencing resting metabolic rate

Further analysis of gut microbiota composition on RMR variation led to the method of artificial neural networks. Neural networks are successfully used in the fields of image and speech recognition or social network analysis. Neural networks have the possibility of learning and can be trained to recognize complex patterns.

In this case, the question was if the neural network is able to identify and create a combination of parameters being able to predict the residual variation of RMR. For proof of principle, a neural network was trained with variables from the linear regression model known to very well predict RMR. The variables age, FFM, fat mass, body temperature, fT_3, leukocytes, creatinine, MCHC, systolic blood pressure and heart rate were mixed among the 1485 OTUs from the gut microbiota to see if a neural network is able to identify important parameters accounting for the RMR variation. A neural network trained with 310 data sets was able to predict RMR in 66 new datasets not initially used for the training, which significantly correlated with measured RMR. The validation set was used to improve continually the generated equation of the training set by applying the generated equation on the validation set and then improving the equation in the training set. If the process of training, improving and verifying is completed the so called “test set” is used to apply the generated equation on an independent set of samples. In all three cases, the prediction significantly correlated with the measured RMR ($P < 0.0001$), which was significantly reproduced in ten individual applied neural network analysis. This result illustrated that a neural network is able to identify important parameters associated with RMR among almost 1500 parameters.

The neural network was then used to identify parameters or cluster of gut microbiota having a possible impact on RMR variation. Therefore, the neural network was applied on all taxonomic levels and until the level of OTUs to predict the residual variation of RMR. The residuals of RMR were calculated with the variable age, FFM, fat mass, body temperature, fT_3, leukocytes, creatinine, MCHC, systolic blood pressure and heart rate from the previous established linear regression model 3 (Table 8). On the level of OTUs, the neural network was able to generate an equation with OTUs to predict the residual variation in RMR (Figure 32). This prediction resulted in a highly significant correlation with the residuals of RMR ($P < 0.05$). However, the neural network was not able to apply this generated equation with OTUs in an independent test set to predict the residual variation in RMR. Not even the validation set was able to improve the training set and resulted therefore also in a non-significant prediction of the residuals. In one out of ten cases a significant correlation of the

prediction and residuals of RMR was observed in the validation set. Since it was only present in one case, this demonstrates to be a random event. On all taxonomic levels the neural network was not able to predict the residuals of RMR, as described for the OTUs.

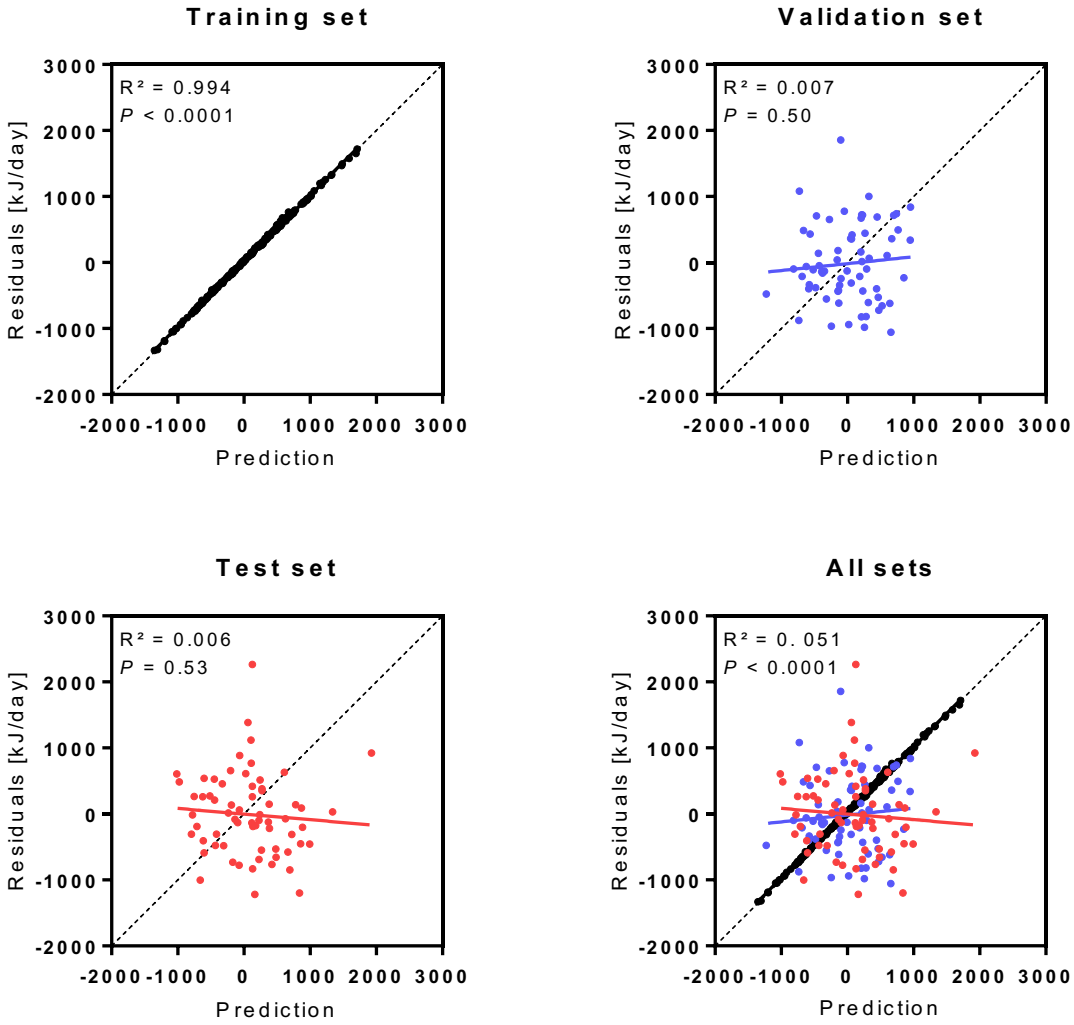

Figure 32: Neural network analysis of gut microbiota on the OTU level. (**A**) Training set, N = 310. (**B**) Validation set, N = 66. (**C**) Test set, N = 66. (**D**) All sets together, depicted by different colors, black = training set, blue = validation set, red = test set, N = 442. Subjects for the individual training, validation and test set were selected randomly by Matlab. (**A-D**) Residuals of RMR were calculated with the variables age, fat mass, FFM, body temperature, MCHC, creatinine, fT_3, leukocytes, systolic blood pressure and heart rate from the linear regression model 3 (**Table 8**).

Taken together, the neural network was able to identify important parameters among many other parameters and to predict the measured RMR by the anthropometric and clinical parameters hidden among more than a thousand other variables. Nevertheless, on all taxonomic levels and on the level of OTUs the neural network was not able to form an

arrangement to predict the residual variation of RMR. Together with the results of PCA, heat-maps and individual correlation analysis, this result illustrates that there is no combination of OTUs or gut bacteria which have an influence on RMR. This leads to the conclusion that gut microbiota composition does not have an influence on RMR variation.

3.4 Liver fat content and inter-individual variation of resting metabolic rate

Inter-individual variation of RMR is determined by variables like sex, age, fat mass and FFM but these variables cannot completely explain the inter-individual variation. High metabolic rate organs were shown to explain 5% of the inter-individual variation of RMR (Javed et al. 2010), however only organ mass was measured and its respective metabolic rate was calculated and not the individual organ activity was measured.

Analyzing the inter-individual variation and variables contributing to RMR variation, a pilot study with 32 subjects was designed to analyze the influence of liver fat content on RMR. The hypothesis was that liver activity may plausibly be associated with fat content and could therefore be used as a marker for liver activity and potentially explain part of the residual variation in RMR. Subjects were recruited based on the phenotyping data raised in the *enable* platform to obtain as far as possible an equal distribution of liver fat in the study cohort. Liver fat was determined by magnetic resonance tomography (MRT) with magnetic resonance imaging (MRI) and magnetic resonance spectroscopy (MRS) scans. The influence of liver fat on RMR variation was analyzed based on the statistical linear regression model, established in the whole *enable* cohort.

3.4.1 Descriptive analysis of the pilot study population

For this pilot study 33 subjects were recruited. After a drop out of three subjects, due to claustrophobia, 30 subjects were left consisting of 17 male and 13 female (Table 14). The mean age of this cohort was 51.0 years in both male and female subjects. The subjects of this cohort are slightly obese, represented by a mean BMI of 27.9 kg/m^2, which was in female slightly higher than in male. The trend of obesity was due to the recruiting criteria, aiming a possible high liver fat content to analyze the influence of liver fat on RMR. One of the selection criteria was the amount of visceral fat, which correlates with an increased body weight and increased abdominal fat.

Table 14: Physical characteristics of the pilot study cohort

	All N = 30			Male N = 17			Female N = 13		
	Mean	±	SD	Mean	±	SD	Mean	±	SD
Age (years)	51.0	±	6.5	50.7	±	6.6	51.5	±	6.6
Height (cm)	174.4	±	8.8	179.4	±	6.5	167.6	±	6.7
Weight (kg)	84.9	±	12.3	89.4	±	10.5	79.1	±	12.4
Body temperature (°C)	36.2	±	0.5	36.1	±	0.6	36.4	±	0.4
Fat mass (kg)	29.6	±	11.8	28.1	±	13.3	31.6	±	9.5
FFM (kg)	55.3	±	9.9	61.3	±	8.6	47.5	±	4.4
RMR (kJ/day)	7134.4	±	1272.7	7931.9	±	1002.7	6091.6	±	703.6
Leukocytes (N/nl)	5.8	±	1.7	5.9	±	1.8	5.6	±	1.7
fT_3 (pg/ml)	3.2	±	0.4	3.4	±	0.2	3.0	±	0.5
Creatinine (mg/dl)	0.8	±	0.1	0.9	±	0.1	0.7	±	0.1
MCHC (g/dl)	34.0	±	0.8	34.4	±	0.7	33.6	±	0.5
BMI (kg/m²)	27.9	±	3.5	27.8	±	2.9	28.1	±	4.2
PDFF (%)	7.6	±	8.4	10.0	±	10.5	4.6	±	2.6
SAT (L)	8.6	±	3.6	7.3	±	2.2	10.3	±	4.4
VAT (L)	3.7	±	2.5	4.6	±	2.6	2.5	±	1.7

PDFF, SAT and VAT were determined by MRI, all other variables were raised at the study center in Freising

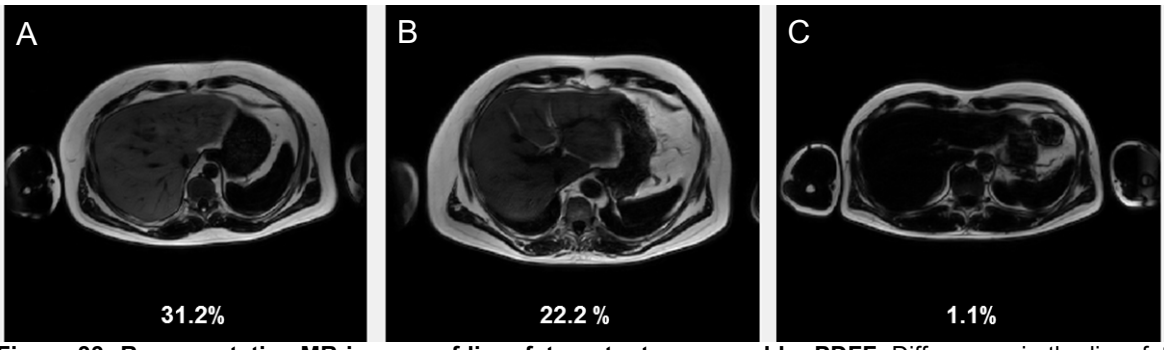

Figure 33: Representative MR images of liver fat content measured by PDFF. Differences in the liver fat content can be seen by appearing brighter with an increasing fat content. Presented are three male subjects with (**A**) a BMI of 29.20 kg/m², (**B**) BMI of 32.42 kg/m² and (**C**) BMI of 22.72 kg/m².

Liver fat content was determined by proton density fat fraction (PDFF) at a defined voxel of 30 x 30 x 20 mm³. The amount of liver fat ranged between 1.1% and 31.2% (Figure 33). By an increasing amount of liver fat, the liver gets brighter and therefore more visible on the MRI, whereas the liver is not visible with little fat content. In all subjects of the pilot study a mean liver fat content of 7.64% was measured, which was in average higher in male (4.64%) than in female subjects (2.50%) (Table 14).

To studying the influence of liver fat on RMR, the aim was to have a study cohort with a wide range of liver fat content (Figure 34). Half of the subjects (N=17) had a low amount of

liver fat between 2 - 4%, eight subjects had elevated amounts of liver fat between 6 10% and five subjects had a fatty liver with 18 - 32% of fat. Besides liver fat, visceral adipose tissue (VAT) and subcutaneous adipose tissue (SAT) were measured during the MRT scans and quantitatively analyzed (Figure 35). The amount of VAT ranged between almost no visceral fat 0.1L and 11L VAT. Half of the subjects (N=17) had low amounts of VAT between 0 - 3L (Figure 34). The other half of the study cohort had high amounts of VAT between 4 - 11L. The VAT content was in female subjects with 2.50L lower than in male subjects with 4.64L, resulting in a mean VAT content of all subjects of 3.71L (Table 14).

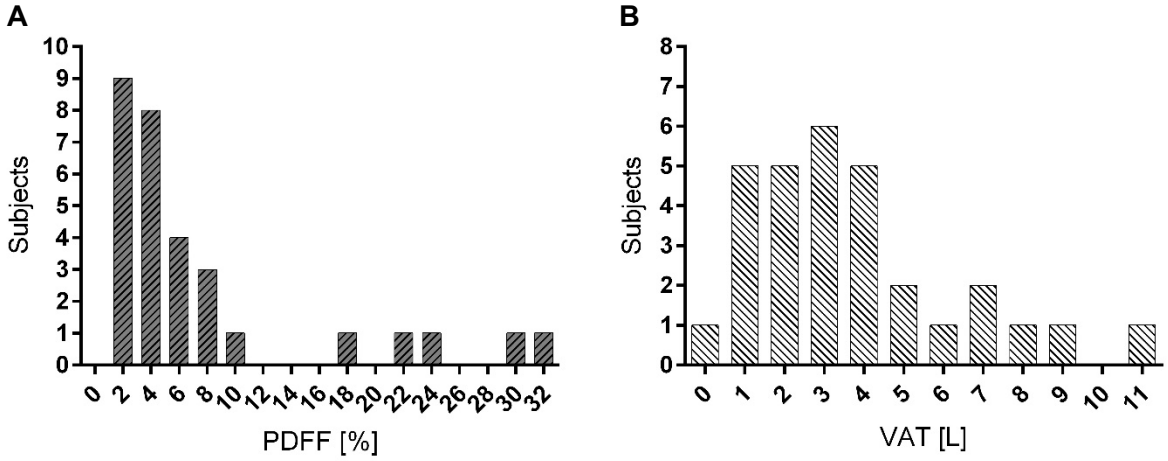

Figure 34: Distribution of liver fat and VAT in the pilot study cohort. (**A**) Frequency distribution of liver fat determined by PDFF at a defined voxel of 30 x 30 x 20 mm³. Presented is the mean liver fat content of 9 segments, N = 30. (**B**) Frequency distribution of the mean visceral fat content (VAT), determined by MR images with a semiautomatic segmentation tool between the apex of the heart and the tip of the femur, N = 30.

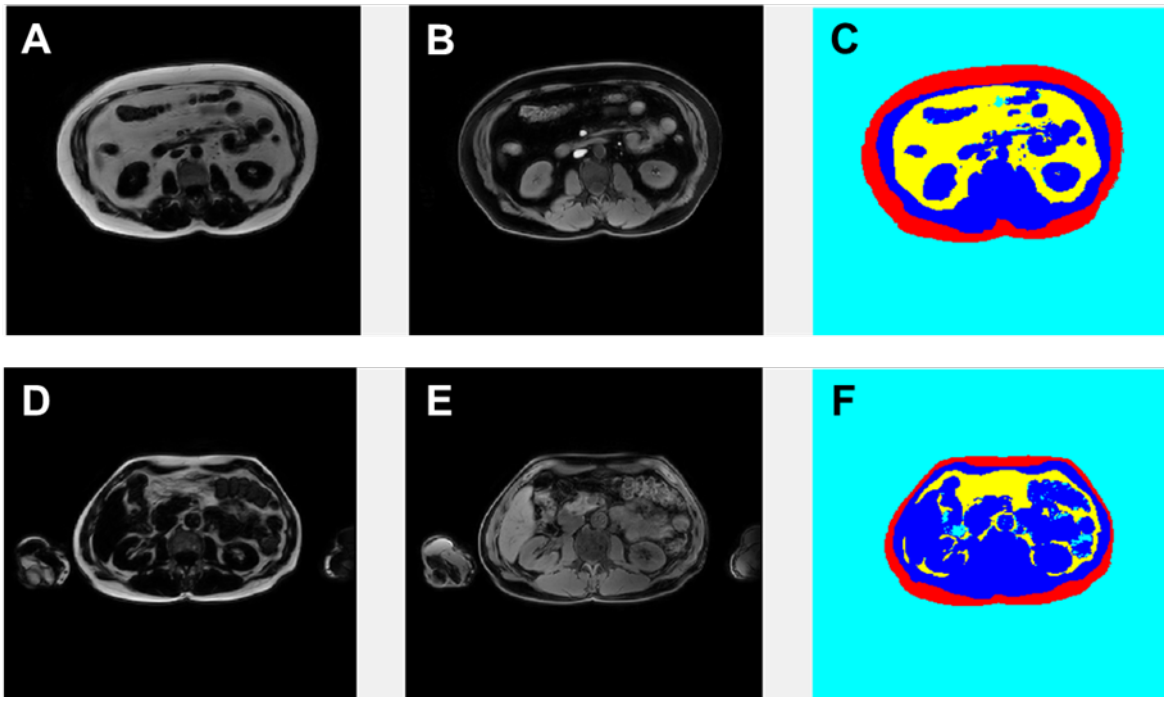

Figure 35: Representative MR images of a 2-point Dixon water-fat image. (**A**) and (**D**) are fat images were fat is presented in white. (**B**) and (**E**) are water images were fat is presented in black. (**C**) and (**F**) are automatic segmentation images of SAT and VAT. SAT is presented in red, VAT in yellow, non-adipose tissue in dark blue and air/bone in cyan blue. (**A** – **C**) Obese subject with a BMI of 29.20 kg/m^2, 8.1 L SAT and 6.6 L VAT. (**D** – **F**) Lean subject with a BMI of 23.23 kg/m^2, 3.5 L SAT and 1.6 L VAT.

To analyze the influence of liver fat on RMR a wide range of liver fat was aimed and achieved. This was accompanied by a wide range of VAT, as VAT was one of the selection criteria to obtain subjects with high liver fat content. Therefore, this small cohort presents a good basis to analyze the influence liver fat on RMR variation.

3.4.2 Influence of liver fat content on the variation of resting metabolic rate

To analyze the effect of liver fat content on RMR variation, the residuals of RMR were calculated. Based on the linear regression model, established in the whole *enable* cohort, the residuals of RMR were calculated for the subject of the pilot study cohort with the variables age, fat mass, FFM, body temperature, fT_3, leukocytes, creatinine and MCHC. The variables systolic blood pressure and heart rate were not available for this pilot study cohort. Therefore, a linear regression model without data about blood pressure was used to calculate the residuals of RMR.

In a linear regression analysis, the effect of liver fat content on the residual variation of RMR was analyzed. No significant correlation (P = 0.52, R^2 = 0.015) of liver fat content and the residuals of RMR was detected. Additionally, the amount of VAT was analyzed regarding its influence on the residual variation of RMR, which resulted in a non-significant correlation

of VAT and residuals of RMR (P = 0.107, R^2 = 0.089). The individual differences in liver fat did not contribute to the inter-individual variation in RMR, despite the high range of liver fat, and did not elucidate if the specific metabolic rate of liver accounts for the residual variation in RMR. The amount of VAT, which was used as a marker to identify subjects with a high liver fat content, was not associated with the residual variation in RMR and therefore not a variable explaining the inter-individual variation in RMR.

Both variables, liver fat and VAT, are included in the variables used to calculate the residuals of RMR. Liver is a high metabolic rate organ and therefore part of FFM, which was used to calculate the residual variation of RMR. Thereby, the amount of liver fat, included in the liver, might already have been taken into account by calculating the residuals of RMR. The same applies for visceral fat, which is a part of fat mass, as well used to calculate the residuals of RMR.

To analyze if the non-existing correlation of liver fat and VAT with the residuals of RMR is due to the adjustment of RMR by fat mass and FFM, liver fat and VAT were analyzed with the unadjusted, measured RMR. No significant correlation of liver fat and measured RMR was observed (P = 0.36) (Figure 37). This verifies the previous result, where liver fat does not explain part of the inter-individual variation of RMR, respectively has an influence on RMR variation.

The linear regression analysis of VAT and measured RMR resulted in a significant correlation (P = 0.004) (Figure 37). This result is in line with the general linear regression model where fat mass is a predictor of RMR. The amount of VAT correlated with RMR, as it is a part of fat mass.

To analyze if the amount of VAT could improve the linear regression model to predict RMR, fat mass was differentiated in general fat mass and visceral fat. Therefore, the amount of visceral fat was subtracted from the total fat mass. To see if the differentiation of the two fat depots can improve the prediction of RMR, both fat depots were included in the linear regression analysis. Thereby the amount of VAT was not an independent predictor of RMR (P > 0.05) and could not improve the linear regression model to predict RMR (data not shown). The total fat mass does influence RMR, but individual difference in the small separate VAT depot did not account for individual differences in RMR.

In conclusion, the amount of liver fat does not contribute to the inter-individual variation of RMR. Despite the significant correlation of VAT and RMR, the amount of VAT could not improve the prediction of RMR as an independent predictor.

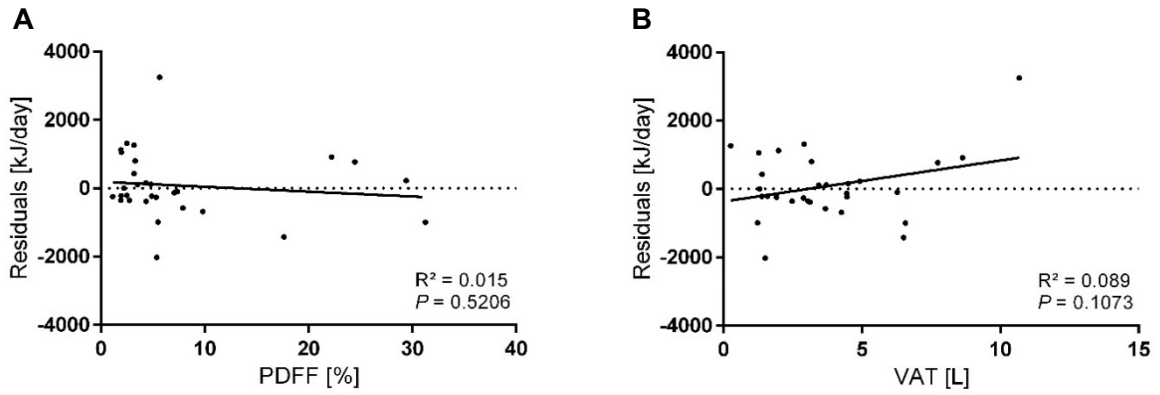

Figure 36: Linear regression analysis of liver fat, VAT and residuals of RMR. (**A**) PDFF was used to determine liver fat content, N = 30. (**B**) VAT presents the visceral fat content, determined by MRI and semiautomatic segmentation tool, N = 30. (**A + B**) Residuals were calculated with the variables age, fat mass, FFM, body temperature, fT_3, leukocytes, creatinine and MCHC.

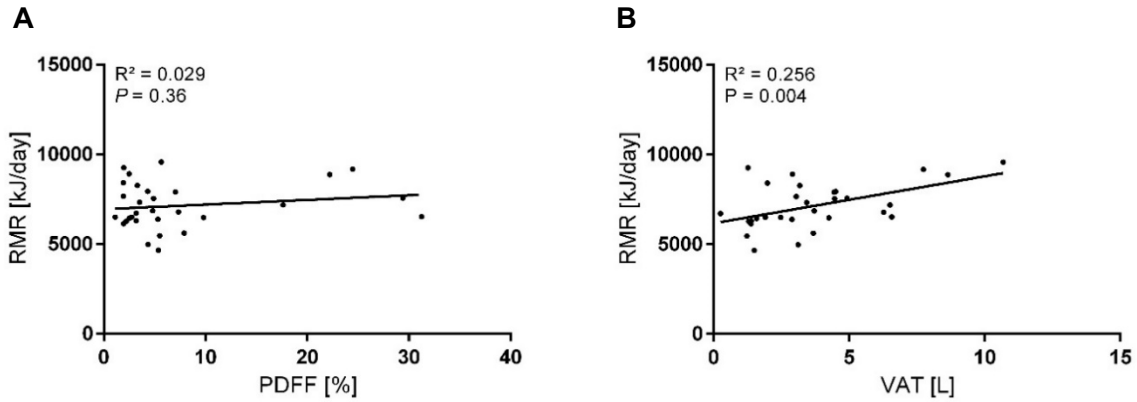

Figure 37: Linear regression analysis of liver fat, VAT and RMR. (**A**) Measured RMR and liver fat represented by PDFF, N = 30. (**B**) Measured RMR and visceral fat content determined by MRI and semiautomatic segmentation, N = 30.

3.4.3 Interaction of liver fat and other metabolic parameters

Increasing liver fat can lead to hepatic steatosis, which has two different reasons. Either alcohol abuse, which leads to alcoholic fatty liver disease or other reasons than alcohol abuse like obesity, which is than termed as non-alcoholic fatty liver disease (NAFLD).

Since an elevated liver fat content is a consequence of either alcohol abuse or unhealthy diet, it is accompanied by other elevated parameters. Therefore, liver fat content was not only analyzed as a variable influencing RMR, but also characterized regarding all other

physical and clinical parameters raised during the phenotyping process. Parameters coming along with obesity might additionally be associated with an increased liver fat content.

Connection of abdominal fat distribution and liver fat was observed by a significant correlation ($P < 0.05$) of liver fat with waist-circumference, waist-to-hip ratio (WHR), VAT and a non-significant correlation with SAT ($P = 0.42$) (Figure 38). Fat distribution in the different fat depots, presented by SAT, VAT and WHR was accompanied by changes of the internal organs, in this case liver fat. In addition, liver fat correlated with BMI ($P = 0.006$) (Figure 39). However, some pre-obese subjects had very high liver fat content, whereas some highly obese subjects had only moderate liver fat content (Figure 39, A). Therefore, BMI alone was not the best parameter to predict liver fat, compared to WHR and VAT.

Studying the relationship of clinical blood parameters and fatty liver, from all the raised blood parameters six were analyzed more in detail (Figure 40). A high insulin concentration was significantly associated with high amount of liver fat ($P = 0.0006$). More than half of the subjects (N = 21) had elevated cholesterol levels above the normal range of 200 mg/dl. The increased amount of cholesterol was significantly associated with liver fat ($P = 0.026$). Seven subjects had elevated blood triglyceride levels which also significantly correlated with the amount of liver fat ($P = 0.018$). Whereas the amount of LDL-cholesterol was not significantly associated with the amount liver fat, thus five subjects had elevated LDL-cholesterol levels above 160 mg/dl.

The progression of fatty liver was presented by the significant correlation of Gamma-glutamyltransferase (GGT) and liver fat ($P < 0.0001$). GGT is an enzyme which is released into the blood when liver cells undergo apoptosis and is therefore a sign for damaged liver cells. The progression of fatty liver and liver damage was supported by the significant correlation of increasing amount of Glutamate-pyruvate-transaminase (GPT) and liver fat ($P = 0.015$). GPT is another enzyme released by liver cells when they are damaged. Even only a few subjects had elevated GGT (> 60U/l) or GPT (> 50 U/l) levels, a strong correlation of liver fat and these enzymes illustrated the progression of hepatic steatosis.

In summary, these results present an increasing liver fat to be associated with several parameters standing for abdominal obesity. The progression of liver damage, caused by fat infiltration, was observed by elevated insulin levels, compensating a reduced glucose tolerance, and elevated enzymes, describing liver cell damage.

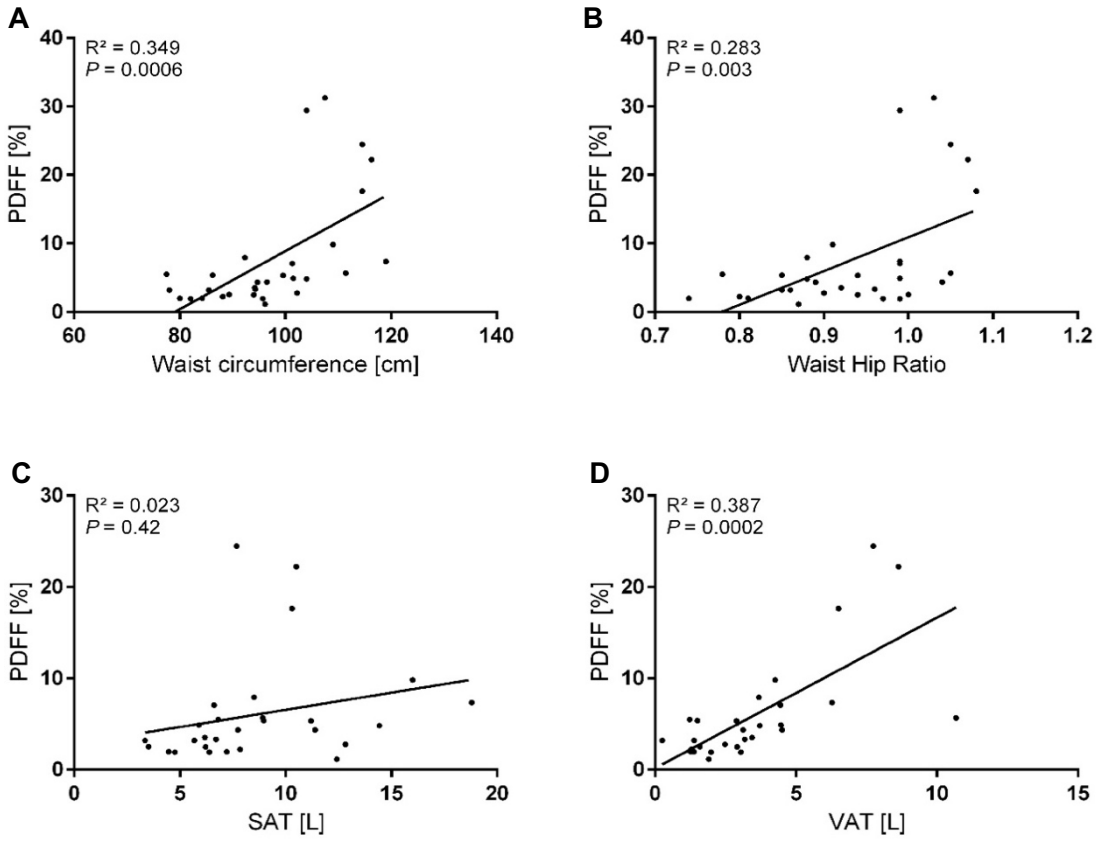

Figure 38: Liver fat and physical characteristics. Linear regression analysis of liver fat content, determined by PDFF and (**A**) waist circumference (**B**) waist to hip ratio (**C**) subcutaneous adipose tissue (SAT) and (**D**) visceral adipose tissue (VAT), N = 30. Waist-circumference, waist to hip ratio and VAT were significantly associated with the amount of liver fat, whereas SAT was not associated with the amount of liver fat.

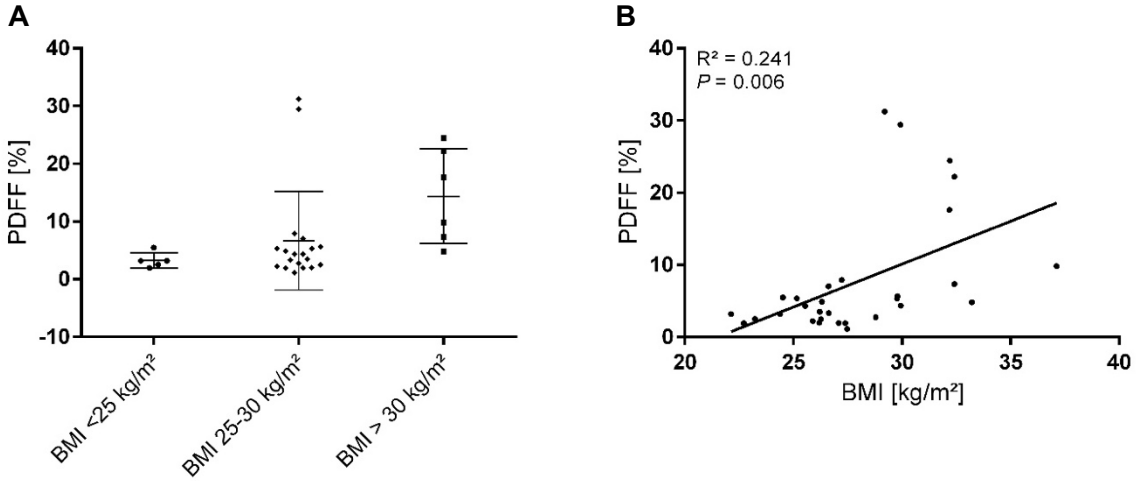

Figure 39: Relationship of liver fat content and BMI. (**A**) Occurrence of liver fat in three BMI classes. Subjects were split in three BMI classes according to the guidelines of WHO, normal weight with a BMI < 25 kg/m² (N = 5), pre-obesity with a BMI between 25 - 30 kg/m² (N = 14) and obesity class I and class II with a BMI between 30 and 39.9 kg/m² (N = 6). (**B**) Increasing liver fat content, depicted by PDFF, significantly correlated with increasing BMI, N = 30.

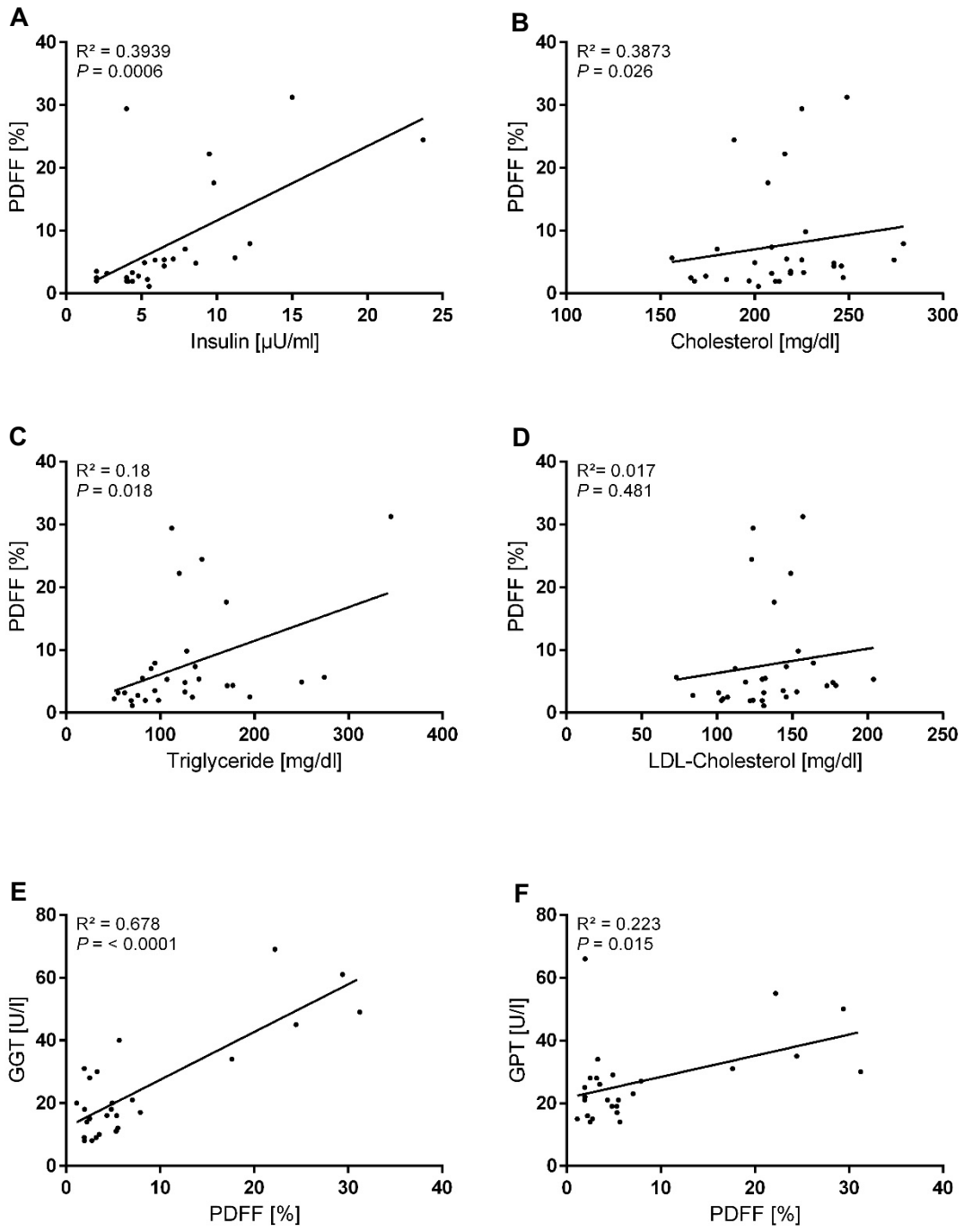

Figure 40: Interaction of liver fat and related blood parameter. (**A - F**) Liver fat content is presented as PDFF in a linear regression analysis with (**A**) Insulin, (**B**) Cholesterol, (**C**) Triglyceride, (**D**) LDL-Cholesterol, (**E**) GGT - Gamma - Glutamyl Transferase and (**F**) GPT - Glutamic Pyruvic Transaminase, N = 26 - 30. All presented blood parameters were significantly associated with liver fat content, except for LDL-Cholesterol.

4 Discussion

The worldwide incidence of obesity has almost tripled in the last 40 years (WHO 2018). The epidemic development of obesity and obesity related diseases requires a precise knowledge of the daily energy requirement to provide adequate dietary recommendations and therapies. The total daily energy expenditure (TDEE) consists of resting metabolic rate (RMR), which accounts for 60 - 80% of TDEE, followed by physical activity with 10 - 30% and adaptive thermogenesis with 10% (Landsberg 2012). RMR is the biggest component of the daily energy expenditure and therefore of particular importance to have a concise knowledge of its functionality and how it is composed.

4.1 Predictors of resting metabolic rate variation

RMR is defined as the energy expenditure at rest to maintain all vital functions. It is characterized by a high inter-individual variation. Variables like sex, age, fat mass, fat free mass (FFM) and race contribute to the variability of RMR and therefore are taken into consideration when analyzing and interpreting RMR (Muller et al. 2004, Javed et al. 2010, Johnstone et al. 2005, Bosy-Westphal et al. 2009a). Even after adjusting RMR for these influencing variables a residual variation of 24 - 30% remains unexplained (Javed et al. 2010, Johnstone et al. 2005). The question arises, which other parameters are influencing RMR and explain the residual variation. Understanding the underlying physiological mechanisms of the variability is of great importance to improve the prediction and calculations of energy requirements for an accurate dietary recommendation.

4.1.1 Body temperature as a predictor of resting metabolic rate

In this work a new equation to calculate RMR is presented, using the variables sex, age, fat mass, FFM and body temperature. Sex, age, fat mass and FFM are parameters which have previously been shown to influence RMR (Javed et al. 2010, Johnstone et al. 2005, Gallagher et al. 2006, Cunningham 1991, Cunningham 1980, Muller et al. 2004). The results of this study presented body temperature to be a new and important variable influencing RMR and thereby contributing to RMR variation. In the context of obesity, a low body temperature was discussed to favor the progression of obesity (Landsberg 2012) due to a reduced RMR. No differences in core body temperature are detected between obese and lean subjects (Hoffmann et al. 2012), but a lower core body temperature may favor the development of obesity in the pre-obese state (Landsberg 2012). However, body

temperature has never been included as a variable in the prediction equations to calculate RMR.

In clinical practice RMR is measured in the thermal neutral zone (TNZ) or thermoneutral environment to avoid heat production or heat loss, which has a major influence on RMR. Increasing temperatures are associated with an increase in metabolic rate (Du Bois 1921), as above the TNZ evaporative heat loss occurs (Roth and Sheard 1950, Kingma et al. 2014) and below the TNZ shivering and non-shivering mechanisms like peripheral vasoconstriction appear to maintain the core body temperature (Landsberg, Saville and Young 1984, Roth and Sheard 1950, Calton et al. 2016). Thus, it is difficult to determine if the subject is really in its individual TNZ. Subjects are not always at their TNZ even when they are measured in an environment of 25°C (Pathak et al. 2017). Consequently, it was proposed to include a forearm to fingertip skin temperature gradient (FFG) measurement to determine if the subject is in its individual TNZ (Pathak et al. 2017).

The results of this study presented body temperature to be an important parameter when predicting and analyzing RMR, which is in line with the proposed measurement of FFG (Pathak et al. 2017). However, based on the results of the present *enable* study it is not possible to distinguish if the differences in the measured body temperature stand either for the individual costs of homeothermy or present the individual deviation from the TNZ during the measurement of RMR.

4.1.2 Resting metabolic rate is influenced by clinical blood parameters and blood pressure

RMR is influenced by the variables sex, age, fat mass, FFM and body temperature. Even after adjusting RMR for these variables a residual variation of 25% remained unexplained (Table 8), raising the question, which other variables contribute to the inter-individual variation of RMR. Analyzing the residual variation of RMR elucidated fT_3, leukocyte number, creatinine, MCHC, systolic blood pressure and heart rate to be important physiological candidates contributing to RMR variation (Table 8, Figure 8).

The results presented a significant impact of the thyroid hormone fT_3 on RMR variation. The residuals of RMR were positively associated with the amount of fT_3 in blood. Thyroid hormones generally play a central role in energy homeostasis and growth (Kim 2008, Lopez et al. 2013). Hypothyroidism is associated with a reduced RMR and weight gain, while hyperthyroidism is associated with an increased RMR and weight loss (Johansen, Hansen and Skovsted 1978, Iwen, Schroder and Brabant 2013). However, so far the function of

thyroid hormones in euthyroid subjects is not fully understood (Kim 2008). In previous studies some authors found a significant correlation of thyroid hormones with RMR (Svendsen et al. 1993, Astrup et al. 1992) some found a moderate influence of thyroid hormones on RMR (Bosy-Westphal et al. 2008) and others found no significant correlation of thyroid hormones and RMR (Meunier et al. 2005, Johnstone et al. 2005, Spadafranca et al. 2015). By analyzing the residual variation of RMR the correlation of fT_3 and RMR is not based on any other variables having a major effect on RMR. Thereby these results proved that differences in fT_3 levels of euthyroid subjects have an influence on RMR and have to be considered when RMR is interpreted and predicted.

Leukocyte number was shown to be positively associated with the residual variation of RMR (Figure 8). Leukocytes are part of the immune system, play an important role in the immune defense and may increase upon an infection. RMR is increased after a vaccination (Cooper et al. 1992) or sepsis (Kreymann et al. 1993), situations in which an immune reaction occurs and therefore leukocytes are increased. Aside from the diseased situations, an increased RMR of healthy Tsimane people was associated with an elevated leukocyte number (Gurven et al. 2016). Nevertheless, the role of leukocytes on healthy Caucasian subjects has not been elucidated so far. The results of this study showed a positive correlation of leukocyte number and residual variation of RMR in healthy Caucasian subjects. Implying minor immune reactions, represented by leukocyte number in a healthy range, play a role in energy requirement and therefore accounted for part of the residual variation in RMR.

Increased levels of creatinine were shown to be negatively associated with the residual variation of RMR (Figure 6). Creatinine is a breakdown product of creatine phosphate, which serves as an energy source of the skeletal muscle. Every day, 1 - 2 % of creatine phosphate is degraded to creatinine, which is excreted by the kidneys. If insufficient fluid is provided by drinking, the kidneys reduce their activity, less creatinine is excreted and, as a consequence, plasma creatinine levels increase. Assuming that increasing creatinine reflects a reduced kidneys activity, plasma creatinine levels might be a suitable method to determine kidney activity. In that case, plasma creatinine levels are an important parameter when analyzing RMR variation.

A positive correlation of MCHC concentration and the residuals of RMR was presented in the results of this study (Figure 6). Hypothetically, a higher RMR causes an increase in hemoglobin per volume of packed red blood cells. As an increased RMR requires more oxygen the amount of hemoglobin per cell is increased to be able to transport more oxygen and compensate for the increased demand of oxygen.

The residuals of RMR were significant association with systolic blood pressure and heart rate (Figure 6, Table 7). In the context of obesity research and cardiometabolic risk factors the relationship of blood pressure and RMR was intensively studied (Bosy-Westphal et al. 2008, Luke et al. 2004, Ali et al. 2017, Creber et al. 2018). Hypertension (Ali et al. 2017, Bosy-Westphal et al. 2008, Luke et al. 2004) and heart rate (Karhunen et al. 1997) are associated with an increased RMR. In obese subjects, blood pressure is associated with RMR, even after adjusting RMR for possible confounder like age and ethnicity (Luke et al. 2004, Snodgrass et al. 2008). However, in healthy individuals the role of blood pressure on RMR variation was not studied so far. There is no equation using blood pressure as a parameter to predict RMR. The results of the present study presented a positive association of systolic blood pressure and heart rate with the residuals of RMR. An increased heart rate reflects an increased activity of the heart, which requires more oxygen and is therefore reflected in an increased RMR. Another possibility might be a stressful situation for the subjects during the measurement, reflected in an increased blood pressure and heart rate. Systolic blood pressure and heart rate were significantly associated with RMR, even after adjusting RMR for the known influencing variables, and are therefore two important parameters having an influence on RMR variation.

Analyzing the residual variation of RMR revealed the thyroid hormone fT_3, leukocyte number, creatinine, MCHC, systolic blood pressure and heart rate to be important physiological candidates influencing RMR variation. All candidates were significantly associated with the residuals of RMR and appeared to be significant predictors of RMR in the linear regression model. However, these six candidates together improved the model by only 3 percentage points (Table 8). Indicating that not just one big variable is missing to explain the residual variation in RMR, but rather several parameters, accounting for the residual variation in RMR. The presented equation with all the blood parameters and blood pressure is more a statistical model elucidating factors contributing to the variability of RMR, rather than an equation for the daily use to predict RMR.

4.1.3 Partitioning of variables contributing to the variation of resting metabolic rate

RMR is influenced by several parameters. It is of added value to understand to which extend the individual variables contribute to RMR variation and how RMR is composed.

In the mixed effect model (Table 6) FFM is with almost 56% the strongest determinant of RMR. This is in line with previous publications, indicating FFM to be the dominant factor, accounting alone for 60 - 72% of RMR variation (Bosy-Westphal et al. 2008, Muller et al. 2004, Johnstone et al. 2005, Karhunen et al. 1997, Ferraro and Ravussin 1992). The close

relationship of FFM and RMR was already described three decades ago (Cunningham 1991). In the present study fat mass was shown to be and independent variable and the second strongest predictor of RMR, being responsible for 11.6% of the variance. Fat mass was identified before, to be an independent variable influencing RMR (Nelson et al. 1992, Svendsen et al. 1993, Ferraro and Ravussin 1992) and being responsible for 6 - 8% of variance in RMR (Johnstone et al. 2005, Ferraro and Ravussin 1992). Sex, age and body temperature accounted together for 12% of the variance in RMR. By combining these variables with FFM and fat mass 80% of the variance were explained by these 5 variables. In previous studies only up to 76% of the variance were explained (Bosy-Westphal et al. 2008), even though HMRO were included in the prediction equation (Javed et al. 2010).

Intra-individual variation was determined to be 4.3% of the total variance in RMR (Schicker 2017). This is in line with previous publications where intra-individual variation was reported to be between 2 - 6% (Weststrate 1993, Zurlo et al. 1986, Adriaens, Schoffelen and Westerterp 2003, Haugen et al. 2003, Bader et al. 2005, Johnstone et al. 2005). The low variation of intra-individual variation presented the indirect calorimetry to be a reliable and repeatable method to determine RMR. The intra-individual variation represents technical and biological day to day variation of the subject. Every subject has a biological variation and every RMR measurement is accompanied by a technical variation, which contributes to the overall inter-individual variation of RMR. By including the intra-individual variation to the overall variance in RMR, 84% of the variance was explained. Leaving a residual variation of less than 16% unexplained.

Adding the parameters fT_3, leukocytes, creatinine, MCHC, blood pressure and heart rate to the linear regression model reduced the effect size of FFM and fat mass. These blood parameters are not only correlating with RMR, but also with FFM and fat mass. A reduced effect size indicates an interaction of the variables among each other, in this case the interaction of blood parameters and blood pressure with FFM and fat mass. Adding parameters to the linear regression model reduced the effect size of the original parameters due to an interaction with the added variables. The addition of blood parameters and blood pressure reduced the influence of FFM on RMR by over 20% and fat mass by 7%, indicating an interaction of the blood parameters, blood pressure and FFM respectively fat mass. FFM was associated with the blood parameters MCHC, creatinine and fT_3. This might be explained by the fact that FFM is not a homogeneous tissue (Gallagher et al. 1998), as it represents high and low metabolic rate organs (Muller et al. 2002, Heymsfield et al. 2002), which have different metabolic rates.

By adding blood parameters and blood pressure to the linear regression analysis new predictors of RMR were identified. Including these physiological candidates to the regression analysis, additionally 3% of the variance in RMR was explained even though each single parameter alone accounted for 3 - 7 % of the variation in RMR. This demonstrates the interwoven complexity of all these factors contributing to RMR. Newly identified factors cannot just be added on top, there are several interactions between the individual variables, even if the effect of the known influencing variables was initially removed. This phenomenon was observed before, by including HMRO and brain to the linear regression model, rendering the effect of age, race and sex non-significant (Javed et al. 2010).

4.1.4 High accuracy of the newly established equation to predict resting metabolic rate

Several equations have been generated to predict RMR, since measuring RMR is a complex and time-consuming method, which requires strictly standardized conditions. However, there is a high inter-individual variation in RMR, and the precision and accuracy of the recommended equations varies. Well-established and commonly used equations are the equation from Harris-Benedict (Harris and Benedict 1918) and Food and Agriculture Organization/World Health Organization/United Nations University (FAO/WHO/UNU) (WHO (1985). The Harris-Benedict equation uses the variables weight, height and age to predict RMR whereas the WHO equation solely uses weight to predict RMR. In current research factors like sex, age, fat mass and FFM (Gallagher et al. 1998, Gallagher et al. 2006) are taken into consideration when predicting RMR, which account for 60 - 70 % of variation in RMR (Muller et al. 2004, Javed et al. 2010). In addition, FFM is the major predictor of RMR (Bosy-Westphal et al. 2008, Johnstone et al. 2005, Ferraro and Ravussin 1992) and was suggested to be used instead of body weight to predict RMR (Nelson et al. 1992, Wang et al. 2000). Therefore, the question arises whether the commonly used equations from Harris-Benedict and WHO adequately predict RMR, which mainly use body weight and thereby differences in body compositing are neglected.

In this work, an equation to predict RMR is presented, characterized by a high accuracy and precision. Precision of the newly developed equation was confirmed by a cross-validation with an independent study cohort. Compared to the commonly used equations from WHO, Harris-Benedict, Tanita and Kleiber, the newly developed equation presented the highest coefficient of determination to predict RMR. However, RMR prediction and comparison of the newly developed equation with the common equations was performed

with the *enable* cohort and not with a completely independent cohort, which might possibly result in a different coefficient of determination. From the analyzed equations the WHO equation predicted RMR with the highest accuracy after the newly developed equation. However, the WHO equation is not one single equation for all ages and sexes. It consists of eight different equations, distinguishing on the one hand between men and women, and on the other hand between four different age groups, whereas the equation from Harris-Benedict only distinguishes men and women. These two equations have been established decades ago and predict RMR by body weight, respectively height and age. Previously, FFM was discussed to be used as the major determinant to predict RMR instead of body weight (Nelson et al. 1992, Wang et al. 2000). The equation embedded in the BIA scale from Tanita consists only of one equation and calculates RMR by the variables FFM, age and weight. This equation predicted RMR the second most accurate after the WHO equation. Nevertheless, the equation provided by the Tanita scale, was not developed to calculate RMR of children.

The equation from Harris Benedict and WHO were previously reanalyzed and evaluated (Muller et al. 2004, Rao et al. 2012, De Lorenzo et al. 2018, Henry 2005). The WHO equation overestimates RMR at low and underestimates at high RMR (Muller et al. 2004), whereas the Harris-Benedict equation predominantly overestimates RMR (Frankenfield, Roth-Yousey and Compher 2005). The specific metabolic rate at low body mass respectively low FFM is increased (Muller et al. 2004), which shows the importance to use FFM as the main variable to predict RMR instead of body weight. The WHO equation is based on a huge study cohort with more than 7000 subjects. However, these subjects are from various ethnicities, different ages, weight and were phenotyped in different study centers with different equipment's. Thus, a not insignificant number of subjects had an BMI below 17 kg/m^2 and were strongly underweight. The presented *enable* study was a homogeneous study cohort of healthy Caucasian subjects. All subjects were phenotyped by trained staff in two equally equipped study centers. However, the presented equation is only applicable for Caucasian subjects and was established on a comparatively small study cohort.

In summary, the presented equation is characterized by a high precision to predict RMR, by using only anthropometric and body composition data. Compared to the commonly used equation provided by WHO and Harris-Benedict, the presented equation is one single equation, applicable for men and women for a wide range of age.

4.2 Peripheral blood mononuclear cells as a biomarker for mitochondrial activity

Mitochondria are the 'powerhouse' of a cell to produce energy in form of ATP. Energy is provided in response to acute or chronic energy demand. Measuring ATP production in response to energy demand gives information about the efficiency and capacity to generate ATP (Jheng et al. 2015, Liesa and Shirihai 2013, Brand and Nicholls 2011). Mitochondrial function can be assessed in peripheral blood mononuclear cells (PBMCs) (Ost et al. 2018). As PBMCs are circulating cells of the blood they are directly affect by systemic changes like inflammatory processes and metabolic stress. Recently, the inflammatory processes of sepsis and diabetes were found to be associated with the respiratory capacity of PBMCs (Hartman et al. 2014, Belikova et al. 2007, Alonso et al. 2004). Therefore, PBMCs might also reflect processes globally affecting RMR variation. However, PBMCs as a biomarker for mitochondrial activity in healthy subjects has not deeply been analyzed so far.

4.2.1 Protocols to measure mitochondrial respiration of PBMCs

For respiration measurements, PBMCs are freshly isolated from blood by density gradient centrifugation (Riedhammer, Halbritter and Weissert 2016). Mitochondrial activity of PBMCs can be assessed by high resolution respirometry, in a chamber-based system. Different respiratory states of intact and permeabilized PBMCs can elucidate functional changes of mitochondria (Doerrier et al. 2018). Substrate uncoupler inhibitor titration protocols (SUIT) combine substrates, uncoupler and inhibitors to assess the different respiratory states like leak, oxidative phosphorylation (OXPHOS) and the capacity of the electron transport system (ETS). However, there are different possibilities how to assess these respiratory states. So far there is no consensus for an ideal isolation procedure, respectively protocol to measure mitochondrial activity of PBMCs.

In the present study, different isolation procedures and respiration protocols were tested, analyzing the respiratory states of leak, OXPHOS and uncoupled respiration. Leak respiration can be either determined by oligomycin, which inhibits the ATP-synthase, or after permeabilizing the cells. Usually leak respiration is assessed by a prolonged waiting time, after permeabilizing the cells with digitonin (Ost et al. 2018). In the present study, leak respiration after permeabilization with digitonin resulted in a reduce OXPHOS capacity, whereas leak respiration induced by oligomycin inhibited the uncoupled respiration under FCCP. The reduced OXPHOS capacity indicates a lot of stress for the cells during the prolonged waiting time after permeabilization. Therefore, these cells could not achieve the same OXPHOS capacity as other cells, which were not exposed to this stressful situation. However, leak respiration under oligomycin was more stable and better reproducible

compared to leak respiration after permeabilization. Both approaches to assess leak respiration have their advantages and disadvantages. On the one hand oligomycin repressed the uncoupled respiration under FCCP and the real maximal uncoupled respiration could not be determined. On the other hand, leak respiration after permeabilizing with digitonin resulted in a reduced OXPHOS capacity due to a lot of stress for the cells.
PBMCs are isolated by density gradient centrifugation and it is recommended to isolate cells directly after taking the blood sample (Hsiao and Hoppel 2018, Corkum et al. 2015). Results of the present study demonstrated that PBMCs can also be isolated a few hours after taking the blood sample, without affecting the mitochondrial activity. This observation is in line with the results of a previous master thesis (Schicker 2017), and another publication (Karabatsiakis et al. 2014). Even no differences in fresh and frozen PBMCs was observed (Karabatsiakis et al. 2014), but if PBMCs could also be cryopreserved for a longer time period has to be further analyzed. One limitation of the present study was the availability of two high-resolution respirometer, therefore the measurement was limited to four blood samples simultaneously. The storage of blood samples, respective cryopreservation of PBMCs, has the advantage that several blood samples of different subjects could be taken on one day, and assess mitochondrial activity later on.

Based on these results, there is no protocol where all respiratory states can perfectly be determined. Depending on the scientific question the different options have to be considered carefully with the knowledge that not every respiratory state can accurately be determined at once. First steps to store blood samples have been undertaken and there are some possibilities to assess mitochondrial activity of PBMCs to a later time point.

4.2.2 Mitochondrial activity of PBMCs has no influence on resting metabolic rate variation

Inter-individual variation of RMR is mainly explained by variables like sex, age, fat mass, FFM and body temperature. Adjusting RMR for these influencing variables, a residual variation of about 20% remains. Recently, mitochondrial activity of skeletal muscles was found to be associated with whole body oxygen consumption (Larsen et al. 2011, Wijers et al. 2008). Energy expenditure, respectively RMR, is determined by measuring oxygen consumption and carbon dioxide production (Atwater 1905). Since mitochondrial respiration takes about 90% of the total oxygen turnover to produce energy in form of ATP by oxidative phosphorylation the question arises whether individual difference in mitochondrial activity account for the inter-individual variation of RMR.

To assess whether PBMCs could be used as a biomarker to determine mitochondrial activity, respiratory capacity of PBMCs was determined. The respiratory activity of PBMCs was not associated with the residual variation of RMR and therefore individual differences in mitochondrial activity did not explain inter-individual variation of RMR. Earlier, basal metabolic rate (BMR) was associated with mitochondrial respiration (Porter and Brand 1993). Mitochondrial proton leak correlates with BMR and it was suggested to be an important parameter accounting for interspecies variation of BMR in mammals (Porter and Brand 1993), thus it was proposed that proton leak contributes with 20 - 25% to the in vivo BMR (Rolfe and Brand 1996). In contrast, recent results found no association of proton leak and BMR (Larsen et al. 2011). Furthermore, mitochondrial coupling, meaning the ATP produced per consumed oxygen, was not associated with BMR (Befroy et al. 2008). However, an increased RMR was associated with a reduced oxygen affinity of skeletal muscle mitochondria (Larsen et al. 2011). Thereby the hypothesis was raised that differences in the oxygen affinity of mitochondria explain inter-individual variation in RMR (Larsen et al. 2011). So far, there is no clear correlation of mitochondria respiration and RMR.

Previously, energy expenditure was associated with an increase in uncoupling respiration of skeletal muscle cells, upon a cold stimulus (Wijers et al. 2008). Since FFM and fat mass are major predictors of metabolic rate, mitochondrial respiration was predominantly studied in skeletal muscle and adipocytes (Jheng et al. 2015, Liesa and Shirihai 2013, Rustin et al. 1994). In contrast to skeletal muscle and adipocytes, PBMCs represent a very small fraction of cells with less than 1% of the whole body cell mass, which is expected to be $3.72 \times 10\text{^}13$ cells (Bianconi et al. 2013). Nevertheless, PBMCs have the advantage to be accessible by a minimal invasive procedure of a venipuncture (Ost et al. 2018), compared to invasive procedure of a muscle biopsy. As circulating cells PBMCs might reflect systemic changes affecting RMR variation, whereas adipocytes and muscle cells reflect only local changes of adipose tissue and muscle.

Leukocyte number was found to explain part of the residual variation of RMR. An increased leukocyte number was associated with an increased RMR. Leukocytes are part of the PBMC population, which is a heterogenous cell population, consisting of lymphocytes, monocytes and dendritic cells (Kleiveland 2015). The frequency and composition of these cells varies among individuals (Kleiveland 2015). Since leukocytes are part of the immune system, they may increase upon an infection. The correlation of leukocytes and RMR might therefore imply that minor immune reactions play a role in energy requirement. Not only leukocytes, but also monocytes and lymphocytes respond to an immune activation.

Especially T-cells, belonging to lymphocytes, can respond to stressful situations by using their spare respiratory capacity to generate additional energy (van der Windt et al. 2012). For the present study, respiration measurements were performed with a defined number of PBMCs, to obtain comparable results. However, there was a big variation of PBMC number between individuals. Since an increased leukocyte number was associated with an increased RMR also the increased PBMC number may explain inter-individual difference in RMR. Moreover, in a recent master thesis an increased leukocyte number was associated with a higher number of isolated PBMCs (Schicker 2017). Differential composition and frequency of PBMCs may play a role in RMR variation. Additionally, measurements of isolated T-cells or other singular cell populations may explain individual differences in RMR. Taken together, mitochondria play an important role in energy metabolism, whether and how mitochondrial respiration affects resting metabolic rate is not clear. The simple, non-invasive and fast approach to assess mitochondrial activity is a clear advantage of PBMCs. However, the possibility of PBMCs as a biomarker for mitochondrial activity in the context of energy homeostasis has to be further analyzed, regarding the different cell populations of PBMCs, their frequency and individual activity.

4.2.3 Declining mitochondrial activity of peripheral blood mononuclear cells with age

The process of aging is associated with physiological changes and loss of fitness. Age related changes are presented in a decline of muscle mass, increase in fat mass, reduced RMR (Bosy-Westphal et al. 2003) and mitochondrial changes (Harman 1956), arising the question whether general physiological processes of aging are reflected in the mitochondrial activity of PBMCs.

Across the three adult cohorts of *enable*, an increased proton leak was associated with increasing age. The tendency of a reduced uncoupled respiration and increased leak respiration resulted in a significantly reduced uncoupled respiratory control ratio (RCRu), indicating an impaired mitochondrial function in elder subjects. The reduced mitochondrial function was accompanied by a trend of reduced basal respiration and OXPHOS capacity. Early on, proton leakage was described to be a factor contributing to the process of aging, due to an impaired inner mitochondrial membrane (Ames et al. 1995). Thus, aging was associated with a reduced efficiency of the respiratory chain (Green, Galluzzi and Kroemer 2011), reflected in a reduced OXPHOS capacity of skeletal muscle cells (Trounce, Byrne and Marzuki 1989), resulting in a reduced ATP production (Green et al. 2011).

The efficiency of ATP generation is based on the integrity of the inner mitochondrial membrane, to build up a membrane potential without compensating too much for proton leakage. Cardiolipin is a large phospholipid comprising 20% of the inner mitochondrial membrane and an important factor to keep up the membrane integrity. Therefore, cardiolipin plays an important role in the OXPHOS efficiency, respectively ATP production (Chicco and Sparagna 2007, Shigenaga, Hagen and Ames 1994). In addition, aging was associated with increasing levels of reactive oxygen species (ROS) (Kauppila, Kauppila and Larsson 2017), which affect cardiolipin by peroxidation (Chicco and Sparagna 2007), resulting in a reduced membrane integrity. The reduced levels of cardiolipin lead to an increase in proton leak (Ames et al. 1995) and reduced ATP generation (Green et al. 2011) in aging subjects. These age-related changes were observed in the respiratory capacity of PBMCs in the *enable* cohort. Elderly exhibited an increased proton leak and a reduced efficiency to generate ATP, reflected in a mildly reduced OXPHOS capacity, which might be due to changes of the membrane integrity of the inner-mitochondrial membrane.

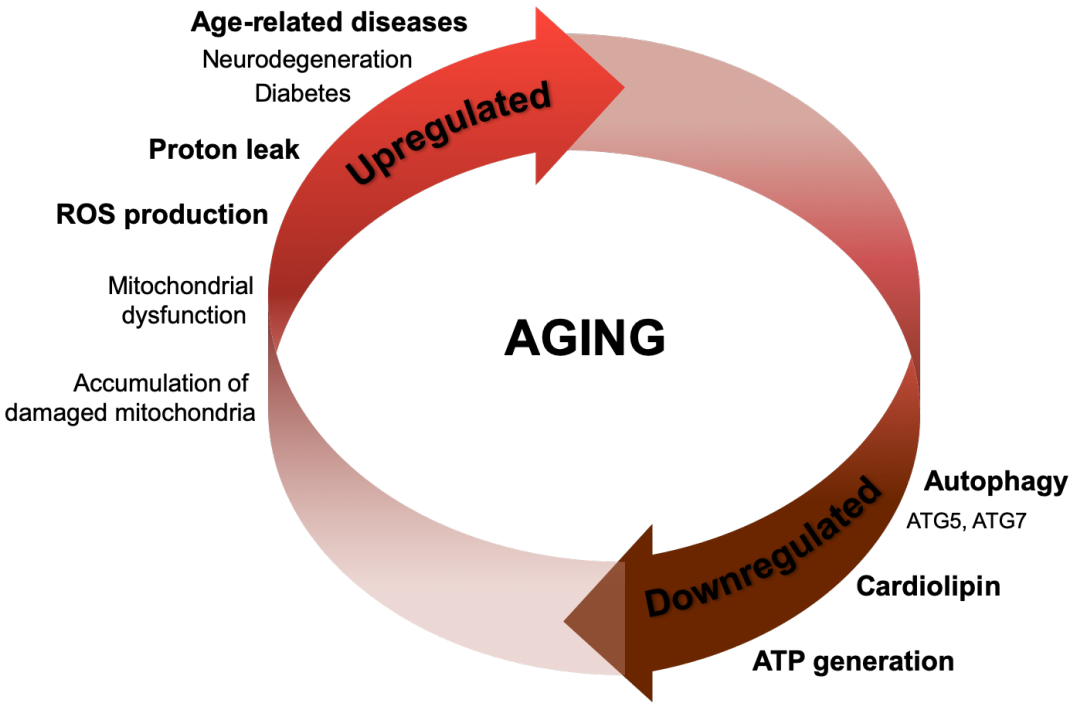

Figure 41: Physiological changes associated with aging Aging is associated with some mechanisms which are 'upregulated' and some are 'downregulated'. Upregulated mechanisms like an increased production of reactive oxygen species (ROS), increased proton leak and mitochondrial dysfunction are presented along the red arrow. Downregulated mechanisms like ATP production, autophagy and cardiolipin are presented along the brown arrow. Enzymes involved in autophagy are ATG5 and ATG7, found to be downregulated in aging subjects. These mechanisms do not elucidate if aging is a cause or consequence of these processes.

The observation of age-related changes in mitochondrial respiration might also be due to an accumulation of damaged mitochondria. Damaged mitochondria are removed by autophagy (Kroemer, Marino and Levine 2010), which is triggered by enzymes and proteins (Tait and Green 2010). Autophagy and the related enzymes and proteins are reduced in aging subjects (Lipinski et al. 2010), leading to an accumulation of damaged mitochondria. The accumulation of damaged mitochondria may favor the development of age-related diseases like diabetes mellitus type 2 or neurodegenerative diseases (Sebastian et al. 2017).

Mitochondrial activity of PBMCs were associated with age related changes, presented by an increased proton leak and the tendency of a reduced ATP generation. These observations could be due to an increased proportion of damaged mitochondria or reduced cardiolipin levels. Analyzing cardiolipin and ROS production could further elucidate age related changes in mitochondria of PBMCs.

4.3 Gut microbiota composition does not explain the residual variation of resting metabolic rate

The gut microbiome is a complex ecosystem consisting of almost 38 billion bacteria (Sender et al. 2016). In the context of obesity an altered gut microbiota composition was found in obese compared to lean subjects (Scheepers et al. 2015). Overweight individuals exhibit an increased ratio of *Firmicutes* to *Bacteroidetes* (Ley et al. 2006, Castaner et al. 2018, Abdallah Ismail et al. 2011, Ley et al. 2005), with the increased capacity to extract energy from the diet (Turnbaugh et al. 2006, Shen et al. 2014). The question arises whether an altered gut microbiota composition influences energy homeostasis and thereby RMR.

Association of RMR with gut microbiota diversity and bacteria from the family level disappeared after RMR was adjusted by the influencing variables sex, age, fat mass, FFM, body temperature, leukocytes, fT_3, MCHC, creatinine and blood pressure, demonstrating clearly that gut microbiota composition has no direct influence on RMR variation. These findings were supported by individual correlation, neural network and principal component analysis on all taxonomic levels. Analysis of gut microbiota and the variables influencing RMR revealed a negative correlation of the family bacteria *Ruminococcaceae*, *Porphyromondaceae* and *Rikenellaceae* with FFM (Figure 29). This explained the previous observed association of these gut bacteria with RMR, since FFM is a major determinant of RMR.

Ruminococcaceae belong to the phylum of *Firmicutes*, which have been associated with obesity (Abdallah Ismail et al. 2011, Ley et al. 2006, Beaumont et al. 2016). The abundance

of *Ruminococcaceae* is associated with body composition (Smith-Brown et al. 2018), fat distribution (Min et al. 2019) and visceral fat mass (Beaumont et al. 2016). Furthermore, they are negatively associated with the metabolic syndrome (Ferrer et al. 2013, He et al. 2018), which is the occurrence of several symptoms like abdominal obesity and high serum triglycerides among other things. Different studies have observed a correlation of an increased abundance of *Ruminococcaceae* and fat mass, respectively overweight. This observation is consistent with the association of an increased abundance of *Firmicutes* in obese people, as *Ruminococcaceae* belong to the phylum of *Firmicutes*. However, the results of the present study showed an opposite trend. Adjusting FFM for body weight eliminated the correlation of FFM and *Ruminococcaceae* (data not shown), illustrating the observed correlation be due to total body mass and not body composition. This presented a reduced body mass to be associated with an increased abundance of *Ruminococcaceae.* This is the opposite as described in literature where a reduced body weight is associated with reduced abundance of *Firmicutes* respectively *Ruminococcaceae*. The results of this study rather indicated that *Ruminococcaceae* do not behave like 'typical' *Firmicutes*, which increase with increasing body mass.

The family *Rikenellaceae* and *Porphyromondaceae* were negatively associated with FFM. *Rikenellaceae* and *Porphyromondaceae* belong to the phylum of *Bacteroidetes*. *Bacteroidetes* stand for a healthy, balanced diet (David et al. 2014) and are increased in lean subjects (Ley et al. 2005). Adjusting FFM for body mass eliminated the correlation of *Porphyromondaceae* with FFM, indicating an association with body mass and not solely FFM (data not shown). The association of an increased abundance of *Porphyromondaceae* and reduced body mass is in line with the observation of an increased abundance of *Bacteroidetes* in lean subjects, as *Porphyromondaceae* belong to the phylum of *Bacteroidetes*.
The correlation of *Rikenellaceae* and FFM still existed after adjusting FFM for body weight (data not shown). This presents a direct association of reduced FFM with increased abundance of *Rikenellaceae*. However, only a few subjects illustrated a really high abundance of *Rikenellaceae*. This indicates some special circumstances lead to an increased abundance of *Rikenellaceae* and reduced FFM but not reduced total body weight. These subjects should be analyzed separately to investigate if a specific diet or a reduced protein intake is leading to this phenomenon.

Taken together, not every bacterium belonging to the phylum of *Firmicutes* and *Bacteroidetes* can simply be accredited with their respective characteristics. Findings of the

present study illustrate the difficulty to identify gut microbiota associated with body composition, respectively body weight. Any association of gut microbiota and RMR disappeared when the effect of FFM and other predictors of RMR was removed, demonstrating clearly that gut microbiota composition does not account for RMR variation.

4.4 Liver fat in the context of resting metabolic rate and abdominal obesity

Inter-individual variation of RMR is determined by variables like body composition, sex, age and clinical blood parameters. FFM accounts for the biggest part of the inter-individual variation with 30 - 60% and was therefore analyzed in several studies regarding its influence on RMR (Gallagher et al. 2006, Gallagher et al. 1998, Javed et al. 2010, Bosy-Westphal et al. 2004). However, FFM is not a homogenous tissue and is resembled by high and low metabolic rate organs. HMRO are heart, liver, spleen, kidneys and brain, which account for less than 6% of body weight but for 60 - 70% of RMR (Elia 1992, Gallagher et al. 1998). Whereas, skeletal muscle, as a low metabolic rate organ (LMRO), accounts only for 20 - 30% of RMR and resembles 40 - 50% of the body weight (Gallagher et al. 1998, Elia 1992). Commonly high and low metabolic rate organs are combined in FFM and are not differentiated. A previous study showed that additionally 5% of the inter-individual variation in RMR are explained by the size of HMRO (Javed et al. 2010). Nevertheless, measuring only organ size does not elucidate if changes in the organ density or lipid accumulation affect the individual organ activity (Javed et al. 2010).

In the present study, liver fat was measured instead of liver activity, based on the hypothesis that increasing amounts of fat result in a reduced organ activity and therefore explain part of the residual variation in RMR. The results did not show an association of liver fat and RMR variation. The hypothesis, that increasing liver fat would reduce the specific organ metabolic rate, was raised before (Bosy-Westphal et al. 2004). However, in a subjects with nonalcoholic steatohepatitis the calculated RMR, based on a theoretical liver fat content of 50%, underestimated the measured RMR (Bosy-Westphal et al. 2004). This led to the assumption that increasing amounts of liver fat lead to a hypermetabolic state to compensate for fat infiltration (Bosy-Westphal et al. 2004). This is in line with the observation of an increased RMR in subjects with liver cirrhosis, presenting also a hypermetabolic state (Perseghin et al. 2002). In the present study no association of liver fat and RMR was observed, and also no tendency indicating an association. This might be due to the small study cohort existing of only 30 subjects, respectively five subjects with really high liver fat content. To analyze the correlation of liver fat on RMR variation a larger sample size with a larger number of high liver fat might be necessary.

For a long time, liver biopsy was the gold standard to determine liver fat, respectively hepatic steatosis (Bravo, Sheth and Chopra 2001, Gaidos, Hillner and Sanyal 2008). A biopsy is an invasive method and therefore unsuitable for the daily and frequent use. In recent years magnetic resonance spectroscopy (MRS) and magnetic resonance imaging (MRI) have become the gold standard to determine liver fat (Reeder, Hu and Sirlin 2012). However, the method of MRI and MRS to determine liver fat by proton density fat fraction (PDFF) is limited and not available at every hospital or study center. Fatty liver is associated with abdominal obesity, especially VAT, but so far the amount of liver fat cannot easily be assessed by anthropometric measurements.

Subjects of the present study were selected based on VAT and body mass index (BMI), to increase the probability of high liver fat. Visceral adipose tissue and BMI were both strongly associated with the amount of liver fat. Additionally, the anthropometric parameters waist-circumference and waist to hip ratio (WHR) were associated with liver fat, whereas the mass of subcutaneous adipose tissue (SAT) was not related to liver fat. The measurement of waist-circumference was already described to be a simple method to determine the abdominal fat distribution, respectively VAT (Alberti et al. 2005, Alberti and Zimmet 1998), which is strongly associated with liver fat (Kotronen et al. 2007, Rocha et al. 2005, Jakobsen et al. 2007). The parameter WHR describes more in detail how the abdominal fat is distributed and would therefore be a more precise parameter to be associated with liver fat. However, the present results showed a weaker association of liver fat with WHR than with waist-circumference.

Liver fat was described to be associated with BMI (Wilman et al. 2017). This observation is in line with the present study results, where liver fat was related to BMI. Nevertheless, a detailed look at the distribution of BMI and liver fat, revealed some subjects with really high liver fat content but pre-obese BMI, whereas some subjects of the obesity class I and II had only slightly elevated liver fat content. BMI does not distinguish between lean and fat mass and was therefore depicted to be an imprecise parameter to determine adiposity (Romero-Corral et al. 2008). The results of the present study revealed VAT to be a better predictor of liver fat, compared to BMI. Visceral adipose tissue was shown before to be associated with liver fat, more than any other anthropometric parameter (Kotronen et al. 2007, Speliotes et al. 2010). Furthermore, there is no association of SAT and liver fat (Kelley et al. 2003), respectively the correlation is controversial (Jakobsen et al. 2007). These observations describe the inaccuracy of BMI to determine liver fat, due to neglecting the distribution of lean and fat tissue, respectively the distribution of adipose tissue depos, described by SAT and VAT. Thus, by using BMI as a parameter to determine adiposity the phenomenon of thin outside, fat inside (TOFI) phenotype is neglected, where a low BMI is

associated with a higher than expected visceral fat content (Thomas et al. 2012). The present study presents several anthropometric parameters to be associated with fatty liver. Thereby VAT was identified to be the best predictor of fatty liver, describing most appropriate abdominal obesity due to its unique location.

Taken together, increasing amounts of liver fat were associated with several parameters describing abdominal obesity. Among the analyzed anthropometric parameters, VAT seemed to be the best predictor of fatty liver, compared to BMI which does not distinguish between the different fat depots, respectively lean and fat mass. HMRO were shown to contribute to the inter-individual variation of RMR (Javed et al. 2010). Based on the hypothesis that fat infiltration might reduce the specific organ metabolic rate of liver, liver fat content was analyzed regarding RMR variation. However, the amount of fat in the HMRO liver did not account for the inter-individual variation of RMR.

4.5 Conclusion

Resting metabolic rate is characterized by a high inter-individual variation, which cannot completely be explained. Understanding the underlying physiological processes causing the inter-interindividual variation of RMR is important to accurately predict RMR by prediction model. To identify the components contributing to RMR variation a prediction model was generated with anthropometric data and body temperature, explaining 80% of the variability. In a more complex model, part of the residual variation in RMR was explained by the blood parameters, free triiodothyronine, leukocytes, creatinine, MCHC and blood pressure, accounting for a substantial predictive improvement. Based on this prediction model the influence of gut microbiota composition, liver metabolism and respiratory capacity of PBMCs was analyzed regarding the inter-individual variation of RMR.

In the first part, the respiratory capacity of PBMCs was analyzed as a biomarker for mitochondrial activity on RMR variation. As mitochondria play an essential role in energy homeostasis, this study adds to the understanding of mitochondrial function of circulating PBMCs on RMR. The respiratory capacity of PBMCs was not associated with the variability of RMR. However, the respiratory capacity of PBMCs was shown to be decreased in aging subjects. Since RMR decreases with aging, the declined mitochondrial function of PBMCs contributes to the understanding of this aging process. This study presents a possibility to determine mitochondrial activity of PBMCs by respirometry, which is not invasive or requires expensive equipment like other approaches to measure mitochondrial function in humans and has therefore a great potential to assess mitochondrial function in large interventional or epidemiological studies.

In the second part, gut microbiota composition was analyzed regarding its influence on RMR variation. Gut microbiota was discussed to play an important role in energy homeostasis due to the association with obesity and the potential to extract additional energy from the diet. The present data confirm by several statistical approaches that gut microbiota is not a significant predictor of RMR. When the effect of FFM and other predictors of RMR were removed, any association of gut microbiota and RMR disappeared, which suggests that previous links between RMR and gut microbiota composition occurred because of inadequate adjustment for the effect of factors contributing to RMR.
In the third part, liver metabolism was studied regarding its influence on the inter-individual variation of RMR. Liver, as a high metabolic rate organ, plays an important role in energy expenditure. Previously, a hypothesis was formulated that fat infiltration might reduce the organ specific metabolic rate of liver. The present results showed no evidence for a decreasing organ metabolic rate due to intrahepatic fat accumulation and intrahepatic fat was not associated with inter-individual variation of RMR. Determining liver fat by MRI based PDFF was shown to be an effective and non-invasive method, allowing a fast and easy assessment of liver fat, which is important in the context of overweight and metabolic diseases.

In conclusion, a novel prediction model for RMR is presented, which will be useful in human studies due to its high precision to predict RMR. The connection of blood parameters, blood pressure, gut microbiota composition, liver fat and respiratory capacity of PBMCs on RMR variation are of added value to better understand the components of RMR causing the inter-individual variation.

5 References

Abdallah Ismail, N., S. H. Ragab, A. Abd Elbaky, A. R. Shoeib, Y. Alhosary & D. Fekry (2011) Frequency of Firmicutes and Bacteroidetes in gut microbiota in obese and normal weight Egyptian children and adults. *Arch Med Sci,* 7**,** 501-7.

Adriaens, M. P., P. F. Schoffelen & K. R. Westerterp (2003) Intra-individual variation of basal metabolic rate and the influence of daily habitual physical activity before testing. *Br J Nutr,* 90**,** 419-23.

Alberti, K. G., P. Zimmet, J. Shaw & I. D. F. E. T. F. C. Group (2005) The metabolic syndrome--a new worldwide definition. *Lancet,* 366**,** 1059-62.

Alberti, K. G. & P. Z. Zimmet (1998) Definition, diagnosis and classification of diabetes mellitus and its complications. Part 1: diagnosis and classification of diabetes mellitus provisional report of a WHO consultation. *Diabet Med,* 15**,** 539-53.

Ali, N., S. Mahmood, M. Manirujjaman, R. Perveen, A. Al Nahid, S. Ahmed, F. A. Khanum & M. Rahman (2017) Hypertension prevalence and influence of basal metabolic rate on blood pressure among adult students in Bangladesh. *BMC Public Health,* 18**,** 58.

Alonso, J. R., F. Cardellach, J. Casademont & O. Miro (2004) Reversible inhibition of mitochondrial complex IV activity in PBMC following acute smoking. *Eur Respir J,* 23**,** 214-8.

Ames, B. N., M. K. Shigenaga & T. M. Hagen (1995) Mitochondrial decay in aging. *Biochim Biophys Acta,* 1271**,** 165-70.

Astrup, A., B. Buemann, N. J. Christensen, J. Madsen, C. Gluud, P. Bennett & B. Svenstrup (1992) The contribution of body composition, substrates, and hormones to the variability in energy expenditure and substrate utilization in premenopausal women. *J Clin Endocrinol Metab,* 74**,** 279-86.

Atwater, W. V., Benedict, F.G., (1905) A respiration calorimeter with appliance for direct determination of oxygen. *Carnegie Institution of Washington,* Publication 42.

Backhed, F., H. Ding, T. Wang, L. V. Hooper, G. Y. Koh, A. Nagy, C. F. Semenkovich & J. I. Gordon (2004) The gut microbiota as an environmental factor that regulates fat storage. *Proc Natl Acad Sci U S A,* 101**,** 15718-23.

Bader, N., A. Bosy-Westphal, B. Dilba & M. J. Muller (2005) Intra- and interindividual variability of resting energy expenditure in healthy male subjects -- biological and methodological variability of resting energy expenditure. *Br J Nutr,* 94**,** 843-9.

Bajaj, J. S., H. E. Vargas, K. R. Reddy, J. C. Lai, J. G. O'Leary, P. Tandon, F. Wong, R. Mitrani, M. B. White, M. Kelly, A. Fagan, R. Patil, S. Sait, M. Sikaroodi, L. R. Thacker & P. M. Gillevet (2019) Association Between Intestinal Microbiota Collected at Hospital Admission and Outcomes of Patients With Cirrhosis. *Clin Gastroenterol Hepatol,* 17**,** 756-765 e3.

Beaumont, M., J. K. Goodrich, M. A. Jackson, I. Yet, E. R. Davenport, S. Vieira-Silva, J. Debelius, T. Pallister, M. Mangino, J. Raes, R. Knight, A. G. Clark, R. E. Ley, T. D. Spector & J. T. Bell (2016) Heritable components of the human fecal microbiome are associated with visceral fat. *Genome Biol,* 17**,** 189.

Befroy, D. E., K. F. Petersen, S. Dufour, G. F. Mason, D. L. Rothman & G. I. Shulman (2008) Increased substrate oxidation and mitochondrial uncoupling in skeletal muscle of endurance-trained individuals. *Proc Natl Acad Sci U S A,* 105**,** 16701-6.

Belikova, I., A. C. Lukaszewicz, V. Faivre, C. Damoisel, M. Singer & D. Payen (2007) Oxygen consumption of human peripheral blood mononuclear cells in severe human sepsis. *Crit Care Med,* 35**,** 2702-8.

Bianconi, E., A. Piovesan, F. Facchin, A. Beraudi, R. Casadei, F. Frabetti, L. Vitale, M. C. Pelleri, S. Tassani, F. Piva, S. Perez-Amodio, P. Strippoli & S. Canaider (2013) An estimation of the number of cells in the human body. *Ann Hum Biol,* 40**,** 463-71.

Bosy-Westphal, A., C. Eichhorn, D. Kutzner, K. Illner, M. Heller & M. J. Muller (2003) The age-related decline in resting energy expenditure in humans is due to the loss of fat-

free mass and to alterations in its metabolically active components. *J Nutr,* 133**,** 2356-62.

Bosy-Westphal, A., E. Kossel, K. Goele, W. Later, B. Hitze, U. Settler, M. Heller, C. C. Gluer, S. B. Heymsfield & M. J. Muller (2009a) Contribution of individual organ mass loss to weight loss-associated decline in resting energy expenditure. *Am J Clin Nutr,* 90**,** 993-1001.

Bosy-Westphal, A., M. J. Muller, M. Boschmann, S. Klaus, G. Kreymann, P. M. Luhrmann, M. Neuhauser-Berthold, R. Noack, K. M. Pirke, P. Platte, O. Selberg & J. Steiniger (2009b) Grade of adiposity affects the impact of fat mass on resting energy expenditure in women. *Br J Nutr,* 101**,** 474-7.

Bosy-Westphal, A., U. Reinecke, T. Schlorke, K. Illner, D. Kutzner, M. Heller & M. J. Muller (2004) Effect of organ and tissue masses on resting energy expenditure in underweight, normal weight and obese adults. *Int J Obes Relat Metab Disord,* 28**,** 72-9.

Bosy-Westphal, A., A. Wolf, F. Buhrens, B. Hitze, N. Czech, H. Monig, O. Selberg, U. Settler, M. Pfeuffer, J. Schrezenmeir, M. Krawczak & M. J. Muller (2008) Familial influences and obesity-associated metabolic risk factors contribute to the variation in resting energy expenditure: the Kiel Obesity Prevention Study. *Am J Clin Nutr,* 87**,** 1695-701.

Brand, M. D., K. M. Brindle, J. A. Buckingham, J. A. Harper, D. F. Rolfe & J. A. Stuart (1999) The significance and mechanism of mitochondrial proton conductance. *Int J Obes Relat Metab Disord,* 23 Suppl 6**,** S4-11.

Brand, M. D. & D. G. Nicholls (2011) Assessing mitochondrial dysfunction in cells. *Biochem J,* 435**,** 297-312.

Bravo, A. A., S. G. Sheth & S. Chopra (2001) Liver biopsy. *N Engl J Med,* 344**,** 495-500.

Calton, E. K., M. J. Soares, A. P. James & R. J. Woodman (2016) The potential role of irisin in the thermoregulatory responses to mild cold exposure in adults. *Am J Hum Biol,* 28**,** 699-704.

Castaner, O., A. Goday, Y. M. Park, S. H. Lee, F. Magkos, S. T. E. Shiow & H. Schroder (2018) The Gut Microbiome Profile in Obesity: A Systematic Review. *Int J Endocrinol,* 2018**,** 4095789.

Chicco, A. J. & G. C. Sparagna (2007) Role of cardiolipin alterations in mitochondrial dysfunction and disease. *Am J Physiol Cell Physiol,* 292**,** C33-44.

Claesson, M. J., A. G. Clooney & P. W. O'Toole (2017) A clinician's guide to microbiome analysis. *Nat Rev Gastroenterol Hepatol,* 14**,** 585-595.

Cooper, A. L., M. A. Horan, R. A. Little & N. J. Rothwell (1992) Metabolic and febrile responses to typhoid vaccine in humans: effect of beta-adrenergic blockade. *J Appl Physiol (1985),* 72**,** 2322-8.

Corkum, C. P., D. P. Ings, C. Burgess, S. Karwowska, W. Kroll & T. I. Michalak (2015) Immune cell subsets and their gene expression profiles from human PBMC isolated by Vacutainer Cell Preparation Tube (CPT) and standard density gradient. *BMC Immunol,* 16**,** 48.

Creber, C., R. S. Cooper, J. Plange-Rhule, P. Bovet, E. V. Lambert, T. E. Forrester, D. Schoeller, W. Riesen, W. Korte, G. Cao, A. Luke & L. R. Dugas (2018) Independent association of resting energy expenditure with blood pressure: confirmation in populations of the African diaspora. *BMC Cardiovasc Disord,* 18**,** 4.

Cunningham, J. J. (1980) A reanalysis of the factors influencing basal metabolic rate in normal adults. *Am J Clin Nutr,* 33**,** 2372-4.

Cunningham, J. J. (1991) Body composition as a determinant of energy expenditure: a synthetic review and a proposed general prediction equation. *Am J Clin Nutr,* 54**,** 963-9.

David, L. A., C. F. Maurice, R. N. Carmody, D. B. Gootenberg, J. E. Button, B. E. Wolfe, A. V. Ling, A. S. Devlin, Y. Varma, M. A. Fischbach, S. B. Biddinger, R. J. Dutton & P.

J. Turnbaugh (2014) Diet rapidly and reproducibly alters the human gut microbiome. *Nature,* 505**,** 559-63.

De Lorenzo, A., L. Di Renzo, P. Morini, R. C. de Miranda, L. Romano & C. Colica (2018) New equations to estimate resting energy expenditure in obese adults from body composition. *Acta Diabetol,* 55**,** 59-66.

Doerrier, C., L. F. Garcia-Souza, G. Krumschnabel, Y. Wohlfarter, A. T. Meszaros & E. Gnaiger (2018) High-Resolution FluoRespirometry and OXPHOS Protocols for Human Cells, Permeabilized Fibers from Small Biopsies of Muscle, and Isolated Mitochondria. *Methods Mol Biol,* 1782**,** 31-70.

Drabsch, T., C. Holzapfel, L. Stecher, J. Petzold, T. Skurk & H. Hauner (2018) Associations Between C-Reactive Protein, Insulin Sensitivity, and Resting Metabolic Rate in Adults: A Mediator Analysis. *Front Endocrinol (Lausanne),* 9**,** 556.

Du Bois, E. F. (1921) The Basal Metabolism in Fever. *Journal of the American Medical Association,* 77**,** 352 - 357.

Eckburg, P. B. & D. A. Relman (2007) The role of microbes in Crohn's disease. *Clin Infect Dis,* 44**,** 256-62.

Elia, M. 1992. *Organ and tissue contribution to metabolic rate*. New York, Raven: In Energy Metabolism: Tissue Determinants and Cellular Corollaries.

Ferraro, R. & E. Ravussin (1992) Fat mass in predicting resting metabolic rate. *Am J Clin Nutr,* 56**,** 460-1.

Ferrer, M., A. Ruiz, F. Lanza, S. B. Haange, A. Oberbach, H. Till, R. Bargiela, C. Campoy, M. T. Segura, M. Richter, M. von Bergen, J. Seifert & A. Suarez (2013) Microbiota from the distal guts of lean and obese adolescents exhibit partial functional redundancy besides clear differences in community structure. *Environ Microbiol,* 15**,** 211-26.

Frankenfield, D., L. Roth-Yousey & C. Compher (2005) Comparison of predictive equations for resting metabolic rate in healthy nonobese and obese adults: a systematic review. *J Am Diet Assoc,* 105**,** 775-89.

Gaidos, J. K., B. E. Hillner & A. J. Sanyal (2008) A decision analysis study of the value of a liver biopsy in nonalcoholic steatohepatitis. *Liver Int,* 28**,** 650-8.

Gallagher, D., J. Albu, Q. He, S. Heshka, L. Boxt, N. Krasnow & M. Elia (2006) Small organs with a high metabolic rate explain lower resting energy expenditure in African American than in white adults. *Am J Clin Nutr,* 83**,** 1062-7.

Gallagher, D., D. Belmonte, P. Deurenberg, Z. Wang, N. Krasnow, F. X. Pi-Sunyer & S. B. Heymsfield (1998) Organ-tissue mass measurement allows modeling of REE and metabolically active tissue mass. *Am J Physiol,* 275**,** E249-58.

Gong, D., X. Gong, L. Wang, X. Yu & Q. Dong (2016) Involvement of Reduced Microbial Diversity in Inflammatory Bowel Disease. *Gastroenterol Res Pract,* 2016**,** 6951091.

Green, D. R., L. Galluzzi & G. Kroemer (2011) Mitochondria and the autophagy-inflammation-cell death axis in organismal aging. *Science,* 333**,** 1109-12.

Gurven, M. D., B. C. Trumble, J. Stieglitz, G. Yetish, D. Cummings, A. D. Blackwell, B. Beheim, H. S. Kaplan & H. Pontzer (2016) High resting metabolic rate among Amazonian forager-horticulturalists experiencing high pathogen burden. *Am J Phys Anthropol,* 161**,** 414-425.

Hallgren, P., L. Sjostrom, H. Hedlund, L. Lundell & L. Olbe (1989) Influence of age, fat cell weight, and obesity on O2 consumption of human adipose tissue. *Am J Physiol,* 256**,** E467-74.

Harman, D. (1956) Aging: a theory based on free radical and radiation chemistry. *J Gerontol,* 11**,** 298-300.

Harris, J. A. & F. G. Benedict (1918) A Biometric Study of Human Basal Metabolism. *Proc Natl Acad Sci U S A,* 4**,** 370-3.

Hartman, M. L., O. S. Shirihai, M. Holbrook, G. Xu, M. Kocherla, A. Shah, J. L. Fetterman, M. A. Kluge, A. A. Frame, N. M. Hamburg & J. A. Vita (2014) Relation of

mitochondrial oxygen consumption in peripheral blood mononuclear cells to vascular function in type 2 diabetes mellitus. *Vasc Med,* 19**,** 67-74.

Haugen, H. A., E. L. Melanson, Z. V. Tran, J. T. Kearney & J. O. Hill (2003) Variability of measured resting metabolic rate. *Am J Clin Nutr,* 78**,** 1141-5.

He, Y., W. Wu, S. Wu, H. M. Zheng, P. Li, H. F. Sheng, M. X. Chen, Z. H. Chen, G. Y. Ji, Z. D. Zheng, P. Mujagond, X. J. Chen, Z. H. Rong, P. Chen, L. Y. Lyu, X. Wang, J. B. Xu, C. B. Wu, N. Yu, Y. J. Xu, J. Yin, J. Raes, W. J. Ma & H. W. Zhou (2018) Linking gut microbiota, metabolic syndrome and economic status based on a population-level analysis. *Microbiome,* 6**,** 172.

Henry, C. J. (2005) Basal metabolic rate studies in humans: measurement and development of new equations. *Public Health Nutr,* 8**,** 1133-52.

Heymsfield, S. B., D. Gallagher, D. P. Kotler, Z. Wang, D. B. Allison & S. Heshka (2002) Body-size dependence of resting energy expenditure can be attributed to nonenergetic homogeneity of fat-free mass. *Am J Physiol Endocrinol Metab,* 282**,** E132-8.

Hoffmann, M. E., S. M. Rodriguez, D. M. Zeiss, K. N. Wachsberg, R. F. Kushner, L. Landsberg & R. A. Linsenmeier (2012) 24-h core temperature in obese and lean men and women. *Obesity (Silver Spring),* 20**,** 1585-90.

Hsiao, C. P. & C. Hoppel (2018) Analyzing mitochondrial function in human peripheral blood mononuclear cells. *Anal Biochem,* 549**,** 12-20.

Iwen, K. A., E. Schroder & G. Brabant (2013) Thyroid hormones and the metabolic syndrome. *Eur Thyroid J,* 2**,** 83-92.

Jakobsen, M. U., T. Berentzen, T. I. Sorensen & K. Overvad (2007) Abdominal obesity and fatty liver. *Epidemiol Rev,* 29**,** 77-87.

Javed, F., Q. He, L. E. Davidson, J. C. Thornton, J. Albu, L. Boxt, N. Krasnow, M. Elia, P. Kang, S. Heshka & D. Gallagher (2010) Brain and high metabolic rate organ mass: contributions to resting energy expenditure beyond fat-free mass. *Am J Clin Nutr,* 91**,** 907-12.

Jheng, H. F., S. H. Huang, H. M. Kuo, M. W. Hughes & Y. S. Tsai (2015) Molecular insight and pharmacological approaches targeting mitochondrial dynamics in skeletal muscle during obesity. *Ann N Y Acad Sci,* 1350**,** 82-94.

Johansen, K., J. M. Hansen & L. Skovsted (1978) The preferential role of triiodothyronine in the regulation of basal metabolic rate in hyper- and hypothyroidism. *Acta Med Scand,* 204**,** 357-9.

Johnstone, A. M., S. D. Murison, J. S. Duncan, K. A. Rance & J. R. Speakman (2005) Factors influencing variation in basal metabolic rate include fat-free mass, fat mass, age, and circulating thyroxine but not sex, circulating leptin, or triiodothyronine. *Am J Clin Nutr,* 82**,** 941-8.

Jost, L. (2007) Partitioning diversity into independent alpha and beta components. *Ecology,* 88**,** 2427-39.

Karabatsiakis, A., C. Bock, J. Salinas-Manrique, S. Kolassa, E. Calzia, D. E. Dietrich & I. T. Kolassa (2014) Mitochondrial respiration in peripheral blood mononuclear cells correlates with depressive subsymptoms and severity of major depression. *Transl Psychiatry,* 4**,** e397.

Karhunen, L., A. Franssila-Kallunki, A. Rissanen, K. Kervinen, Y. A. Kesaniemi & M. Uusitupa (1997) Determinants of resting energy expenditure in obese non-diabetic caucasian women. *Int J Obes Relat Metab Disord,* 21**,** 197-202.

Karlsson, F., V. Tremaroli, J. Nielsen & F. Backhed (2013) Assessing the human gut microbiota in metabolic diseases. *Diabetes,* 62**,** 3341-9.

Kauppila, T. E. S., J. H. K. Kauppila & N. G. Larsson (2017) Mammalian Mitochondria and Aging: An Update. *Cell Metab,* 25**,** 57-71.

Kelley, D. E., T. M. McKolanis, R. A. Hegazi, L. H. Kuller & S. C. Kalhan (2003) Fatty liver in type 2 diabetes mellitus: relation to regional adiposity, fatty acids, and insulin resistance. *Am J Physiol Endocrinol Metab,* 285**,** E906-16.

Keys, A., H. L. Taylor & F. Grande (1973) Basal metabolism and age of adult man. *Metabolism,* 22**,** 579-87.

Kim, B. (2008) Thyroid hormone as a determinant of energy expenditure and the basal metabolic rate. *Thyroid,* 18**,** 141-4.

Kingma, B. R., A. J. Frijns, L. Schellen & W. D. van Marken Lichtenbelt (2014) Beyond the classic thermoneutral zone: Including thermal comfort. *Temperature (Austin),* 1**,** 142-9.

Kleiber, M. (1947) Body size and metabolic rate. *Physiol Rev,* 27**,** 511-41.

Kleiveland, C. R. 2015. Peripheral Blood Mononuclear Cells. In *The Impact of Food Bioactives on Health: in vitro and ex vivo models,* eds. K. Verhoeckx, P. Cotter, I. Lopez-Exposito, C. Kleiveland, T. Lea, A. Mackie, T. Requena, D. Swiatecka & H. Wichers, 161-167. Cham (CH).

Kotronen, A., J. Westerbacka, R. Bergholm, K. H. Pietilainen & H. Yki-Jarvinen (2007) Liver fat in the metabolic syndrome. *J Clin Endocrinol Metab,* 92**,** 3490-7.

Kramer, P. A., S. Ravi, B. Chacko, M. S. Johnson & V. M. Darley-Usmar (2014) A review of the mitochondrial and glycolytic metabolism in human platelets and leukocytes: implications for their use as bioenergetic biomarkers. *Redox Biol,* 2**,** 206-10.

Kreymann, G., S. Grosser, P. Buggisch, C. Gottschall, S. Matthaei & H. Greten (1993) Oxygen consumption and resting metabolic rate in sepsis, sepsis syndrome, and septic shock. *Crit Care Med,* 21**,** 1012-9.

Kroemer, G., G. Marino & B. Levine (2010) Autophagy and the integrated stress response. *Mol Cell,* 40**,** 280-93.

Lagkouvardos, I., S. Fischer, N. Kumar & T. Clavel (2017) Rhea: a transparent and modular R pipeline for microbial profiling based on 16S rRNA gene amplicons. *PeerJ,* 5**,** e2836.

Lam, Y. Y. & E. Ravussin (2017) Indirect calorimetry: an indispensable tool to understand and predict obesity. *Eur J Clin Nutr,* 71**,** 318-322.

Landsberg, L. (2012) Core temperature: a forgotten variable in energy expenditure and obesity? *Obes Rev,* 13 Suppl 2**,** 97-104.

Landsberg, L., M. E. Saville & J. B. Young (1984) Sympathoadrenal system and regulation of thermogenesis. *Am J Physiol,* 247**,** E181-9.

Larsen, F. J., T. A. Schiffer, K. Sahlin, B. Ekblom, E. Weitzberg & J. O. Lundberg (2011) Mitochondrial oxygen affinity predicts basal metabolic rate in humans. *FASEB J,* 25**,** 2843-52.

Ley, R. E., F. Backhed, P. Turnbaugh, C. A. Lozupone, R. D. Knight & J. I. Gordon (2005) Obesity alters gut microbial ecology. *Proc Natl Acad Sci U S A,* 102**,** 11070-5.

Ley, R. E., P. J. Turnbaugh, S. Klein & J. I. Gordon (2006) Microbial ecology: human gut microbes associated with obesity. *Nature,* 444**,** 1022-3.

Li, Y., H. Wang, X. Li, H. Li, Q. Zhang, H. Zhou, Y. He, P. Li, C. Fu, X. Zhang, Y. Qiu & J. L. Li (2019) Disordered intestinal microbes are associated with the activity of Systemic Lupus Erythematosus. *Clin Sci (Lond)*.

Liesa, M. & O. S. Shirihai (2013) Mitochondrial dynamics in the regulation of nutrient utilization and energy expenditure. *Cell Metab,* 17**,** 491-506.

Lipinski, M. M., B. Zheng, T. Lu, Z. Yan, B. F. Py, A. Ng, R. J. Xavier, C. Li, B. A. Yankner, C. R. Scherzer & J. Yuan (2010) Genome-wide analysis reveals mechanisms modulating autophagy in normal brain aging and in Alzheimer's disease. *Proc Natl Acad Sci U S A,* 107**,** 14164-9.

Lopez, M., C. V. Alvarez, R. Nogueiras & C. Dieguez (2013) Energy balance regulation by thyroid hormones at central level. *Trends Mol Med,* 19**,** 418-27.

Lozupone, C. A., J. I. Stombaugh, J. I. Gordon, J. K. Jansson & R. Knight (2012) Diversity, stability and resilience of the human gut microbiota. *Nature,* 489**,** 220-30.

Luke, A., A. Adeyemo, H. Kramer, T. Forrester & R. S. Cooper (2004) Association between blood pressure and resting energy expenditure independent of body size. *Hypertension,* 43**,** 555-60.

Meunier, N., J. H. Beattie, D. Ciarapica, J. M. O'Connor, M. Andriollo-Sanchez, A. Taras, C. Coudray & A. Polito (2005) Basal metabolic rate and thyroid hormones of late-middle-aged and older human subjects: the ZENITH study. *Eur J Clin Nutr,* 59 Suppl 2**,** S53-7.

Milani, C., S. Duranti, F. Bottacini, E. Casey, F. Turroni, J. Mahony, C. Belzer, S. Delgado Palacio, S. Arboleya Montes, L. Mancabelli, G. A. Lugli, J. M. Rodriguez, L. Bode, W. de Vos, M. Gueimonde, A. Margolles, D. van Sinderen & M. Ventura (2017) The First Microbial Colonizers of the Human Gut: Composition, Activities, and Health Implications of the Infant Gut Microbiota. *Microbiol Mol Biol Rev,* 81.

Min, Y., X. Ma, K. Sankaran, Y. Ru, L. Chen, M. Baiocchi & S. Zhu (2019) Sex-specific association between gut microbiome and fat distribution. *Nat Commun,* 10**,** 2408.

Mosca, A., M. Leclerc & J. P. Hugot (2016) Gut Microbiota Diversity and Human Diseases: Should We Reintroduce Key Predators in Our Ecosystem? *Front Microbiol,* 7**,** 455.

Muller, M. J., A. Bosy-Westphal, S. Klaus, G. Kreymann, P. M. Luhrmann, M. Neuhauser-Berthold, R. Noack, K. M. Pirke, P. Platte, O. Selberg & J. Steiniger (2004) World Health Organization equations have shortcomings for predicting resting energy expenditure in persons from a modern, affluent population: generation of a new reference standard from a retrospective analysis of a German database of resting energy expenditure. *Am J Clin Nutr,* 80**,** 1379-90.

Muller, M. J., A. Bosy-Westphal, D. Kutzner & M. Heller (2002) Metabolically active components of fat-free mass and resting energy expenditure in humans: recent lessons from imaging technologies. *Obes Rev,* 3**,** 113-22.

Nelson, K. M., R. L. Weinsier, C. L. Long & Y. Schutz (1992) Prediction of resting energy expenditure from fat-free mass and fat mass. *Am J Clin Nutr,* 56**,** 848-56.

Ost, M., C. Doerrier, P. Gama-Perez & S. Moreno-Gomez (2018) Analysis of mitochondrial respiratory function in tissue biopsies and blood cells. *Curr Opin Clin Nutr Metab Care,* 21**,** 336-342.

Pathak, K., E. K. Calton, M. J. Soares, Y. Zhao, A. P. James, K. Keane & P. Newsholme (2017) Forearm to fingertip skin temperature gradients in the thermoneutral zone were significantly related to resting metabolic rate: potential implications for nutrition research. *Eur J Clin Nutr,* 71**,** 1074-1079.

Perseghin, G., V. Mazzaferro, S. Benedini, A. Pulvirenti, J. Coppa, E. Regalia & L. Luzi (2002) Resting energy expenditure in diabetic and nondiabetic patients with liver cirrhosis: relation with insulin sensitivity and effect of liver transplantation and immunosuppressive therapy. *Am J Clin Nutr,* 76**,** 541-8.

Porter, R. K. & M. D. Brand (1993) Body mass dependence of H+ leak in mitochondria and its relevance to metabolic rate. *Nature,* 362**,** 628-30.

Rao, Z. Y., X. T. Wu, B. M. Liang, M. Y. Wang & W. Hu (2012) Comparison of five equations for estimating resting energy expenditure in Chinese young, normal weight healthy adults. *Eur J Med Res,* 17**,** 26.

Ravussin, E., S. Lillioja, T. E. Anderson, L. Christin & C. Bogardus (1986) Determinants of 24-hour energy expenditure in man. Methods and results using a respiratory chamber. *J Clin Invest,* 78**,** 1568-78.

Reeder, S. B., H. H. Hu & C. B. Sirlin (2012) Proton density fat-fraction: a standardized MR-based biomarker of tissue fat concentration. *J Magn Reson Imaging,* 36**,** 1011-4.

Riedhammer, C., D. Halbritter & R. Weissert (2016) Peripheral Blood Mononuclear Cells: Isolation, Freezing, Thawing, and Culture. *Methods Mol Biol,* 1304**,** 53-61.

Robert, C. & A. Bernalier-Donadille (2003) The cellulolytic microflora of the human colon: evidence of microcrystalline cellulose-degrading bacteria in methane-excreting subjects. *Fems Microbiology Ecology,* 46**,** 81-89.

Rocha, R., H. P. Cotrim, F. M. Carvalho, A. C. Siqueira, H. Braga & L. A. Freitas (2005) Body mass index and waist circumference in non-alcoholic fatty liver disease. *J Hum Nutr Diet,* 18**,** 365-70.

Rodriguez, J. M., K. Murphy, C. Stanton, R. P. Ross, O. I. Kober, N. Juge, E. Avershina, K. Rudi, A. Narbad, M. C. Jenmalm, J. R. Marchesi & M. C. Collado (2015) The composition of the gut microbiota throughout life, with an emphasis on early life. *Microb Ecol Health Dis,* 26**,** 26050.

Rolfe, D. F. & M. D. Brand (1996) Contribution of mitochondrial proton leak to skeletal muscle respiration and to standard metabolic rate. *Am J Physiol,* 271**,** C1380-9.

Romero-Corral, A., V. K. Somers, J. Sierra-Johnson, R. J. Thomas, M. L. Collazo-Clavell, J. Korinek, T. G. Allison, J. A. Batsis, F. H. Sert-Kuniyoshi & F. Lopez-Jimenez (2008) Accuracy of body mass index in diagnosing obesity in the adult general population. *Int J Obes (Lond),* 32**,** 959-66.

Rontoyanni, V. G., O. Nunez Lopez, G. T. Fankhauser, Z. F. Cheema, B. B. Rasmussen & C. Porter (2017) Mitochondrial Bioenergetics in the Metabolic Myopathy Accompanying Peripheral Artery Disease. *Front Physiol,* 8**,** 141.

Roth, G. M. & C. Sheard (1950) Relation of basal metabolic rate to vasodilatation and vasoconstriction of the extremities of normal subjects as measured by skin temperatures. *Circulation,* 1**,** 1142-7.

Rustin, P., D. Chretien, T. Bourgeron, B. Gerard, A. Rotig, J. M. Saudubray & A. Munnich (1994) Biochemical and molecular investigations in respiratory chain deficiencies. *Clin Chim Acta,* 228**,** 35-51.

Scheepers, L. E., J. Penders, C. A. Mbakwa, C. Thijs, M. Mommers & I. C. Arts (2015) The intestinal microbiota composition and weight development in children: the KOALA Birth Cohort Study. *Int J Obes (Lond),* 39**,** 16-25.

Schicker, C. (2017) Association of intra-individual variability between basal metabolic rate and mitochondrial respiration in Peripheral Blood Mononuclear Cells. *Master Thesis*.

Sebastian, D., M. Palacin & A. Zorzano (2017) Mitochondrial Dynamics: Coupling Mitochondrial Fitness with Healthy Aging. *Trends Mol Med,* 23**,** 201-215.

Sender, R., S. Fuchs & R. Milo (2016) Revised Estimates for the Number of Human and Bacteria Cells in the Body. *PLoS Biol,* 14**,** e1002533.

Shen, W., H. R. Gaskins & M. K. McIntosh (2014) Influence of dietary fat on intestinal microbes, inflammation, barrier function and metabolic outcomes. *J Nutr Biochem,* 25**,** 270-80.

Shigenaga, M. K., T. M. Hagen & B. N. Ames (1994) Oxidative damage and mitochondrial decay in aging. *Proc Natl Acad Sci U S A,* 91**,** 10771-8.

Smith-Brown, P., M. Morrison, L. Krause & P. S. W. Davies (2018) Male-specific Association Between Fat-Free Mass Index and Fecal Microbiota in 2- to 3-Year-Old Australian Children. *J Pediatr Gastroenterol Nutr,* 66**,** 147-151.

Snodgrass, J. J., W. R. Leonard, M. V. Sorensen, L. A. Tarskaia & M. J. Mosher (2008) The influence of basal metabolic rate on blood pressure among indigenous Siberians. *Am J Phys Anthropol,* 137**,** 145-55.

Spadafranca, A., C. Cappelletti, A. Leone, L. Vignati, A. Battezzati, G. Bedogni & S. Bertoli (2015) Relationship between thyroid hormones, resting energy expenditure and cardiometabolic risk factors in euthyroid subjects. *Clin Nutr,* 34**,** 674-8.

Speliotes, E. K., J. M. Massaro, U. Hoffmann, R. S. Vasan, J. B. Meigs, D. V. Sahani, J. N. Hirschhorn, C. J. O'Donnell & C. S. Fox (2010) Fatty liver is associated with dyslipidemia and dysglycemia independent of visceral fat: the Framingham Heart Study. *Hepatology,* 51**,** 1979-87.

Srinivasan, S., M. Yeh, E. C. Danziger, M. E. Hatley, A. E. Riggan, N. Leitinger, J. A. Berliner & C. C. Hedrick (2003) Glucose regulates monocyte adhesion through endothelial production of interleukin-8. *Circ Res,* 92**,** 371-7.

Suomalainen, A. & B. J. Battersby (2018) Mitochondrial diseases: the contribution of organelle stress responses to pathology. *Nat Rev Mol Cell Biol,* 19**,** 77-92.

Svendsen, O. L., C. Hassager & C. Christiansen (1993) Impact of regional and total body composition and hormones on resting energy expenditure in overweight postmenopausal women. *Metabolism,* 42**,** 1588-91.

Tait, S. W. & D. R. Green (2010) Mitochondria and cell death: outer membrane permeabilization and beyond. *Nat Rev Mol Cell Biol,* 11**,** 621-32.

Thomas, E. L., J. R. Parkinson, G. S. Frost, A. P. Goldstone, C. J. Dore, J. P. McCarthy, A. L. Collins, J. A. Fitzpatrick, G. Durighel, S. D. Taylor-Robinson & J. D. Bell (2012) The missing risk: MRI and MRS phenotyping of abdominal adiposity and ectopic fat. *Obesity (Silver Spring),* 20**,** 76-87.

Tilg, H. & A. Kaser (2011) Gut microbiome, obesity, and metabolic dysfunction. *J Clin Invest,* 121**,** 2126-32.

Tremaroli, V. & F. Backhed (2012) Functional interactions between the gut microbiota and host metabolism. *Nature,* 489**,** 242-9.

Trounce, I., E. Byrne & S. Marzuki (1989) Decline in skeletal muscle mitochondrial respiratory chain function: possible factor in ageing. *Lancet,* 1**,** 637-9.

Turnbaugh, P. J., F. Backhed, L. Fulton & J. I. Gordon (2008) Diet-induced obesity is linked to marked but reversible alterations in the mouse distal gut microbiome. *Cell Host Microbe,* 3**,** 213-23.

Turnbaugh, P. J., R. E. Ley, M. A. Mahowald, V. Magrini, E. R. Mardis & J. I. Gordon (2006) An obesity-associated gut microbiome with increased capacity for energy harvest. *Nature,* 444**,** 1027-31.

Tzankoff, S. P. & A. H. Norris (1977) Effect of muscle mass decrease on age-related BMR changes. *J Appl Physiol Respir Environ Exerc Physiol,* 43**,** 1001-6.

van der Windt, G. J., B. Everts, C. H. Chang, J. D. Curtis, T. C. Freitas, E. Amiel, E. J. Pearce & E. L. Pearce (2012) Mitochondrial respiratory capacity is a critical regulator of CD8+ T cell memory development. *Immunity,* 36**,** 68-78.

van Marken Lichtenbelt, W. D., J. W. Vanhommerig, N. M. Smulders, J. M. Drossaerts, G. J. Kemerink, N. D. Bouvy, P. Schrauwen & G. J. Teule (2009) Cold-activated brown adipose tissue in healthy men. *N Engl J Med,* 360**,** 1500-8.

Wang, Z., S. Heshka, D. Gallagher, C. N. Boozer, D. P. Kotler & S. B. Heymsfield (2000) Resting energy expenditure-fat-free mass relationship: new insights provided by body composition modeling. *Am J Physiol Endocrinol Metab,* 279**,** E539-45.

Wang, Z., T. P. O'Connor, S. Heshka & S. B. Heymsfield (2001) The reconstruction of Kleiber's law at the organ-tissue level. *J Nutr,* 131**,** 2967-70.

Weinsier, R. L., Y. Schutz & D. Bracco (1992) Reexamination of the relationship of resting metabolic rate to fat-free mass and to the metabolically active components of fat-free mass in humans. *Am J Clin Nutr,* 55**,** 790-4.

Weir, J. B. (1949) New methods for calculating metabolic rate with special reference to protein metabolism. *J Physiol,* 109**,** 1-9.

Weststrate, J. A. (1993) Resting metabolic rate and diet-induced thermogenesis: a methodological reappraisal. *Am J Clin Nutr,* 58**,** 592-601.

WHO (1985) Energy and protein requirements. Report of a joint FAO/WHO/UNU Expert Consultation. *World Health Organ Tech Rep Ser,* 724**,** 1-206.

WHO (2018) Obesity and overweight. *Fact sheet (World Health Organization)*.

Wijers, S. L., P. Schrauwen, W. H. Saris & W. D. van Marken Lichtenbelt (2008) Human skeletal muscle mitochondrial uncoupling is associated with cold induced adaptive thermogenesis. *PLoS One,* 3**,** e1777.

Wilman, H. R., M. Kelly, S. Garratt, P. M. Matthews, M. Milanesi, A. Herlihy, M. Gyngell, S. Neubauer, J. D. Bell, R. Banerjee & E. L. Thomas (2017) Characterisation of liver fat in the UK Biobank cohort. *PLoS One,* 12**,** e0172921.

Zurlo, F., Y. Schutz, P. Frascarolo, G. Enzi, O. Deriaz & E. Jequier (1986) Variability of resting energy expenditure in healthy volunteers during fasting and continuous enteral feeding. *Crit Care Med,* 14**,** 535-8.

6 Acknowledgments

An dieser Stelle möchte ich mich gerne bei allen bedanken, die mich auf persönlicher und wissenschaftlicher Ebene während meiner Promotionszeit unterstützt und zu dem Gelingen dieser Arbeit beigetragen haben.

Ein besonderer Dank geht an Prof. Martin Klingenspor für die Bereitstellung des Themas, die Betreuung durch zahlreiche Diskussionen, Anregungen, Ratschläge und die Unterstützung durch seine freundliche und motivierende Art.

Ein weiterer Dank gilt dem *enable*-Kompetenzcluster mit allen *enable*-Partnern und *enable*-Doktoranden für die erfolgreiche Zusammenarbeit. Ein besonderer Dank gilt dem *enable*-Studienteam und Prof. Thomas Skurk, der mich in all meinen Fragen bezüglich Ethikantrag und klinischer Studien unterstützt hat. Außerdem möchte ich mich bei mein Kooperationspartnern am Klinikum rechts der Isar, Priv.-Doz. Dr. Dimitrios Karampinos, Priv.-Doz. Dr. med Thomas Baum, Dr. med. Daniela Franze und Jan Syväri für die Messung und Zusammenarbeit bei der Pilot-Studie bedanken.

Ein großer Dank geht an Tobi für all seine Ratschläge und Unterstützung, sowohl wissenschaftlich als auch persönlich. Vielen Dank für die Geduld bei all meinen statistischen Fragen und für das Korrekturlesen dieser Arbeit. Außerdem möchte ich mich bei der gesamten Arbeitsgruppe für die angenehme Arbeitsatmosphäre, die Hilfsbereitschaft und vielen lustigen Momenten bedanken. Insbesondere bedanke ich mich bei Sabine, Samira und Anika für ihre Hilfe und Unterstützung im Labor.

Ein besonderer Dank gilt meiner Familie und Freunden, die immer für mich da waren und mich stets unterstützt haben. Ein großes Danke geht an meine Eltern, die mir ermöglicht haben zu studieren, mich immer wieder ermutigt und emotionalen Rückhalt gegeben haben. Bei meiner Schwester Claudia bedanke ich mich herzlich für das Korrekturlesen dieser Arbeit. Ich möchte mich bei all mein Freunden bedanken, vor allem bei Claire, Johanna und Isabel, die stets für mich da waren, immer ein offenes Ohr hatten und auch für Abwechslung gesorgt haben.

Dieses Projekt wurde im Rahmen des *enable*-Kompetenzclusters durchgeführt und vom Bundesministerium für Bildung und Forschung finanziert.